VeloElectric

California Polytechnic State University San Luis Obispo 2015

Project Sponsor: Lynne Slivovsky

Faculty Advisor: John Ridgely

Pedl Team Members:
Austin Hall-auhall@calpoly.edu
Daniel Stohr-dstohr@calpoly.edu
TJ Fox-tjfox@calpoly.edu

Creating a device that harnesses energy from mountain biking to power mobile devices.

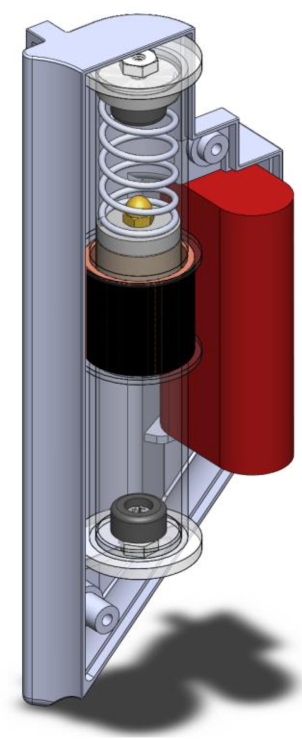

Statement of Disclaimer

Since this project is a result of a class assignment, it has been graded and accepted as fulfillment of the course requirements. Acceptance does not imply technical accuracy or reliability. Any use of information in this report is done at the risk of the user. These risks may include catastrophic failure of the device or infringement of patent or copyright laws. California Polytechnic State University at San Luis Obispo and its staff cannot be held liable for any use or misuse of the project.

Acknowledgements

The Pedl team would like to thank the Endowment for Excellence in Project-Based Learning and Student success for funding this entire project and making it possible for the design team to create their final prototype. The design team would also like to give a special thanks to the following people for helping the design team throughout the year:

- Professor John Ridgely: Senior Project Advisor
- Professor Lynne Slivovsky: Project Sponsor
- Staff at the Innovation Sandbox: 3D Printing Prototypes
- Larry Coolidge: Rapid Prototyping Assistant
- Jaime Carmo: Assisted in Soldering the BQ25504 to the Printed Circuit Board

Table of Contents

Abstract

Long distance mountain bikers, bike-packers, and many bikers in developing countries rely on electrical devices for safety and communication. These specific groups of people operate in areas with little to no electricity, and often times have no power to sustain their devices. The purpose of this Cal Poly senior project, VeloElectric, was to design, build, and test a kinetic energy harvester for bicycles that can be used to charge common mobile devices via USB. This senior project team created a device that attaches directly to a bicycle and uses vibrations to generate energy, which in turn powers a variety of portable devices. The final product will be used by Professor Lynne Slivovsky on a bike ride from Canada to Mexico. This document contains information on the entire project during the 2014-2015 school year. The "Background" section summarizes research and case studies including dynamo chargers and an electromagnetic induction charger called the nPower PEG. The Pedl team used this information to generate initial design ideas such as using piezoelectrics and other kinetic energy harvesting devices. This research was also used to gain a better understanding of the current state of art for this type of product. The end of the background section provides details of the project management plan that was used through the course of the projects focusing heavily on the tasks completed during Spring quarter. Following the "Background" section is an explanation of the development of conceptual designs that lead to the final product. Conceptual designs included decision matrices to decide on a 3D printed exterior casing, Velcro straps for attachment, electromagnetic induction for energy generation, and a battery for energy storage. Diagrams, models and pictures of the end product are displayed and analyzed in the "Description of Final Design" section. This section shows the exterior casing that was created to house the inner casing, battery, and printed circuit board. The "Product Realization" section focuses on how a lathe was used to create the final inner casing, 3D printing for the exterior casing and inner casing caps, and simple soldering for the electrical components. The section also explains how the final prototype cost the team about $200, but through mass production could be lowered to about $45. The "Design Verification" section discusses how the final iteration was tested and includes test descriptions and photos while documenting the results of these tests. Example tests include weight, bike transfer time, USB compatibility, and vibrational tolerance. The document concludes by discussing the progress that was made on the project throughout the year and the recommendations that the design team has for possible future teams assigned to this task.

List of Tables

List of Figures

Chapter 1: Introduction

The primary purpose of this senior project, VeloElectric, is to harness kinetic energy in an efficient and sustainable way. Specifically, the Pedl team wants to take the excess energy of a moving bike and use it to charge a large range of mobile devices. Cell phone and MP3 device use has increased exponentially over the past decade to the point where it is often times necessary to carry a mobile device at all times. That, of course, includes times when a person is working out. Many mountain bikers listen to music, use GPS apps, and even take calls on the go. Additionally, mountain biking is a relatively dangerous activity that may require a participant to make an emergency call at any time. The project sponsor, Lynne Slivovsky, will be conquering The Great Divide Mountain Bike Route which is a continuous long distance bicycle touring route from Banff, Alberta, Canada to Antelope Wells, New Mexico, USA. As of 2010, the route is 2745 miles. The created product will be heavily used during this trip to help charge three devices that Lynne extensively uses while she rides. Other stakeholders include general bike packers and bikers in developing countries such as Kenya, Uganda, and Tanzania. This area presents a large opportunity, because many of the roads in these parts of Africa are extremely rugged causing many people to bike. In addition, many of the same people that have bikes also use cell phones, but the electrical grid in Africa is often unreliable and their phones can't be charged. The overall goal of the team is to have a working device by June that can be used by many bikers to power their mobile devices.

Chapter 2: Background

Existing Products/Current State of Art

There have been many attempts at creating devices that fulfill the goals of the Pedl team's intended product. One of these devices is the Siva Cycle Atom. This device attaches to the rear hub on a bicycle and converts the rotational energy of the wheel into electrical energy. This electrical energy is used to either charge a battery pack or directly charge a mobile device. It has a charge rate of 5V at 500mA, is water resistant, and weighs 300g.[1] The device itself is also about as large as an iPhone with dimensions of 7.5" by 3.0" by 1.2". The other advantage of this device is that it technically only has three moving parts: a drive gear, idler gear, and magnet rotor. This makes the Siva a very dependable device. The Siva also has a detachable Lithium-polymer battery that can be used to charge devices while users are on the go and away from their bike. The size of the battery is 1300 mAh and can charge an iPhone from dead to 70% once per charge. [1] The Atom's energy delivery works in the following manner. When the bike travels at a rate of 3mph, the Atom outputs 0.75W; at 10mph, 3W, and at 15mph it is maxed out at 4.5W. Power is always delivered in a regulated manner (5V @ up to 500mA; 2.5W), providing only the amount of energy the device specifically demands. Excess power charges the battery or (if battery is full) is

Figure 2-1: Siva Bicycle Atom on Rear Hub

Source: http://www.wired.com

released to protect electronics. [1] A picture of the Siva Cycle Atom attached to a bicycle hub is shown in Figure 2-1.

The second device that seems to be common uses a dynamo on one of the wheels to generate electricity. The Nokia bicycle charger consists of three components: a bottle dynamo, a charger and a phone holder. A bottle dynamo is specific for bicycles and is essentially a small electrical generator. A roller is placed on the front tire of a bicycle and, as the tire rotates and the bicycle moves, the roller begins to spin and energy is generated. This rotational motion is harvested in a generator and creates electrical energy. The bottle dynamo fits to the front of the bike with a mounting bracket. The charger and phone holder attach securely to the handlebars. The charger, phone holder and phone can be removed easily whenever the bike is parked. While riding, the Nokia Bicycle Charger Kit starts charging at walking speed (6 km/h) and stops when speed reaches 50 km/h. [2] This specific design only charges phones that have a 2 mm interface.

Figure 2-2: Shimano Hub Dynamo Example

Source: http://www.wikimedia.com

A hub dynamo is another option that bikers currently use to power LED front and back lights. A hub dynamo consists of a typical bicycle hub with a generator inside that operates and produces electricity by rotation of the hub shell relative to a hub axle. [3] Most of these hub dynamos generate about 3 Watts at 6 Volts. The downside of this type of device is that they are always engaged while the rider is biking and they cause the rider to exert more energy to the pedals to overcome this resistance. They also require quite a bit of retrofitting to the bike because the entire hub is removed and replaced for the dynamo hub. This makes transferring the device to multiple bikes more difficult and time consuming. Figure 2-2 shows a hub dynamo installed on a bicycle.

Piezoelectrics is another option that could be used for energy harvesting. Piezoelectricity is the act of taking crystals, such as quartz, and doing work on the crystals to create a current. In technical terms, "Piezoelectricity (also called the piezoelectric effect) is the appearance of an electrical potential (a voltage, in other words) across the sides of a crystal when it is subjected to mechanical stress (by squeezing it)."[4] The crystal essentially becomes a battery with a positive charge on one face and a negative charge on the opposite face. Current will flow when the two faces are connected together to make a circuit. Figure 2-3 shows how a piezoelectric would work in terms of bicycle vibrations. The vibrations of the bicycle would cause stress to the piezoelectric. This stress would induce a current that could be used to charge a battery which would be connected to a load. In a study done by Dejan Vasic, Yu-Yin Chen, and François Costa, it was determined that by using piezoelectrics, 9mW could be produced with an acceleration of 8 m/s^2. This is enough to power a flashing light on a bicycle.[5]

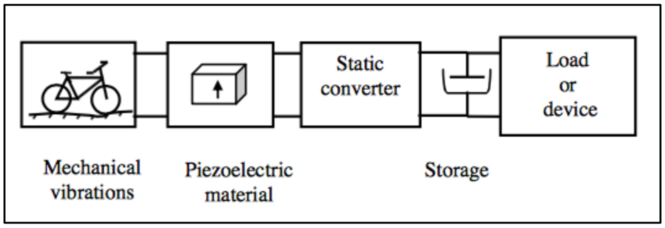

Figure 2-3: Block Diagram of Piezoelectric Energy Generation

Source: http://www.ieeexplore.ieee.org

Most recently, a group of three engineers from Northwestern University created a device that harvests energy from inductors and is geared toward active individuals. It essentially captures kinetic energy when the user is moving and stores that energy in a 1000 mAh battery. They call the device AMPY and the project has raised over $300,000 on Kickstarter. [6] AMPY is currently available for pre-order and is scheduled to begin shipping in July 2015. It is a very versatile device that can be used in many different situations due it its shape and size. The design incorporates the device itself with an armband, clip, and sleeve to protect the device while in use and make it usable in many situations. According to their website, a cell phone can regain 3 hours of use by walking 10,000 steps, cycling for an hour, or 30 minutes of running. [6] A prototype assembly of the AMPY is shown in Figure 2-4.

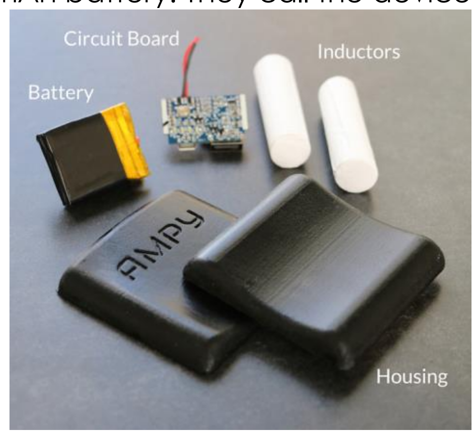

Figure 2-4: AMPY Prototype Assembly

Source: http://www.kickstarter.com

The final device that was previously manufactured harvests energy from motion. This device is called the nPower PEG. The nPower PEG is a rod-shaped mobile power generator that harvests energy "while you walk, ride in a car or bus, or even shake it up and down."[7] It includes a built-in 2000 mAh lithium ion polymer battery that can charge mobile devices from its mini USB port. The devices uses electromagnetic induction to generate AC power that it rectifies through a printed circuit board and stores that resulting DC power in a battery. The device contains only a couple of major parts including a printed circuit board, copper coil, magnet, springs, and all of this is enclosed in a thick plastic housing. The device is not waterproof, but according to its designers, it is water resistant and can withstand thunderstorms when carried in the side pocket of a backpack. In terms of energy generation, the device will recharge an iPhone to about 20% after a full day of walking. [7] Weighing about 1 pound and having a length of 10.5", it is a pretty large device, as shown in Figure 2-5, and can best be utilized when placed in a bag where the user does not have to carry it around.

Figure 2-5: nPower PEG in use

Source: http://www.sectionhiker.com

In order to meet protection requirements, the final product will need to meet certain IP Codes (Ingress Protection Rating) for solids and liquids. IP Codes classify and rate the "degree of protection provided against intrusion (body parts such as hands and fingers), dust, accidental contact, and water by mechanical casings and electrical enclosures." [8] These codes specify what type of conditions the device can withstand and continue to function in. The IP rating for water that will need to be met is 4, which is described as "water splashing against the enclosure from any direction which should have no harmful effect." [9] The IP rating for solids required by a product like this is 4, which is effective against wires and screws. [9] The device will also need to withstand a specific magnitude of vibrations. Research and test results suggest that the maximum G-forces on a bicycle max out around 30G where an accelerometer is placed on the fork of a bicycle.[10]

During an October 16th meeting with the sponsor, some of the requirements that she wanted to see in the final design were discussed.[10] These engineering requirements have been specifically highlighted with grey in the objectives section.

Project Requirements

The ultimate objective of this project is to design, prototype, and produce a bike powered device charger that meets all intended specifications. Based on the customer requirements that were established over the course of initial meetings, as well as the QFD exercise (Appendix B-1), the Pedl team has compiled a list of general and specific parameters for the intended product. These parameters cover the majority of this product and if met will signify an overall success.

Pedl Project Engineering Requirements

Table 2-1: Pedl Project Engineering Requirements

Spec. Number	Parameter Description	Requirement or Target with Units	Tolerance	Risk	Compliance
1	Battery Capacity	5000 mAh	Min	L	A,T,S
2	USB Output	5V DC, 0.5-0.9A	Min	L	I,T
3	Weight	250g	100g<x<300g	H	A,T,S
4	Bike Transfer Time	5 minutes	Max	M	T
5	Waterproofing	IPX-4 rating	Min	M	T,S
6	Particle-proofing	IPX-4 rating	Min	M	T,S
7	Vibration Tolerance	30g (acceleration)	Min	M	A,T
8	Charge Rate	2.0-2.5W	Min	H	A,T
9	Direct Angular Resistance to Wheel	0 ft-lbs	Max	L	T,I
10	Noise while riding	20 dB	Max	L	T,I
11	Time to Charge Battery	6-15 Hours	Min	H	T,A

Table 2-1 serves as a brief parameter outline. The following table shows the meaning of the letters used in the table.

Compliance:

A: Analysis **T**: Testing **S**: Similarity to Existing Devices **I**: Inspection

Risk:

L: Low **M**: Medium **H**: High

1. In order to charge the wide variety and large amount of devices (as explained by the sponsor) the Pedl team has decided that the battery capacity should be at least 5000 mAh. This battery size will be able to fully charge a phone, bike computer, and GPS with a little extra capacity to account for DC-DC losses. Meeting this battery specification will not be difficult, however, the size of the battery is directly proportional to size and weight.

2. Because almost every portable device is charged by USB, a USB port will be used as the main method of charging. The voltage specification provides for no more than 5.25 V and no less than 4.75 V (5 V ± 5%) between the positive and negative bus power lines (V_{BUS} voltage). [11] The current limit for USB 2.0 is 500mA which results in 2.5W of maximum power.

3. As specified by the client, the entire device will ideally be around 250 grams[10]. The Pedl team believes that this may be the most difficult specification to meet. Many similar devices on the market today weigh close to a pound and the lightest battery on the market that fits the capacity specifications (>=5000 mAh) weighs around 102 grams[12]. That being said, weight is still a very high priority and will take a major role in guiding the design process.

4. The client also mentioned that the device would ideally be easily transferred from one bike to another. [10] The Pedl team has determined that a 5 minute maximum detachment and attachment time would be suitable.

5. Because this device is specifically for use outside, the Pedl team will be designing it to withstand water splashing against the enclosure from any direction which should have no harmful effect (IPX-4 waterproof rating).

6. Mountain biking is generally done on dirt paths, and it is very likely that the device will be exposed to mud, dirt, and other large particles. The product will have a particle-proofing rating of IPX-4.

7. It is very likely that the finished project will be entirely, or at least partially fastened to the seat tube in order to harness vibration. Additionally, the entire bike will be vibrating and dropping over the course of the entire ride. The Pedl team will be designing a product that can withstand at least a 30g impact. This number was provided from the sponsor as an extreme mountain biking acceleration. Additional testing will need to be completed in order to ensure the accuracy of this requirement.

8. The Charge rate of this device will be at least 2.5 Watts. With the correct circuit architecture and specifications, this should be a pretty easy specification to achieve.

9. The client made it clear that this device was not to inhibit the forward motion of the bicycle [10]. Therefore, there can be no direct contact with the wheels. Energy will need to be harvested from a different part of the bicycle's motion.

10. The sponsor also explained that she did not want to hear the device while she was riding her bike. A 20dB target was chosen because this will give room for the device to make noise without being heard by the rider while biking.

Project Management

In order for this project to succeed, the Pedl team needed to approach the project by completing a conceptual design report in the Fall, a critical design report in the Winter, and major deadlines throughout the Spring quarter. These major tasks included an initial prototype that was to be tested on a bike while iterating the design as needed until the final design was achieved. The Pedl team decided on a schedule for the spring quarter of the school year that greatly helped the project remain on schedule and deliverable by the end of the quarter. This schedule is shown below in Table 1:

Table 2-2: Detailed Project Schedule

Task ID	Description	Predecessor	Start Date	Duration (days)	Responsible Party
A	3-D Print Outer Housing for Physical Verification	none	3/13/2015	5	Danny/Austin
B	3-D Print Inner Housing for Physical Verification	none	3/13/2015	5	Danny/Austin
C	Complete Purchases of New Mechanical Parts	none	3/13/2015	1	Danny/Austin
D	Verify/Obtain Tolerance and Fitting of Outer and Inner Housing Assemblies	A,B	3/30/2015	2	Danny/Austin
E	Complete Inner Casing Subassembly	C,D	4/2/2015	2	Danny/Austin
F	Complete Testing of Circuit Subassembly	none	3/13/2015	25	TJ
G	Finalize PCB Layout	F	4/7/2015	2	TJ
H	Order and Receive PCB	G	4/09/1015	7	TJ
I	Solder Battery and Coil to PCB	H	4/16/2015	1	TJ
J	Create Assembly of Outer Housing, Inner Housing, and EE Components	E,I	4/17/2015	1	All
K	Perform Mechanical Tests	J	4/19/2015	2	Danny/Austin
L	Perform Electrical Tests	J	4/19/2015	3	TJ
M	Document Findings and Implement Possible Changes to Design	K,L	4/22/2015	20	All
N	3-D Print/Machine Final Inner and Outer Housing Design	M	5/13/2015	5	Danny/Austin
O	Complete Final Assembly	N	5/18/2015	2	All
P	Final Testing	O	5/20/2015	7	All
Q	Document Results and Finalize Report	P	5/27/2015	15	All

In order to ensure that the deadlines above were met, the Pedl team needed to meet outside of class at least twice every week. That being said, a large amount of the parts needed for this project were shipped in the mail, so work related meetings only occurred when the necessary materials arrived. This is why the specific dates were chosen as start dates to allow for specific parts to be shipped and delivered. There are also gaps in between task completion dates and task start dates that allowed for some slack time for other outside school work to be completed giving the design team enough time to finish tasks in reasonable amount of time. Additionally, it was not necessary for

specific group members to attend meetings where they were not needed at. Specific group members were assigned to each of the tasks which allowed for accountability of tasks as well as an understanding of what each of the group members needed to complete. This allowed for a more effective use of time during what was a very busy quarter.

Appendix H includes a PERT (Program Evaluation Review Technique) Chart for the project which was effective in identifying the tasks that were most important and which tasks had slack time. The PERT chart is displayed in a block diagram format which makes it easy to follow and very easy to read. It also clearly identified which tasks needed to be completed, or the predecessors, of the tasks that followed them. It made it simple to refer to this chart and management plan during various points of the project to understand what tasks needed to be done next and when specific tasks could be started. The chart shows the early start and finish time for each of the tasks that needed to be completed as well as the number of days that each task would take. The chart was built for information in Table 2-2 and task identifiers can be found in this table. The critical path was highlighted in green so that they could be easily identified and this identified the tasks that were rate determining for the entire project. These tasks together are what caused the project to take 59 days as shown on the right-hand side of the chart. Any delays in the tasks that are shown in green past the estimated completion time would have caused the project to slip and take more time than what was estimated. The design team was prepared to follow this management plan in order to finish the project in a timely fashion and successfully deliver a working product to Lynne.

Chapter 3: Design Development

Preliminary Design Decisions

A decision matrix process was chosen in order to narrow down the many solutions that could possibly solve the problem provided by the sponsor. The datum that was used to compare possible solutions was the Siva Cycle Atom described in the background section of the report. There are four primary subsystems that serve as the core of the device. These subsystems include housing, bike attachment, power generation, and power storage. The decision making process for each of these subsystems is described in detail below and Figure 3-1 shows an example of the housing matrix.

		Siva Cycle Atom	Weight (grams)	Noise (dB)	Durability (max G force)	Aesthetically Pleasing	Manufacturability (seconds)	Weighted Sum +	Weighted Sum -	Weighted Sum S	Total Score
	Specification Weight		20	15	35	5	25				
Housing	3-D Printed Plastic		S	S	S	S	+	25	0	75	48
	Aluminum	S	-	S	+	+	-	40	45	15	-1
	Rubber		-	+	-	-	-	15	85	0	-70

Figure 3-1: Housing Decision Matrix

Appendix B-2 shows the completed decision matrix for the housing of the device. The three possible solutions that were explored were rubber, plastic, and aluminum. These three solutions were compared on the basis of weight, noise, durability, aesthetics, and manufacturability. The various weighting of these specifications can also be seen in Appendix B-2. 3-D Printed plastic proved to be the best possible solution for the housing of the device. It is not as durable as something like aluminum, but plastic does have much more versatility in terms of manufacturability and this is very important to the design team. As more and more iterations are made, it is going to be much more difficult to make aluminum housings to test than it will to print 3-D plastic models. In terms of durability, the housing will not encounter very large

forces while on the bike. The stresses from the components inside will be very minimal. Many 3-D printed plastics, such as ABS, have tensile strengths ranging from 20-35 MPa which is more than enough for the stress that the Pedl while endure.[13] Stress calculations have been done to prove that the exterior casing will withstand the force of a magnet at 30 G's. (See Appendix E-3). The one case where it would need to withstand structural integrity is during a crash when outside forces act on it. The design team also agreed that the plastic housing would best blend in with the other components on the bike and could be aesthetically pleasing. 3-D Printed Plastic is also relatively light in weight and would be the best material for keeping water and particles from getting inside the housing.

The next subsystem (shown in Appendix B-3) that Pedl team investigated was the bicycle attachment system. It was important to address this component because, like the housing, the attachment needs to be very durable and usable with the design of current bikes. The possible solutions included zip ties, Velcro straps, bungee cords, and a mounting bracket. These solutions were compared based on similar specifications as the housing with the addition of transfer time. Transfer time is an important specification because the sponsor has indicated that the device must be transferable between bikes within five minutes. With the help of the decision matrix, the design team found that Velcro straps would be the most favorable option. Velcro straps are very versatile and are able to be used in many applications. Straps can wrap around objects and keep them secure with reasonable strength that suits the current application. The Velcro straps would also reduce the transfer time to a matter of seconds which is highly desirable to users with multiple bicycles. Transfer time was a critical need of the sponsor, Lynne Slivovsky, and the Velcro straps help address this need.

Energy generation is arguably the most important part of the device. Appendix B-4 shows the matrix that was used to determine how the device is going to harvest energy. Some of the initial ideas that were considered included solar, wind, and piezoelectric materials and these are not shown on the decision matrix. The reason for this is that the design team determined these sources of energy would not be feasible for this project. Some of the research shown in the background section reveals that piezoelectric materials would not be able to produce the energy needed to fully charge a 5000 mAh battery in 6-15 hours. Additionally, solar energy would be extremely difficult to implement on the bike. The solar cell would need to be oriented in such a way to point in the direction of the sun and the architecture of the bike does not allow for this when the size of the solar panel is taken into account. The design team also felt that wind would be compatible and calculations prove that it could be possible, however, there would be direct resistance to the pedaling of the rider. The client expressed that the design not directly restrict her pedaling and the design team feels that an option of wind would generate enough energy, but would require too much work from the rider.

The remaining solutions included electromagnetic induction as a free magnet and as a fixed magnet. The difference between these two concepts is that the fixed magnet would be attached to the front fork of a front suspension bicycle and move with respect to the fork to force the magnet through the copper coil, while the free magnet would move independently and could be placed anywhere on the bicycle. The decision matrix shows that the free and fixed magnets are very comparable in terms of weight, durability, angular resistance, and manufacturability. Their final scores were nearly identical and the design team decided that they needed to have criteria that discussed how the design would function with all bicycle designs. Front suspension is not a feature included on all bikes, including the sponsor's, and the fixed magnet approach would limit the number of bikes that the device is compatible with. The free magnet system is also a more simple design with less

moving parts, which will allow it to properly work for a longer amount of time. The fixed magnet requires too many prerequisites from the bike and is not suitable for the presented problem.

The final subsystem is the energy storage system (Appendix B-5). The possible solutions were a capacitor, battery, and capacitor and battery working together. The fuel cell and super capacitor ideas were quickly thrown out of the final decision matrix due to the size of the super capacitor needed and the cost of the fuel cell. The design team determined that the capacitor and battery combination would be the best option for this device. Much like how the electromagnetic induction flashlights work, the capacitor and battery combination is necessary to harvest the AC current generated by the magnet and convert it to DC current necessary to charge the battery. The circuit architecture for this type of set up has been described and explained in the initial prototype section previously.

Preliminary Electrical Analysis/Initial Prototypes

The initial prototype, involved modifying and extensively testing two different faraday flashlights. An example of this type of flashlight is shown in Figure 3-3. These self-sustaining flashlights recharge their battery via kinetic energy converted to electrical energy. Faraday's law (shown in Figure 3-2) states that any change in the magnetic environment of a coil wire will cause a voltage to be induced in the coil. The flashlight houses a magnet in the center of a coil. By shaking the flashlight, the magnet passes back and forth through the coil housing, causing a voltage to be induced in the wire. With a simple full wave rectifier and a capacitor, this energy is harvested and stored in the battery. In order to test the initial prototype the flashlight was taken apart and leads were soldered to all of the essential electrical components of the flashlight (shown in Figure 3-4). In Figure 3-4, 1 & 2 represent the positive and negative sides of the capacitor, 3 & 4 are where the flashlight's switch is connected, and 5 & 6 are the output terminals of the battery. Using a breadboard, a 1.5 ohm resistor was placed across the battery terminal where the LED used to be. Next, the device was shaken for approximately 30 seconds, giving the battery sufficient time to fully charge. Then the switch was closed and the voltage across the resistor was recorded. A 4 volt output was observed at 80 milliamps for approximately six seconds.

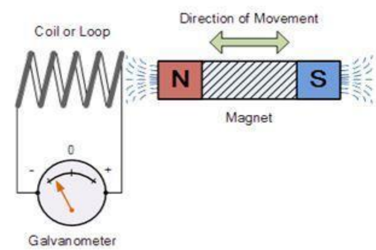

Figure 3-2: Diagram describing Faraday's Law

Source: http://electrical4u.com

Figure 3-3: Example Faraday Flashlight

Source: http://www.amazon.com

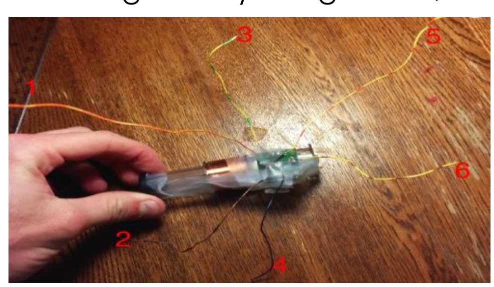

Figure 3-4: Modified Flashlight Circuit

This data succeeded as a proof of concept and from here, tests were performed to try to charge a portable external battery via USB. The battery pack that was chosen was a 5000 mAh Mophie Powerstation Mini. The circuit for this test is shown below in Figure 3-5. After shaking the modified flashlight, it was determined that the circuit was not producing enough current to charge the portable battery.

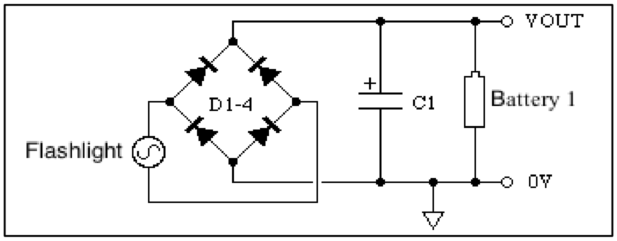

Figure 3-5: Test Circuit Architecture

Source: http://newton.ex.ac.uk

Many of these devices have regulators in them that force a current threshold to be achieved and kept for a specified amount of time or they will not charge. The circuit that was designed was specific for the flashlight in powering the LED, but was not designed to charge a battery with a higher current threshold. It was not possible to try to identify where this regulator was in the circuit and try to remove it without sacrificing the integrity of the battery, so alternative tests were performed.

For the next iteration of the electrical design, the nPower PEG, which was explained in the Background chapter of the report, was purchased. This device was originally intended to be a personal energy generator for people to wear while walking around and performing daily activities. The PEG, shown in Figure 3-6, works identically to the flashlight prototype, harnessing Faraday's law to transform kinetic energy into usable electricity. As described previously, this device comes standard with a 2000 mAh, 3.7 volt battery and a 5 volt, 500 mA USB output port. This is the ideal output requested by the sponsor. The built in springs are tuned for people walking and ideally oscillate at 2 Hz. The mechanical analysis in the next section will describe how these springs were not strong enough to test on a bicycle so results were obtained by shaking the device by hand. After taking apart the device, the team observed that the internal components are very similar to those of the original flashlight prototype. The device has a built in printed circuit board that uses a rectifier circuit and a capacitor to smooth the output of the coils.

Figure 3-6: nPower PEG Device

Source: http://www.wired.com

New analysis was available after successfully machining the inner casing assembly (described in the Preliminary Mechanical Analysis section). The team was able to determine the amount of peak-to-peak voltage produced through electromagnetic induction using an oscilloscope of the new inner casing assembly. The coil leads were attached to an oscilloscope to measure the peak to peak voltage and 0.2V was measured shown in Figure 3-7. This voltage seemed very low and the team also noticed that the magnet was experiencing a lot of friction when travelling through the casing. It was determined that the copper wire used was uncoated and this was causing a large amount of voltage loss through the wire. The design team then bought some magnetic copper wire, wound it around the casing, and tried the test again. This greatly improved the results and peak-to-peak voltages of 20V was observed.

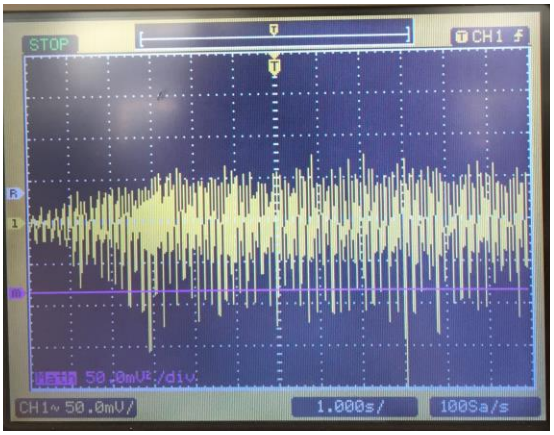

Figure 3-7: Oscilloscope Screen Capture of Original Inner Casing Assembly

After the inner casing assembly was finalized with the new magnetic coil, the 20V peak to peak AC voltage was rectified through a full-wave rectifier on a breadboard. The output DC voltage after the rectifier varied between 2 and 5 volts. This voltage was an acceptable range and the design team moved on to design a circuit to charge the 3.7 V Li-Ion battery.

A Texas Instruments BQ25504 Ultra Low Power Boost Converter with Battery Management for Energy Harvester chip was chosen as an optimal energy harvesting chip. The data sheet, shown in Appendix J, stated that it was able to continually harvest energy from an input source as low as 80mV. [14] The 16 pin chip layout is shown in Figure 3-8 and, after research, it was determined that solar cell applications with this chip were similar to the induction charging circuit. A full-wave rectifier would be needed before the input node in order to convert the voltage from the induction charger from AC to DC.

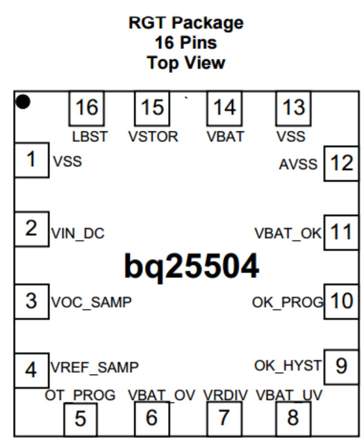

Figure 3-8: Texas Instruments BQ25504 RGT Package Pin Layout Assembly

Source: http://www.ti.com

PSpice was used to design the test circuit that would be used on the breadboard. Intermediate calculations determined the proper resistor divider values for battery overvoltage and under voltage pins. The final PSpice design is shown in Appendix C-9.

All of the PSpice components listed in Appendix C-9 were purchased and the Texas Instruments BQ25504 was mounted to a Proto-Advantage QFN-16 to DIP SMT Adapter shown in Figure 3-9.

With the help of Jaime Carmo, the equipment technician for the electrical engineering department, the BQ25504 was soldered to the adapter. Initially, the plan was to use the reflow oven. However, after applying the solder paste, it was decided that a hot air gun would be the best option. While this may have been more tedious, it was more accurate and allowed the team to constantly monitor the solder to ensure no pins became bridged together in the process.

After this process was completed, the test circuit was built on a breadboard shown in Figure 3-10 by attaching all of the necessary components: both ends of the coil to the positive and negative input terminals and a 3.7 V Li-Ion battery to the battery terminal. Two tests were then run on this circuit with the battery starting at different voltage levels. The test results are shown in Table 3-1.

Figure 3-9: Proto-Advantage QFN-16 to DIP-16 SMT Adapter

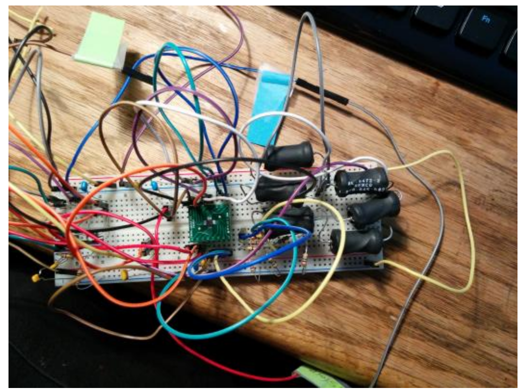

Figure 3-10: Breadboard Test Circuit of PSpice Design

Table 3-1: Testing Results of Breadboard Test Circuit

	Charge on Battery (Volts)	Charge on Battery (Volts)
Time of Shaking (Minutes)	Test 1	Test 2
0	3.695	3.995
1	3.696	3.995
2	3.696	3.996
5	3.699	3.998
10	3.703	4.001
15	3.706	4.004

The results of the above table indicated to the team that the chosen circuit design would successfully harvest energy at an acceptable rate. Also through this testing, the design team was able to prove that the circuit would charge the battery to its maximum capacity of 4 volts which is shown in Test 2. It is clear from the tests that the circuit is much more efficient at charging the battery when it is initially at a smaller voltage or charge. The voltage increase over 15 minutes in the first test was 0.011 volts while the voltage increase in the second test was .009 volts. This proof of concept allowed the design team to move forward and begin PCB design.

Preliminary Mechanical Analysis

Testing was performed to not only verify the 30G maximum acceleration provided by the sponsor, but also to verify the best possible position for the device on a bicycle. The team used a YEI 3-Space Data Logger, shown in Figure 3-11, to quantify accelerations on different parts of the bicycle. The YEI 3-Space Data Logger logs both gyroscope and accelerometer data and stores this information into a mini-SD card within the device which can be read out and interpreted on a computer. The data logger was secured to the bike in the following places: fork, seat post, handlebars, and down stem. During each of these tests, the design team rode the bicycle on the same path which included normal terrain, bumpy terrain, and a 3 foot drop. It was quickly identified that the fork was the best place for the device because it experienced larger accelerations for longer periods of time compared to other locations on the bicycle. A maximum acceleration was calculated to be 24Gs. This force was experienced both during the 3-foot drop and on the bumpy terrain path. This indicated that the entire design needs to be resistant to extremely high accelerations. In some cases, devices attached to the front fork could experience up to 30 g's which will create large amounts of forces on the casing. This force will directly act on the magnet which bounces through the copper wire coils and will cause stress on the spring that hold the magnet assembly.

Figure 3-11: YEI 3-Space Data Logger

Source: https://www.yeitechnology.com

Figure 3-12 is a graphical representation of the acceleration data collected during one of the bike riding tests. Specifically this data shows the acceleration on the front fork for the extreme case of riding down stairs. An overwhelming majority of this data falls between -5g and 5g. This means that the team will select springs with spring coefficients that can handle forces caused by this range of accelerations. The accelerometer used to acquire these test results had a maximum reading of 24g which is reached on the graph 3 separate times. In rarer cases like these where the acceleration spikes to values which are 10g and more, it will be very convenient to have a rubber stopper at each end of the device to keep the springs from bottoming out and to ensure that the device stays silent throughout the ride.

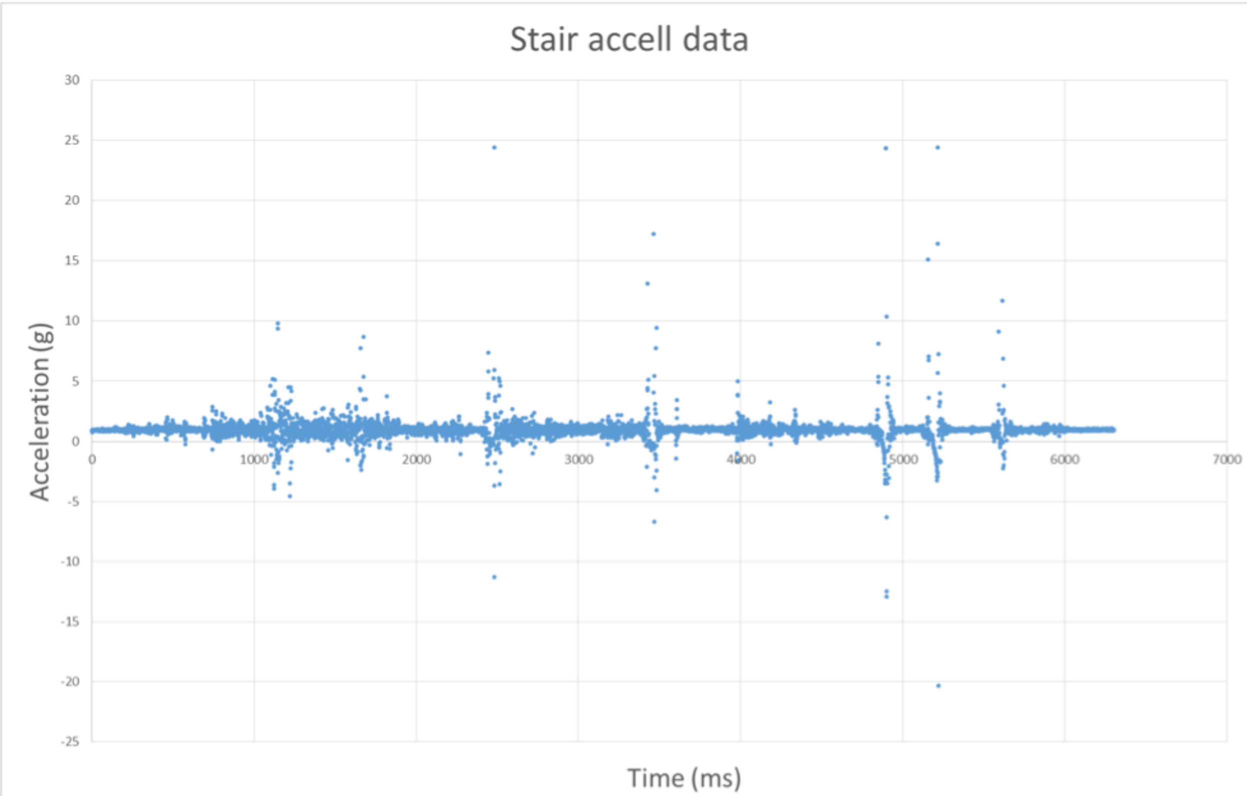

Figure 3-12: Acceleration Data of YEI Data Logger for Bike Stair Test

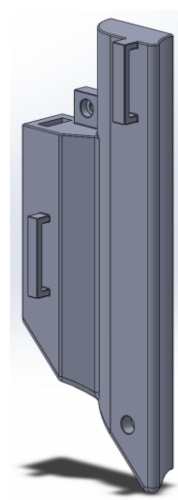

Figure 3-13: SolidWorks Model of Exterior Casing

Physically, the design of the Pedl e- has changed significantly throughout the design process due to space limitations which were results of the size of necessary parts. Originally the exterior design was a single cylinder. However, because the device uses a large battery, a multitude of possible shapes and arrangements were created and proposed to incorporate a 5000+ mAh battery. The final physical concept utilized a single cylinder design with an attached chamber for the battery. This casing fits snuggly around the charging mechanism, electrical board, and battery. Figure 3-13 shows a preliminary high-level design of the outer casing which restricts movement of inner components and fits securely onto the seat tube of a bicycle. The casing design has two curved surfaces which allows the device to fit in the space between the seat tube and the down tube. Two rubber pads will be placed on the curved surfaces touching the seat and down tubes which are designed to significantly increase the static friction between the device and the bicycle. By using rubber pads alongside Velcro attachment straps, the Pedl e- will stay safe and secure during the entire ride.

Following the competition of this testing and the critical design presentation, it became evident that the initial design was not compatible with the client's specific bicycle frame. The client uses a Jones Titanium Spaceframe with a Truss Fork Thru-Axle. This is a very specific design that Jones has released and is shown in Figure 3-14. The front fork has a small diameter and the first iteration of the Pedl was not going to securely fit onto the fork. It was also not possible to change the diameter on the fitting of the exterior casing based on the internal components. After evaluating the new frame and examining the data logger information in different bicycle locations, it was decided that the device would need to be placed on the seat tube. This would allow the magnet's motion in the inner casing to continue to move in a linear motion. This motion is also consistent with the maximum accelerations experienced by the bicycle.

Figure 3-14: Jones Titanium Spaceframe with Truss Fork Thru-Axle
Source: http://www.jonesbikes.com/

A second test was performed and the YEI data logger was placed on the seat tube of the clients bicycle. The client and a member of the design team then went on a bike ride around the Cal Poly campus and the client chose to ride in locations that were similar to the terrain of the The Great Divide Mountain Bike Route. After the ride, the data for the YEI data logger was analyzed and is graphically shown in Figure 3-16.

The acceleration data displayed in Figure 3-16 shows far smaller accelerations when compared to the data from the previous stair test. This is due to the fact that the trail terrain is much more calm than the stairs, and it can be expected that the majority of trails and roads will produce data that is far closer to the data shown in Figure 3-16. Additionally, the seat post does experience slightly smaller accelerations than the fork does. These results support the idea that the majority of the acceleration values experienced by the magnet during riding will be between 5g and negative 5g. In order to harness these smaller accelerations a change in the spring design was necessary which is shown in Figure 3-15. The previous design requires at least 1g to get the magnet up off of the bottom of the inner casing, which wasn't a problem given the older data. However, with the new location, the design team has decided to use a single spring system where the magnet and the top of the casing are connected by a spring. This spring suspends the magnet in the exact center of the inner casing where the copper coil is, ensuring that even the smallest accelerations move the magnet through the coils and generate current.

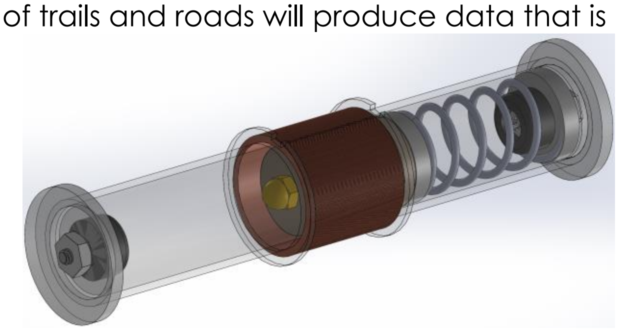

Figure 3-15: Inner Casing Spring Assembly

Like the stair test results, these new results also contain data where accelerations were relatively high. The data contains accelerations up to 17G's. Because the spring is only designed to hold the magnet in oscillation for accelerations between -5g and 5g, two soft rubber stoppers are at either end of the inner casing and ensure that the magnet is stopped during extreme terrain riding. (See Appendix E-1)

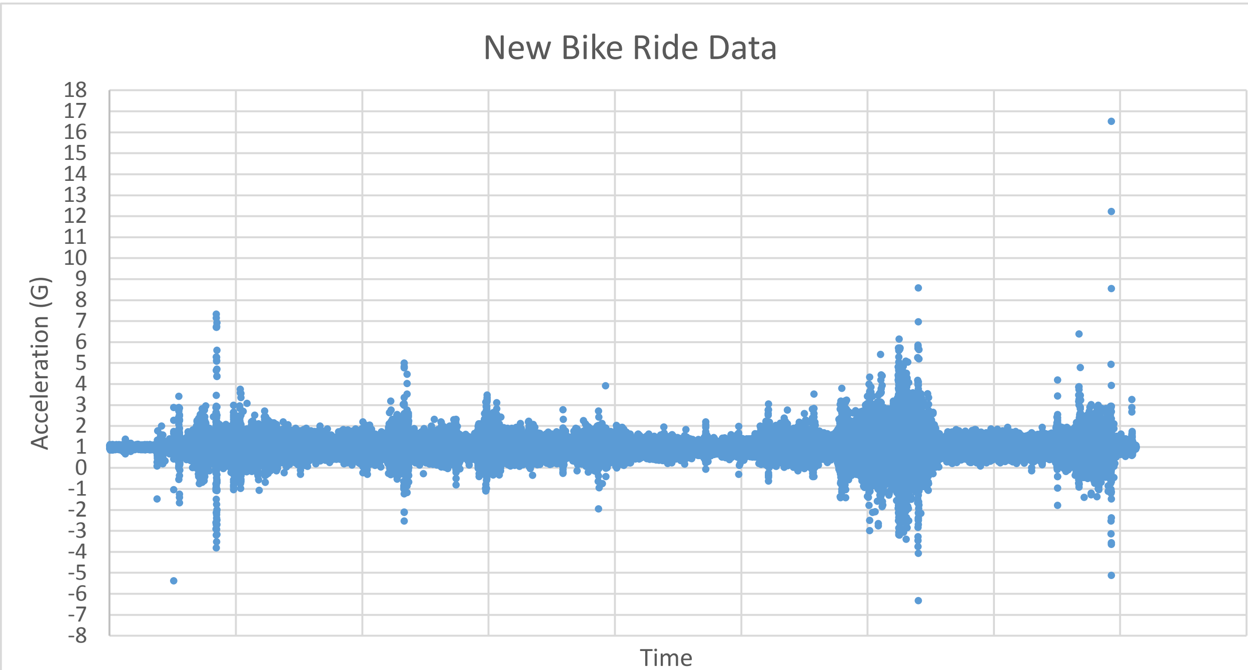

Figure 3-16: Acceleration Data for Bike Ride Test on Seat Tube

After the preliminary design was created, the team utilized Sculpteo.com which is a 3D printing service that accepts part files and mails the physical part to the designer. The inner casing for the inductor as well as the two caps were printed using this service. The team was very happy with the precision of the printed parts, but there was one problem with the casing. The printed part was a little bit rough and the design team worried that friction with the magnet would have a significant negative effect on the efficiency of the device. In order to avoid this the team decided to manufacture the final part from delrin plastic which is very smooth and easy to machine.

Chapter 4: Description of the Final Design

Final Mechanical Design

The final design contains 27 parts and utilizes a single electromagnetic induction charger (see Figure 4-1). This induction charger is made up of a black plastic casing with caps on either end which allows for simple assembly, and disassembly if necessary. Within the casing, there is a magnet, one spring, and two rubber stoppers. The spring allows the magnet to maintain its kinetic energy and ultimately increases the amount of charge created, while the rubber stoppers exist to cope with the larger accelerations and keep the spring from bottoming out, which will increase the longevity of the product. Only one spring is utilized and it holds the magnet in the exact middle of the inner casing because the closer that magnet is to the copper coil, the higher the charge rate will be. Appendix E-1 includes calculations showing minimum requirements for spring. The spring chosen for this application needs to be able to take the force of the magnet accelerated to 5 g's before the magnet touches the rubber safety pad. The selected spring (mentioned in Appendix E-1) can handle accelerations of over 6 g's before the rubber stopper is touched allowing the Pedl e$^-$ to utilize an even greater range of accelerations. The clear casing will fit snuggly into the exterior casing and allows for a central concentrated copper coil which is necessary for efficient AC power production.

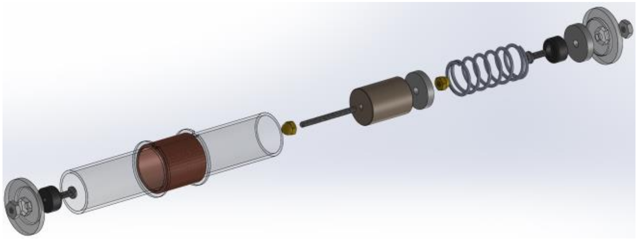

Figure 4-1: Exploded View of Electromagnetic Induction Components

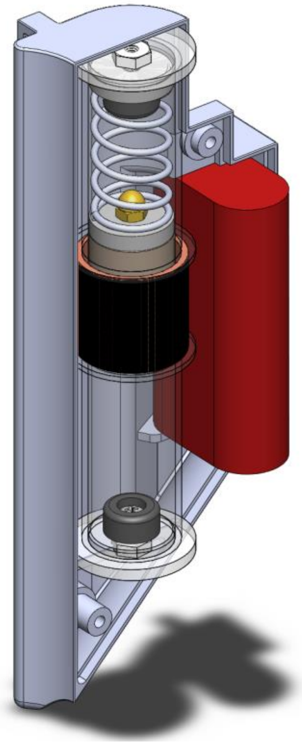

Figure 4-2: Inner Component Arrangement

The inner casing, battery. and electrical board are shown in place in Figure 4-2. This figure is the simple layout of the system. The electrical board was incorporated into the design which allows for storage of all of the electrical components and wiring. As can be seen in Figure 4-2, the battery (which is red) is held by the casing leaving room for the electrical board on the right hand side. The electrical boards are adhered to the exterior casing which prevents them from moving during vibration. Every interior component is contained snugly by some part of the exterior casing. It is imperative that there is no movement of interior components (except the magnet) at any point, otherwise life span and efficiencies would be significantly decreased. The top and bottom casings are connected using 4-40 steel screws and nuts which allow for simple assembly and disassembly.

Finally, the entire device will be attached to a bicycle using thin Velcro straps (Appendix D-3). These straps will loop through the protruding components on the flat sides of the casing and tighten around the bike tube pressing the rubber friction pads securely against the bike. Simple statics analysis shows that the normal force provided by the straps will need to be above 10 lbs. (See Appendix E-2). This is definitely achievable, because the straps and casing are designed to withstand forces far greater. Additionally all downward movement will be negated by the tube that contacts the bottom of the device.

Mechanical Material Selection

Due to the complexity and wide variety of the custom parts needed for this project, 3D printing will be utilized for the two exterior casings, and the two inner casing caps. Based on strength data for different plastics, ABS (Acrylonitrile Butadiene Styrene) was chosen for the exterior casing because it is rigid and can hold up to the forces that will be exerted by the magnet and the straps. ABS also has great impact resistance (tensile strength 20-35 MPa) which will be necessary if the device is ever dropped or becomes detached during riding.[13] 3D Printed plastics such as PVA (dissolves in water) and Nylon were considered, but were not suitable for the outer casing because of material properties. The inner casing will be made from delrin (which is a slippery and easily machinable polymer) and caps will be made from Objet Vero White which is a rigid inexpensive polymer.

Appendix C displays Mechanical drawings of all of the parts used by this design and provides some visual insight as to why certain parts are 3D printed as opposed to cast, machined, or molded.

Final Electrical Design

The final electrical design was chosen based off of the Faraday flashlight, nPower PEG circuits, and the proof of concept from the PSpice circuit described in the "Detail Design" section of this report. The PCB of the nPower PEG was an original prototype that was used because the inputs and outputs of the circuit were specifically designed for this application and would require small changes to be used as the test circuit. A 2300 mAh, 3.7V phone battery was charged using the circuit of the nPower PEG after shaking the device for 10 minutes. Results from shaking the nPower PEG are detailed in Appendix E-4 and the results are very favorable. After 10 minutes of shaking, a 3% increase in battery percentage occurred. This proves that the charge rate is 1.573W. The devices that Lynne will need to charge during riding include a bike computer (3.5Wh), GPS (3.12 Wh), SPOT Device (3.6 Wh), and a Samsung Galaxy S4 Mini: (7.22 Wh). A 30% efficiency loss was assumed for the losses in the circuit from

a buck converter and typical battery charging losses. This produced a charge rate of 1.10W and proved that all of the devices could all be fully charged in around 15 hours of riding. This fits the requirement given by the sponsor of fully charging the internal battery in 6-15 hrs.

For the final design, a custom printed circuit board was built. The specifications and design of this board were based on the results, and data from the breadboard circuit described in the "Detail Design" section of the report. The circuitry is shown in a PSpice schematic in Appendix C-9. In order to design the board layout, a PCB editing program needed to be chosen. Based on sponsor recommendations, CadSoft EAGLE was originally chosen. After completing some online research, the design team discovered a company called Fritzing FAB. Their software was more intuitive to use and the entire design process was able to be streamlined. Fritzing's software was chosen to complete rest of the board design and the final schematic of the board is shown in Appendix C-9 and C-10.

Figure 4-3: Tenergy 5200 mAh Battery

Conversations with the sponsor implied that all of the devices will not need to be charged daily and this allowed for a smaller capacity battery to be used in the device. Originally, a Li-Ion 5200mAh Stick Rechargeable Battery Module was chosen. It was made up of two 2600 mAh cylindrical cells with a built in PCB (protected circuit battery) and poly switch. After the exterior casing was redesigned, the battery needed to be changed because it was not going to be compatible with the new location on the bike. A 3.7 V, 5200 mAh lithium-ion Tenergy battery was chosen as a replacement. This battery is almost identical to the previous battery choice, but the two 2600 mAh cells are placed side by side instead of stacked which allows it to be compatible with the new exterior casing design. It contains a built-in IC chip which will prevent the battery pack from over charging and over discharging and will also prolong the battery life. [15] Additionally, the lithium-ion makeup of the battery allows for an extremely safe battery in a wide variety of conditions in comparison to Li-Polymer batteries which tend to be explosive when subject to too much heat or improper charging. This battery, shown in Figure 4-3, has sufficient storage to adequately charge all of Professor Slivovsky's devices based off the calculations shown in Appendix E-4

Figure 4-4: Adafruit Powerboost 500 Basic

In order to regulate the USB output at 5 volts with a steady current, a DC/DC boost converter needed to be purchased. After research and recommendations from the sponsor, the design team chose the Adafruit PowerBoost 500 Basic, as shown in Figure 4-4. This particular device was chosen due to features such as low battery detection, 2A internal switch, synchronous conversion, and high efficiency. It also has a very compact and simple design that fits nicely into the exterior casing. It uses a Texas Instrument TPS61090 which claims 96% efficiency. [16] This device connects straight into the Tenergy 5200 mAh battery highlighted in the paragraph above and allows the user to plug directly into its USB connector to universally charge their devices.

A summary of the electrical connections is shown in Figure 4-5. Essentially, the electromagnetic induction generator's positive and negative leads are connected to the VIN_AC+ and VIN_AC- of the circuit board. This voltage is then initially rectified using a full-wave rectifier and the voltage is both boosted and stored in inductors and capacitors as well as sent directly into the Tenergy 5200mAH battery. The battery leads are connected to the BAT+ and Ground terminal on the circuit board and the Adafruit PowerBoost 500 Basic are also connected in parallel to the battery which boosts the voltage from 3.7V to 5.0V to provide steady and universal charging.

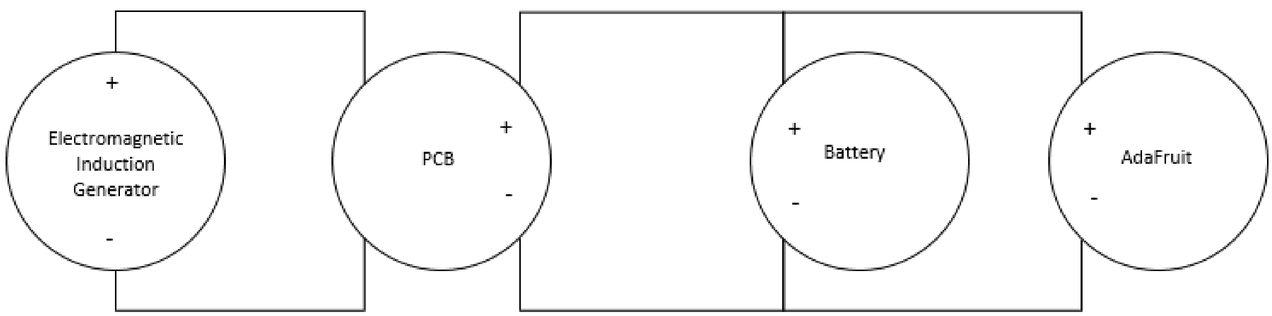

Figure 4-5: Summary of Electrical Connections

Chapter 5: Product Realization

Manufacturing Processes

The design team used a combination of 3D printing and machining (as well as other methods) to create parts that fit together perfectly in the main exterior case. These manufactured custom parts are listed below along with an explanation of the processes used to create them.

Exterior Casing:

The exterior casing shown in Figure 5-1 was created using filament deposition modeling, which is a very common 3D printing process. This type of manufacturing was necessary because of the high level of precision that this design requires. It would be nearly impossible to machine anything that fits these requirements, and creating a mold would be far too expensive for single use, so it was determined that 3D printing would be the best way to create a suitable case.

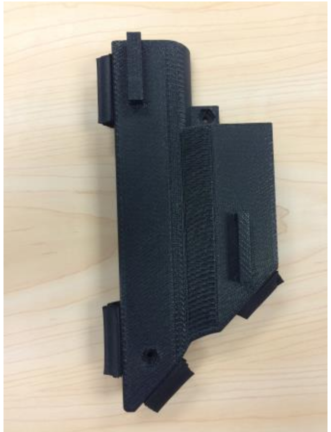

Figure 5-1: Final 3D Printed Exterior Casing

Interior Casing:

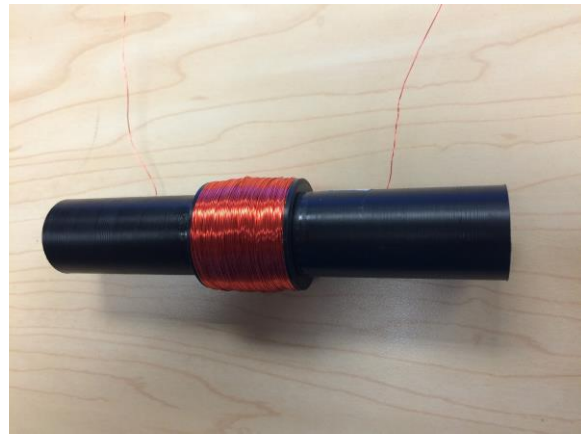

Figure 5-2: Final Machined Delrin Inner Casing

The interior casing shown here was created from delrin plastic using a lathe and a file. Delrin was used because it is relatively rigid, easily machinable, and incredibly slippery, which is very beneficial for the movement of the magnet. A simple cutting tool on a lathe was used to take the outer diameter of the cylinder stock down to size, and a boring tool was used to achieve the correct inner diameter. It was necessary that the inner diameter be nearly perfect because the magnet needs to move inside of it easily without getting stuck, and without moving too much from side to side. In order to achieve this, a thousandth of an inch tolerance was created on either side of the magnet.

Interior Casing Caps:

Figure 5-3: Final 3D Printed Inner Casing Caps

The interior casing caps, shown in Figure 5-3, were created using a powder deposition printer. This type of 3D printing was used because it is the most precise form of manufacturing that was available. Ideally, the exterior casing would have also been made using this process, however, the powder deposition printer on campus was broken for the final 7 weeks of this quarter, and online outlets had proved slow and unreliable in the past.

Copper Coil:

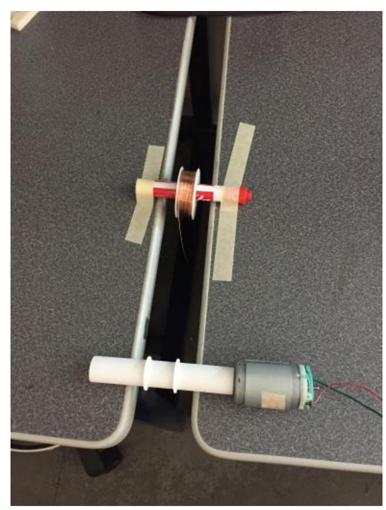

Figure 5-4: Servo Motor Setup

The design team used a small electric servo motor in order to coil the copper around the interior casing. The specific setup can be seen in Figure 5-4. Essentially by attaching the case to the shaft of the motor and spinning the motor, fine layers of copper wire can be quickly and accurately added to the case.

After the main components listed above were created and the remaining parts were purchased, the assembly of the device was a relatively simple process. All of the internal components fit snugly in a way that inhibited movement, which in turn allows for smooth and quiet operation.

Electrical Components:

The design team used a couple of different processes in order to assemble and manufacture all of the electrical components. Many of the components were purchased with little to no manufacturing needs including the battery and Adafruit chip and simply needed to be put together using electrical pins. As described in the "Description of Final Design" section, the printed circuit board was created using a software called Fritzing. After the board was successfully designed, the design was submitted to Fritzing. Fritzing first

collects, designs and produces many PCBs together on one large PCB. The boards are then manufactured by a professional board house here Berlin and shipped globally. After the PCB was received, all of the electrical components were soldered onto the board and the Texas Instruments BQ25504 was installed using solder paste. The final PCB is shown in Figure 5-5. All of the electrical components were then connected together using pins and the circuit was complete.

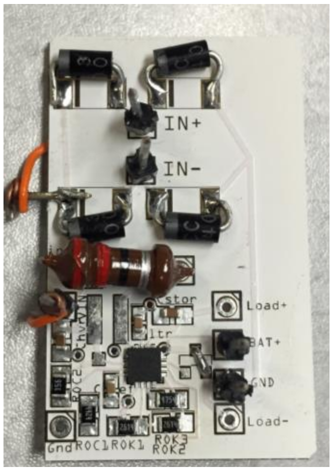

Figure 5-5: Final PCB

Cost Breakdown/Bill of Materials

A complete bill of materials (BOM) was created and can be found in Appendix D. The purpose of the BOM is to visually display the different components and assemblies that make of the Pedl e-. The bill of materials displays the components that make up the larger subassemblies (exterior casing, inner casing, magnet, and electrical) and how these all connect to make up the final assembly. These assemblies have been broken down into individual parts and a BOM cost breakdown is displayed below in Figure 5-6. Complete vendor information and pricing for each items can also be found in Appendix D-2 and D-3. As mentioned in the previous section, the assembly only consists of 27 parts which is a benefit in that each part can be easily exchanged if needed. The costs that are shown reflect the cost of a single prototype and parts if purchased individually. The parts that do not have a cost were taken from previous products and the costs are therefore negligible. The cost of a single prototype is relatively high ($198.92), especially for someone in the developing world, but mass manufacturing and bulk ordering parts would bring this cost down considerably. For example, both the exterior and inner casings are being 3D printed which is a fairly expensive manufacturing process. The cost of the casings alone is $88.00 and this is for a single assembly. Mass producing the casing would require injection molding which would significantly lower the cost/unit and, with the other assumptions, reach a price point that is attainable for the developing world around $50.00.

Bill of Materials				
Part Number	Part Name	Quantity	Description	Cost
100	Exterior Casing	1	3D Printed Casing with unthreaded holes for screws	$ 80.00
101	Interior Casing	1	Machined Delrin Plastic Cylinder	$ 8.00
102	Interior Casing Cap	2	3D Printed ABS Cap	$ 4.00
103	Magnet	1	1" T, 3/4" OD, 1/9" ID Neodymium Magnet, 54.3 g	$ 3.08
104	Magnet Assembly Nut	2	Brass Acorn Nut 4-40, 1/4" W, 1/4" H	$ 0.32
105	Magnet Assembly Screw	1	1 1/4" long, .106" dia, Brass Screw	$ -
106	Magnet Assembly Washer	1	ABS Plastic Washer w/ Spring Fitting	$ -
107	Inner Assembly Washer	1	ABS Plastic Washer w/ Spring Fitting	$ -
108	Inner Casing Cap Screws	2	#5-40 x 3/8 in. Machine Screws	$ 0.50
109	Inner Casing Cap Nut	2	5-40 Thread Size, 5/16" W, 7/64" H, Steel Hex Nut	$ 0.30
110	Spring	1	2" Conical Compression Spring (k=11.35 lbs/in.)	$ 6.00
111	Copper Wire	1	2000 turns of 30 gauge copper wire	$ 7.00
112	PCB	1	Custom Printed PCB	$ 15.96
113	PCB Components	1	All electrical components used on PCB	$ 36.72
114	Adafruit PowerBoose 500 Basic			
115	Battery	1	Li-Ion 18650 3.7V 5200mAh Cell	$ 19.99
116	Screws	2	Steel Pan Head Phillips Screw (4-40 Thread, 5/16")	$ 4.20
117	Nuts	2	Zinc Plated Steel Narrow Hex Nut (4-40, 1/16")	$ 2.36
118	Straps	1	Camco 42503 12" Awning Straps	$ 4.19
119	Rubber Stopper	2	Rubber Feet, 1/4" H x 1/2" D	$ 1.80
120	Rubber Pad	1	.75" wide, .125" thick neoprenes strip with adhesive	$ 4.50
			Total:	**$198.92**

Figure 5-6: Complete Bill of Materials

Final Prototype

The final iteration of this project is almost exactly what was planned by the design team. It did not fit all of the requirements given to us by the sponsor, but from the beginning it was understood that some of the criteria would simply not be met. The technology is sound, and the induction component is very much capable of charging a battery. As the device is now it would not be an effective method of charging, further development would be required to create something that meets all of the requirements set by the sponsor. One specific recommendation to future teams that work on this project, is to print a case that keeps the magnet farther away from the battery. The current iteration holds the two close together which inhibits axial movement of the magnet by causing increased friction between the magnet and the inner casing. Because this is a project that requires electrical components, it is very necessary to ensure that the magnet does not interfere with or harm any surrounding parts. Realistically, it would only take one more iteration to produce a product that would work in the manner that the design team intended. That being said the progress made over the past three quarters is satisfactory.

Chapter 6: Design Verification

FMEA

The design team incorporated a Failure Modes Effect Analysis (FMEA) during the design of the Pedl e- This analysis was helpful in identifying areas of the product that effect the customer most, how likely these events are to occur, and how difficult these events are to detect. A severity, occurrence, and detection rating was given (1-10) to each potential failure mode of each subsystem of the design. These rating were then multiplied to develop a risk priority number. Appendix F shows a table of the FMEA analysis as well as possible recommendations. After this process was applied to each potential failure mode, the design team chose the RPN numbers that were high, relative to the whole, and brainstormed to determine if there were any recommended controls or redesigns that could be implemented to reduce the RPN.

The Velcro straps were first evaluated due to their high severity level and RPN. The straps could loosen or break while on the bicycle and this could result in a loss or breaking of the device. In order to decrease the occurrence of this failure, we have decided to use new straps that have rubber on the portion that touches the device in order to create more friction and less likelihood for loosening.

The nuts in the nut and bolt assembly were the next item of inspection. The nuts that were being used were standard nuts, but due to the vibrations that the device will endure, there is a chance that these nuts could loosen during riding. However, after testing, it was found that the nuts that were chosen were very suitable and worked for this particular product.

These were the two design changes that were discussed using the FMEA analysis and this analysis also led the design team to begin developing test plans for the entire system.

Test Descriptions and Results

In order to test each iteration of the product, biking and durability analysis were performed for product verification. Bike testing included riding on rough terrain for different periods of time and recording the amount of energy harvested by the device. Durability testing will include a water test, a drop test, a particle test, vibration tolerance test, attachment test, and a magnetic clearance test. The design team will also test bike transfer time, weight, USB output compatibility, and charge rate of the device. All of these tests will be verified thorough physical and electrical inspection to guarantee that the final iteration can hold up to the most extreme outdoor environments. The tests were developed with the help of the project requirement specifications as well as an FMEA that was performed on each subassembly of the device. The detailed test descriptions for each of the tests listed above is included in Appendix G. Some of the tests could not be performed because of the problem explained early in the final prototype subsection. As described, the magnet and battery fit too close together in the exterior casing and this caused increased friction of the magnet travelling up and down the inner casing. Because of this unexpected occurrence, some of the tests were not performed due to the compatibility and safety issues involved.

Test one (which was the weight test) was performed using a mechanical scale which can be seen in Figure 6-1. All of the components were weighed together a number of times and then averaged to ensure that an accurate result was found. The final mass of the device was found to be 298 grams which is barely within the intended parameters, and is still greater than ideal. A smaller battery and or magnet would be required to lower this weight.

Figure 6-1: Mechanical Scale Used for Weight Test

Test two was performed by attaching the device to a bike and timing the speed at which one could comfortably transfer the device to another bike. By using the Velcro straps the device could be easily transferred in under 30 seconds. Some bikes were more difficult to attach to than others simply due to the shape and placement of different components, so the average transfer time found was 34 seconds.

The third test was the USB compatibility test. In order to complete this test multiple different USB cables from different devices were plugged into the device. Every device fit easily into the USB port which is perfect for the intended use. Figure 6-2 shows the USB compatibility test for an iPhone USB cable.

Figure 6-2: USB Compatibility Test Example

Test four was only partially done which is why NA is shown in the results section in Appendix G. The attachment point of the outer case was tested by splashing a direct stream of water on it. It was found to be resistant to water, however a sealing gasket could definitely improve the water resistance. The reason that the entire device was not tested was because the USB port is open and water would damage the interior electrical components.

Test five was also not entirely completed. The attachment between the two exterior casing parts is entirely particle resistant, however, as mentioned before, the USB port of this prototype is still open to the environment.

Test six was the vibration tolerance test which was performed by attaching an accelerometer to the device and shaking it manually until it reached 30 G acceleration. This method was used because it was more effective in allowing for testing on the three main axes, and because the vibration tables are not as capable of recreating the random vertical movement of a bike.

Test seven was done by shaking the inductor component for 10 minutes which transferred a certain amount of charge to the battery. Then, that charge was input to a cell phone and the charge rate from the battery was calculated and recorded. This test was completed and satisfied the desired parameters.

Test eight was the noise test and it was performed in the library where is it silent, but regular ambient noise still exists. By using a device that measures decibels of an environment, sound tests were done when the device was shaking and when the device was not shaking. Even when the device was close to the noise reader, the ambient noise only increased by about 10 decibels (from 50 to 60).

Test nine was performed using the first iteration of the exterior casing. The case was filled with weight until it reached a similar mass to the actual device (to ensure that impact force would be similar). Then the device was dropped from varying heights. There were some small scratches on the exterior casing, but it held up and was not cracked or deformed after the testing even when it landed on a corner.

The tenth test was done to see how long it took to fully charge the main battery. Testing was done to charge the battery, but ultimately these results were inconclusive due to the nonlinear charging nature of lithium ion batteries.

The eleventh test was performed to ensure that the clearance of the inner casing was enough to allow for easy and smooth sliding by the magnet. This was tested by shaking the inductor up and down and feeling possible resistance. After shaking, a .01 inch clearance around the entire circumference was determined to be perfect.

Finally, the twelfth test was done to ensure that the device would stay on the bike during riding. The device was attached to a bike (as seen in Figure 6-3) which was then ridden through rough terrain. The Velcro straps, combined with the sticky rubber pads was enough to secure the device to the bike.

Figure 6-3: Attachment Testing Setup

Chapter 7: Conclusions and Recommendations

The design team has performed the research, background, and supporting analysis to follow through with the request of the sponsor Lynne Slivovsky. The design process, decisions, and calculations have been highlighted in this report to identify how the Pedl team solved the problem that project VeloElectric presents. The project management plan helped to guide the team through the school year to finish the project on time and deliver a prototype for the sponsor by spring of 2015. There are a few recommendations that the design team believes would improve the final product.

The exterior casing was initially designed in a way that kept all components tightly packed which worked well for durability, but the problem was that the magnet was too close to the battery and caused an increase in friction which inhibited the magnets motion. The exterior casing should be redesigned so that the battery sits farther away from the magnet while still employing a compact design. The USB port in the exterior casing is another area of improvement. The waterproof and particle proof specifications were unable to be met because a suitable design was not developed that would allow for the entire device to have a complete seal. A twist-on cap was a design that was developed late in the project that would adequately seal the USB input from water and dust to meet the required specifications. Another water and particle proofing addition was a rubber sealant that would line the inside of the inner casing which would greatly help protect the electrical components. On the electrical side of the design, the design team would recommend upgrading the components to allow for the user to have a better knowledge of their overall battery percentage. The Adafruit PowerBoost 500 basic has a low battery LED indicator integrated into the circuit, but it only allows the user to know when their battery is very low and not when it is fully charged.

Further additions and reconfigurations mentioned above could greatly improve the device. The design team is happy with the progress that has been made over the course of this project and is hopeful that this prototype can act as a significant step towards the creation of a final product that could reach a wide range of users.

Appendix A: References

[1] Delcourt, David. "Siva Cycle | Bicycle Power Your USB Devices." *Bicycle Power Your USB Devices*. 18 Aug. 2011. Web. 16 Oct. 2014.

[2] Quick, Darren. "Nokia's Bicycle Charger Kit a Stroke of Genius." *Nokia's Bicycle Charger Kit a Stroke of Genius*. Gizmag, 4 June 2010. Web. 23 Oct. 2014. <http://www.gizmag.com/nokia-bicycle-charger-kit/15312/>.

[3] Endo, Takahiro. Bicycle Hub Dynamo Assembly. Shimano, assignee. Patent US7048546 B2. 23 May 2006.

[4] Vasic, Dejan. "Self-Powered Piezoelectric Energy Harvester for Bicycle." IEEE, 13 Nov. 2013. Web. 23 Oct. 2014. <http://ieeexplore.ieee.org/xpls/abs_all.jsp?arnumber=6699414&tag=1>.

[5] Woodford, Chris. (2009) Piezoelectricity. <http://www.explainthatstuff.com/piezoelectricity.html.>

[6] Shastry, Tejas. "AMPY: Power Your Devices from Your Motion." *Kickstarter*. Web. 09 Jan. 2015.

[7] LeMieux, Aaron. "NPower PEG Kinetic Energy Charger and Interview with Inventor Aaron Lemieux | Section Hikers Backpacking Blog." *Section Hikers Backpacking Blog*. 09 Oct. 2012. Web. 06 Jan. 2015.

[8] "IP Code." *Wikipedia*.,16 Oct. 2014. Web. 23 Oct. 2014. <http://en.wikipedia.org/wiki/IP_Code>.

[9] IEC 60529, "Degrees of Pretection Provided by Enclosures (IP Codes)," Ed. 2.1 (Geneva: International Electrotechnical Commision, 2011

[10] "October 16th Requirements Meeting." Interview by Lynne Slivovsky. *Bonderson Engineering Projects Center* 16 Oct. 2014

[11] Peacock, Craig. "Connectors." *USB in a NutShell*. Beyond Logic, 17 Sept. 2010. Web. 01 Nov. 2014.

[12] "All-Battery.com: AT: Tenergy Li-Ion 18650 3.7V 5200mAh Stick Rechargeable Battery Module." *All-Battery.com*. Web. 16 Jan. 2015.

[13] Grimm, Todd. "FUSED DEPOSITION MODELLING: A TECHNOLOGY EVALUATION." *Time-Compression Technologies*. RPMA, 13 May 2003.

[14] Texas Instruments Incorporated. Ultra Low Power Boost Converter with Battery Management for Energy Harvester App (Rev. B) (n.d.): n. pag. Web. <http://www.ti.com/lit/ds/symlink/bq25504.pdf>.

[15] Tenergy Corporation. "Energy Li-Ion 18650 3.7V 5200mAh Rechargeable PCB Protected Battery Pack." <http://www.tenergy.com/31001>.

[16] Adafruit Industries. "PowerBoost 500 Basic - 5V USB Boost @ 500mA from 1.8V+." <http://www.adafruit.com/products/1903>.

Appendix B: QFD and Decision Matrices

B-1: QFD

Customer (Step #1) Requirements (Whats)

Customer Requirements (Step #2)

Customer Requirements	Weighting (1 to 5)	> 5000mAh	USB Output (5V)	< 100g	Transferable in 5 minutes	IP 3 Waterproof Rating	IP 4 Solids Rating	Can Experience up to 15G's	Charge Rate >= 2.5 Watts	No additional angular resistance	< 20 dB	Manufacturability (seconds)									Siva Cycle Atom	Hub Dynamo	
Portable	3			6	9																		
Water Proof	4					9						3											
Light Weight	2			9																			
Charge 3 devices	5	9	9																				
Durable	5						9	9															
No Resistance to Pedaling	5									9													
Nice Looking	1					3	3					3											
Small Size	2			3	6																		
Fully Charge Battery in 6-15 hours	4	6	3						9														
Vibration	4							9			6												
Quiet	4										9												
Usable on All Bicycles	4				3			3															
																					Top Contender	Inhibits Wheel	
Units																							
Targets																							
Benchmark #1																							
Benchmark #2																							
Importance Scoring		69	57	42	51	39	48	93	36	45	60	15	0	0	0	0	0	0	0	0			
Importance Rating (%)		74	61	45	55	42	52	100	39	48	65	16	0	0	0	0	0	0	0	0			

● = 9 Srong Correlation

○ = 3 Medium Correlation

Δ = 1 Small Correlation

B-2: Housing Decision Matrix

		Siva Cycle Atom	Weight (grams)	Noise (dB)	Durability (max G force)	Aesthetically Pleasing	Manufacturability (seconds)		Weighted Sum +	Weighted Sum -	Weighted Sum S	Total Score
Specification Weight			20	15	35	5	25					
Housing	3-D Printed Plastic	S	S	S	S	S	+		25	0	75	48
	Aluminum		-	S	+	+	-		40	45	15	-1
	Rubber		-	+	-	-	-		15	85	0	-70

B-3: Attachment Decision Matrix

		Siva Cycle Atom	Weight (grams)	Transfer Time (seconds)	Durability (max G force)	Aesthetically Pleasing	Manufacturability (seconds)		Weighted Sum +	Weighted Sum -	Weighted Sum S	Total Score
Specification Weight			5	30	30	20	15					
Attachment	Zip-Ties	S	+	+	-	-	+		50	50	0	0
	Velcro Straps		+	+	S	S	+		50	0	50	65
	Bungie Cord		-	+	-	-	+		45	55	0	-10
	Mounting Bracket (Screws)		S	+	S	S	-		30	15	55	32

B-4: Power Generation Decision Matrix

		Siva Cycle Atom	Weight (grams)	Transfer Time (seconds)	Mechanical Resistance to Pedaling (Nm)	Noise (dB)	Size (in x in x in)	Durability (max G force)	Manufacturability (seconds)	Can be incorporated into all bike forks	Weighted Sum +	Weighted Sum -	Weighted Sum S	Total Score
Specification Weight			10	15	20	5	5	5	10	30				
Power Generation	Electromagnetic Induction (Free Magnet)	S	-	+	+	-	+	+	+	+	85	15	0	70
	Electromagnetic Induction (Fixed Magnet)		-	S	+	+	+	+	S	-	35	40	25	3

B-5: Power Storage Decision Matrix

		Siva Cycle Atom	Weight (grams)	Charge Rate of Battery (W)	Battery Capacity (mAh)	Size (in x in x in)	Manufacturability (seconds)		Weighted Sum +	Weighted Sum -	Weighted Sum S	Total Score
Specification Weight			5	20	40	15	20					
Power Storage	Capacitor	S	-	-	+	S	S		40	25	35	26
	Battery		-	-	+	S	S		40	25	35	26
	Capacitor and Battery		-	+	+	S	S		60	5	35	66

B-6: Summary of Decisions

Subsystem	Decision
Housing	3-D Printed Plastic
Attachment	Velcro Straps
Power Generation	Electromagnetic Induction (Free Magnet)
Power Storage	Capacitor and Battery

Appendix C: Final Mechanical Drawings and Electrical Schematics

C-1: 3D Model of Exterior Casing Bottom

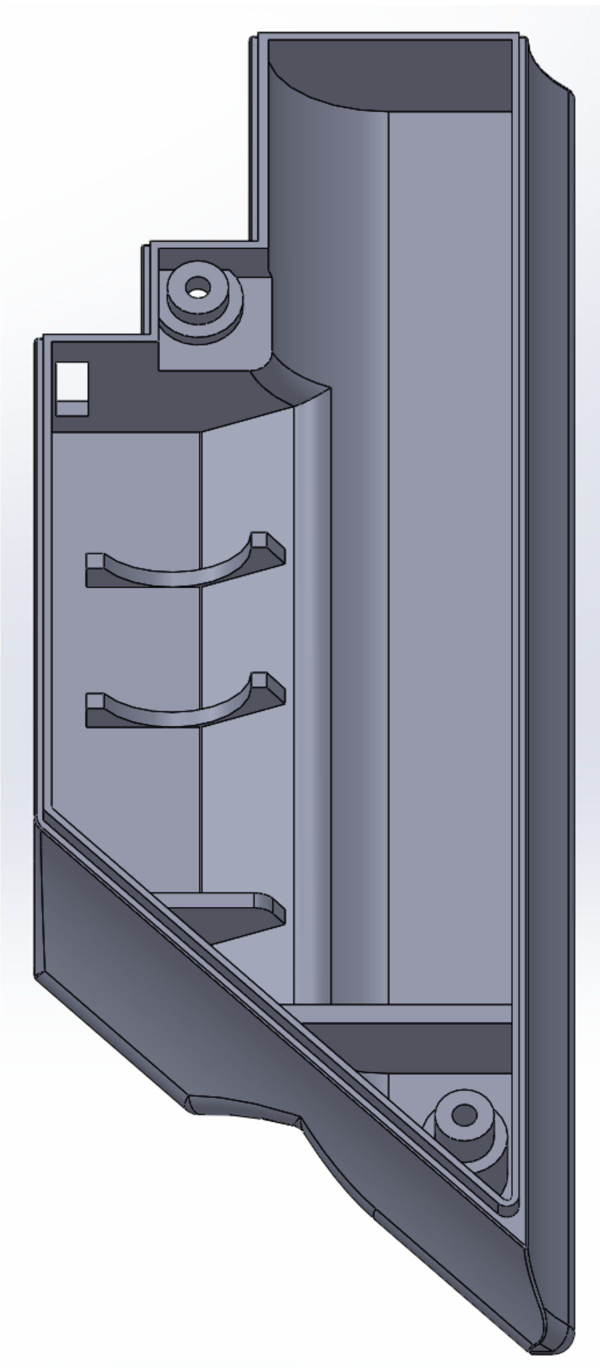

C-2: 3D Model of Exterior Casing Top

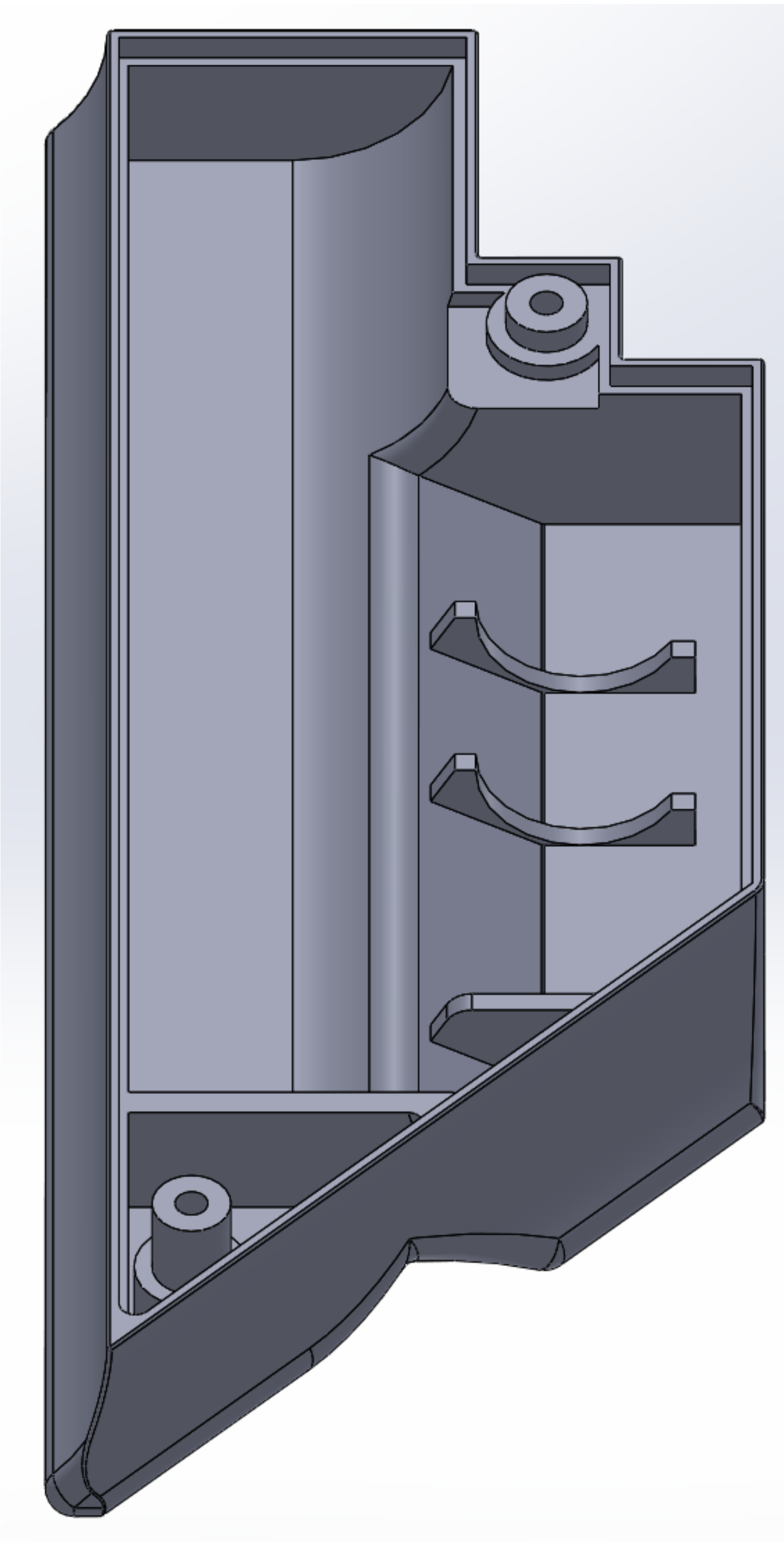

C-3: 3D Model Inner Casing

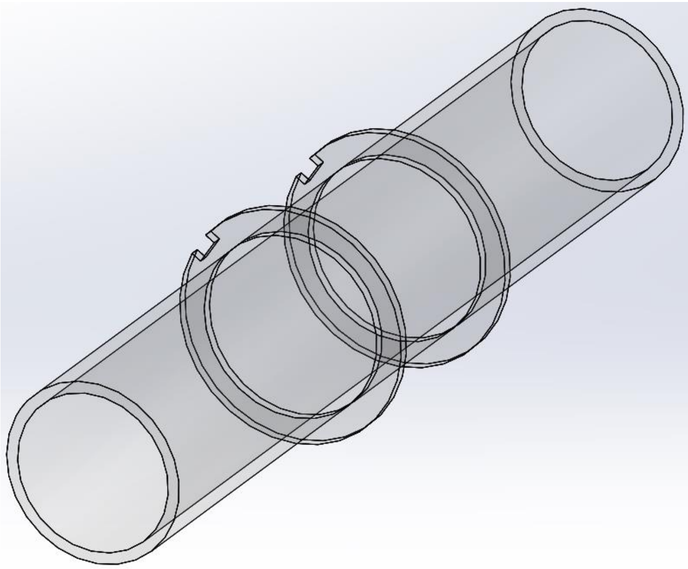

C-4: 3D Model of Inner Casing Cap

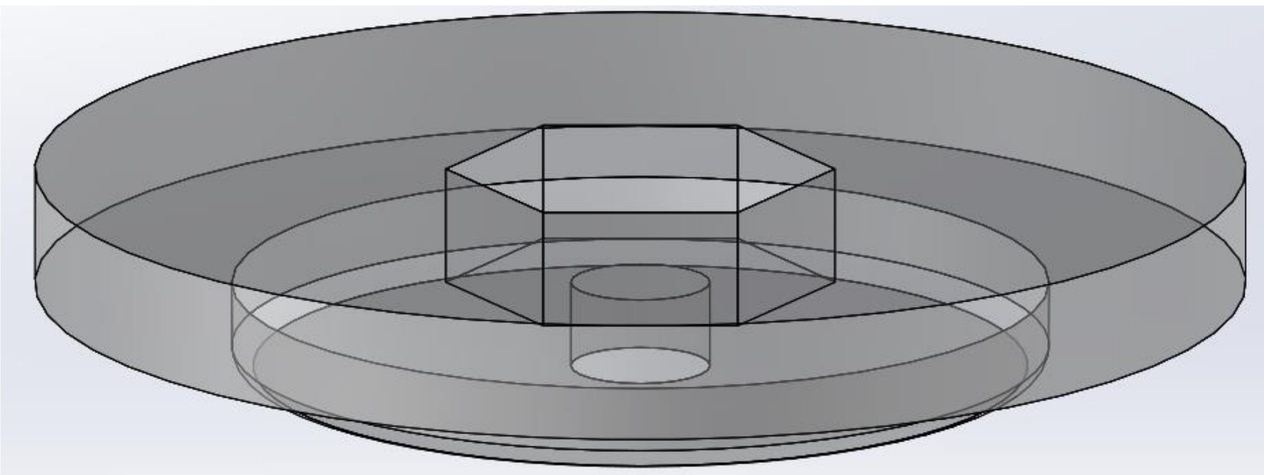

C-5: Exterior Casing Top Part Drawing

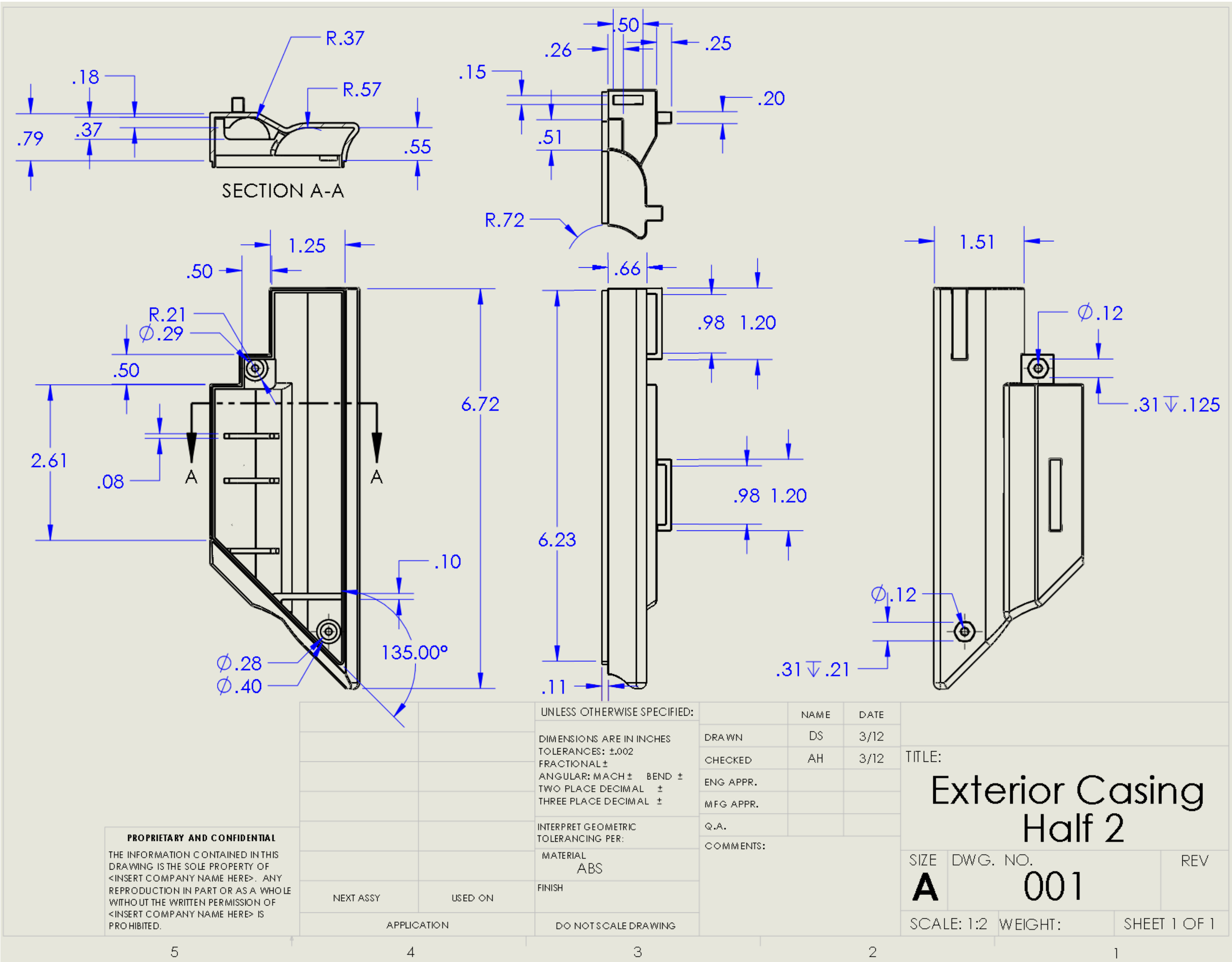

C-6: Exterior Casing Bottom Part Drawing

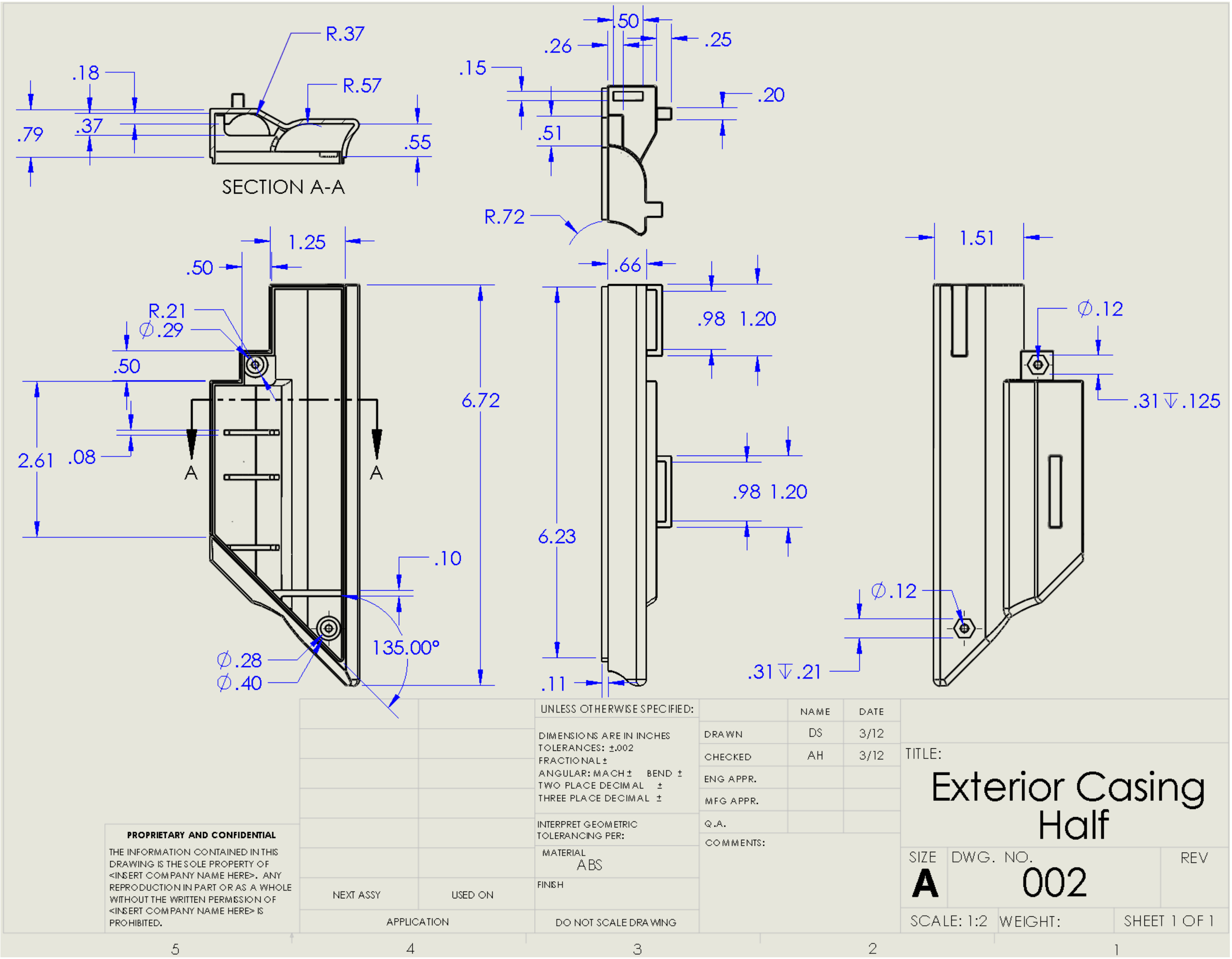

C-7: Inner Casing Part Drawing

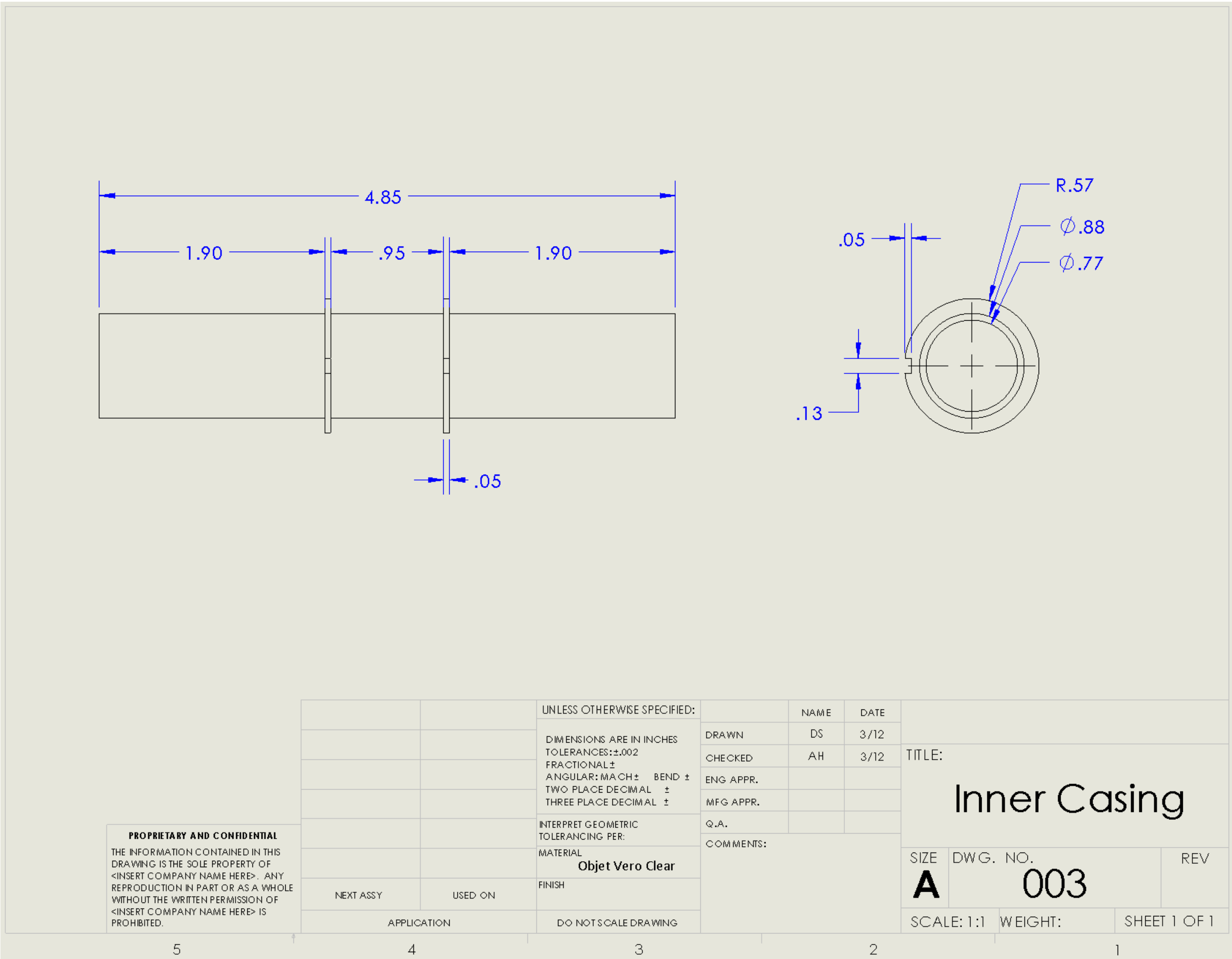

C-8: Inner Cap Part Drawing

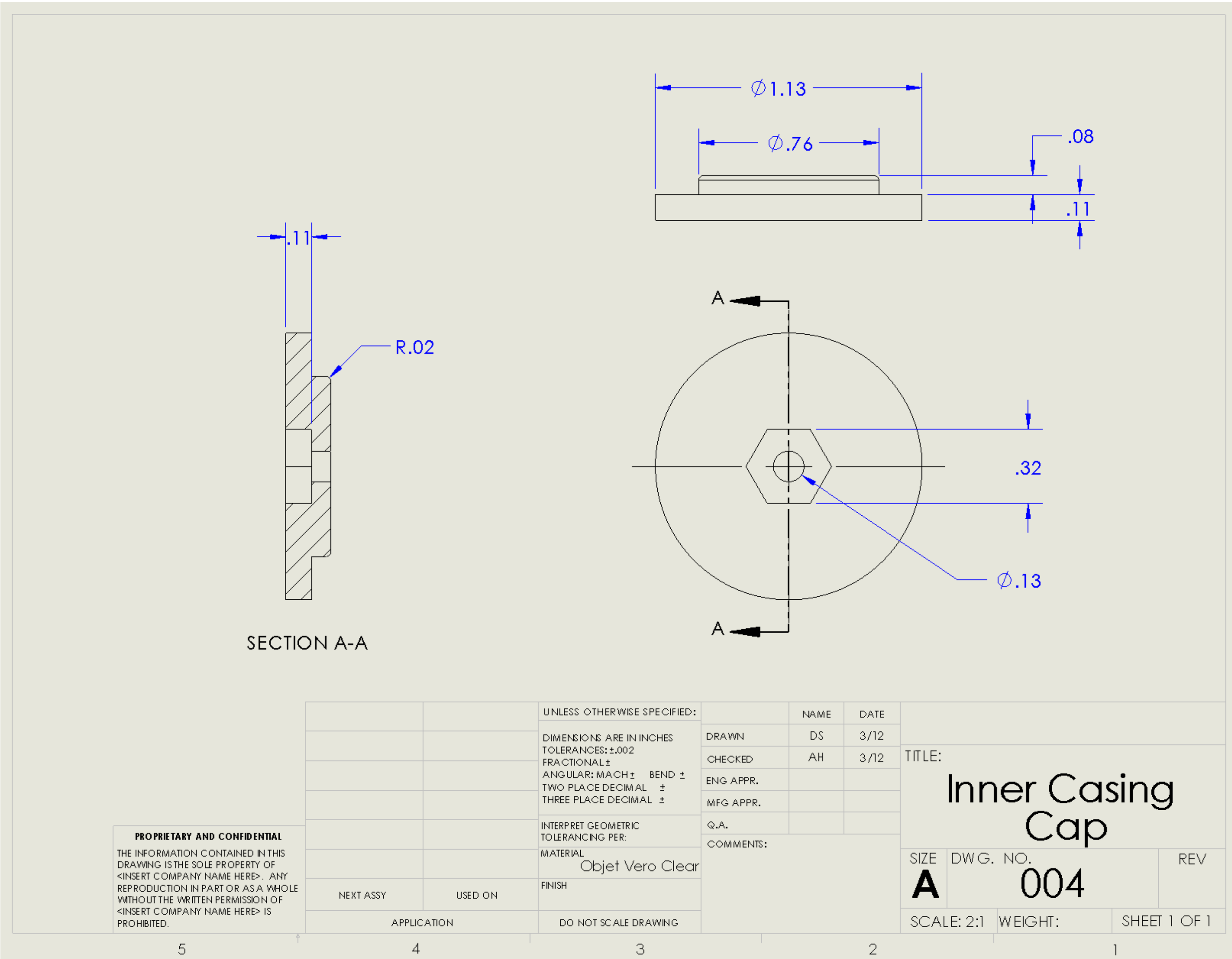

C-9: PSpice Final Circuit Schematic

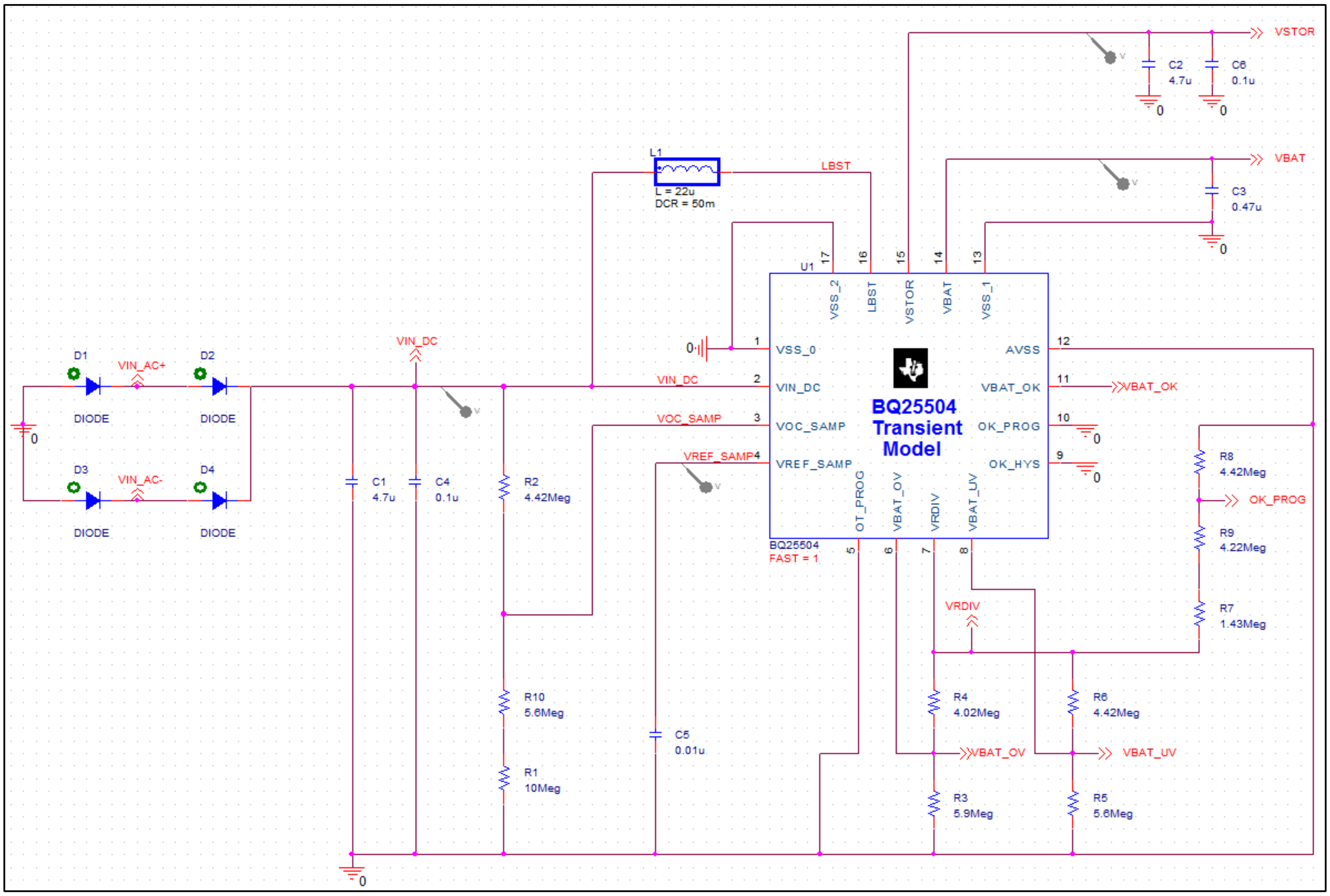

C-10: Fritzing PCB Final Design

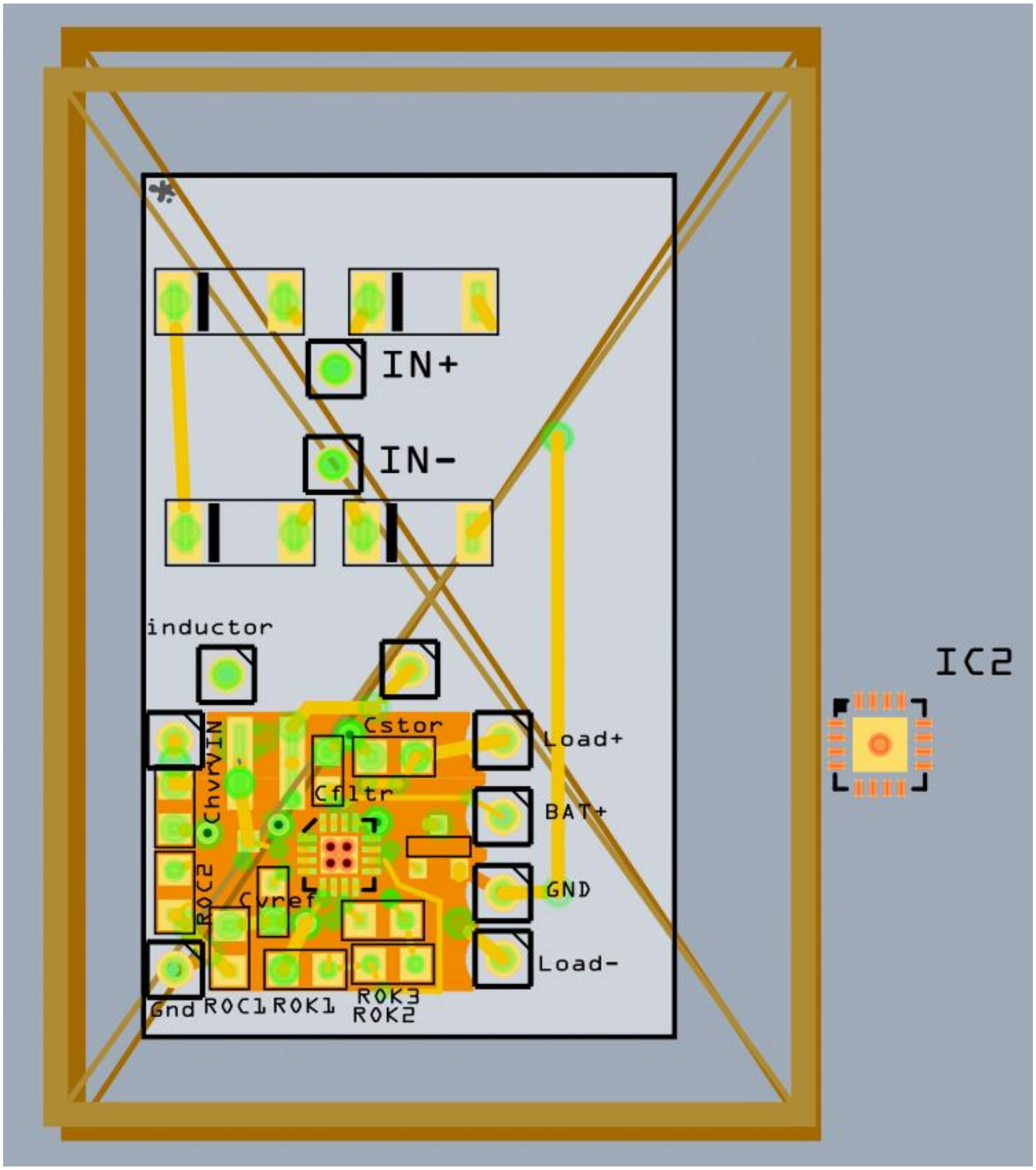

Appendix D: Bill of Materials and Vendor Information

D-1: Bill of Materials Organization Chart

D-2: Bill of Materials Cost Breakdown

Bill of Materials

Part Number	Part Name	Quantity	Description	Cost
100	Exterior Casing	1	3D Printed Casing with unthreaded holes for screws	$ 80.00
101	Interior Casing	1	Machined Delrin Plastic Cylinder	$ 8.00
102	Interior Casing Cap	2	3D Printed ABS Cap	$ 4.00
103	Magnet	1	1" T, 3/4" OD, 1/9" ID Neodymium Magnet, 54.3 g	$ 3.08
104	Magnet Assembly Nut	2	Brass Acorn Nut 4-40, 1/4" W, 1/4" H	$ 0.32
105	Magnet Assembly Screw	1	1 1/4" long, .106" dia, Brass Screw	$ -
106	Magnet Assembly Washer	1	ABS Plastic Washer w/ Spring Fitting	$ -
107	Inner Assembly Washer	1	ABS Plastic Washer w/ Spring Fitting	$ -
108	Inner Casing Cap Screws	2	#5-40 x 3/8 in. Machine Screws	$ 0.50
109	Inner Casing Cap Nut	2	5-40 Thread Size, 5/16" W, 7/64" H, Steel Hex Nut	$ 0.30
110	Spring	1	2" Conical Compression Spring (k=11.35 lbs/in.)	$ 6.00
111	Copper Wire	1	2000 turns of 30 gauge copper wire	$ 7.00
112	PCB	1	Custom Printed PCB	$ 15.96
113	PCB Components	1	All electrical components used on PCB	$ 36.72
114	Adafruit PowerBoose 500 Basic			
115	Battery	1	Li-Ion 18650 3.7V 5200mAh Cell	$ 19.99
116	Screws	2	Steel Pan Head Phillips Screw (4-40 Thread, 5/16")	$ 4.20
117	Nuts	2	Zinc Plated Steel Narrow Hex Nut (4-40, 1/16")	$ 2.36
118	Straps	1	Camco 42503 12" Awning Straps	$ 4.19
119	Rubber Stopper	2	Rubber Feet, 1/4" H x 1/2" D	$ 1.80
120	Rubber Pad	1	.75" wide, .125" thick neoprenes strip with adhesive	$ 4.50
			Total:	**$198.92**

D-3: Vendor Specifications and Data Sheets

Magnet

1" thick, 3/4" outer diameter, 1/9" inner diameter Neodymium Magnet

Pull Force: 36.6 lbs

Source: http://www.kjmagnetics.com/

Camco Straps
http://www.amazon.com/Camco-42503-12-Awning-Straps/dp/B000EDOSSI/ref=sr_1_4?ie=UTF8&qid=1423551206&sr=8-4&keywords=velcro+straps

Source: http://www.amazon.com/

Length: 12”
Width: 1”

Rubber Stopper:
http://www.amazon.com/AmplifiedParts-Rubber-Feet-Pkg/dp/B0062P2KHS/ref=pd_sim_hi_2?ie=UTF8&refRID=08EH40SC8CWMP34EHG75

- **Rubber Feet, 1/4" H x 1/2" D**

Source: http://www.amazon.com/

McMaster-Carr:

Magnetic Copper Wire:
Description

- 785 feet long
- 30 gauge

Magnet Assembly Nut:

Inch/Metric	Inch Sizes
Thread Size	4-40
Width	1/4"
Height	1/4"
Minimum Thread Depth	3/32"
Additional Specifications	Brass
RoHS	Compliant

Source: http://www.mcmaster.com/

Inner Casing/Exterior Casing Cap Nuts:

Thread Size	5-40
Width	5/16"
Height	7/64"
Additional Specifications	Zinc-Plated Steel
RoHS	Not Compliant

Source: http://www.mcmaster.com/

Exterior Casing Screw 1:

Length	1"
Additional Specifications	18-8 Stainless Steel 5-40—#2 Drive
RoHS	Compliant

Source: http://www.mcmaster.com/

Exterior Casing Screw 2:

Length	3/8"
Additional Specifications	18-8 Stainless Steel 5-40—#2 Drive
RoHS	Compliant

Source: http://www.mcmaster.com/

Rubber Pads:

- Super-Soft Neoprene Rubber
- 6"x6"
- 1/8" thick

Lee Spring's:
http://www.leespring.com/product_spec.asp?partnum=LP029M06S316&springType=C&subType=

Specification	
Part Number	LP 029M 06 S316
Outside Diameter	0.660 in
Hole Diameter	0.687 in
Wire Diameter	0.029 in
Load At Solid Length	0.927 lb
Free Length	2.000 in
Rate	0.53 lb/in
Solid Length	0.277 in
Rod Diameter	0.563 in
Number of Coils	6.5
Total Coils	8.5
Finish	ULTRASONICALLY PASSIVATE WITH CITRIC ACID FOR 10 MINS AT 131 DEG F
Material	SS316
Click Here for Tolerances and Engineering Notes	

Home Depot:
http://www.homedepot.com/p/Unbranded-5-40-x-3-8-in-Phillips-Fillister-Head-Machine-Screws-3-Pack-97358/203538502?N=5yc1vZc27iZ1z0sfyi
Inner Casing Cap Screws

Source: http://www.homedepot.com/

- Zinc-plated finish
- #5-40 x 3/8 in.
- Fillister head phillips drive

Cal Poly 3D Printing Services:

Exterior Casing Top:

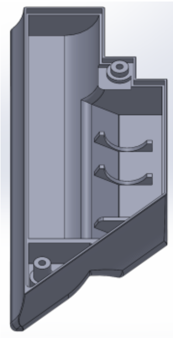

Exterior Casing Bottom:

Sculpteo:
https://www.sculpteo.com/en/account/login/?next=/en/upload_design/3D/%3Faffiliate%3D3dprintingpricecheck

Inner Casing Caps:

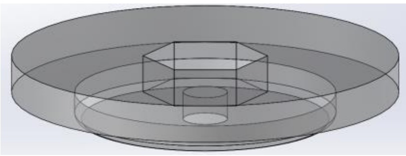

<u>All-Battery</u>:
http://www.all-battery.com/li-ion1865037v5200mahrechargeablebatterypcbmodulewithbareleads.aspx

Source: http://www.all-battery.com/

<u>Fritzing:</u>
http://fritzing.org

Custom Printed Circuit Board:

<u>Adafruit</u>
https://www.adafruit.com/products/1903

Adafruit PowerBoost 500 Basic

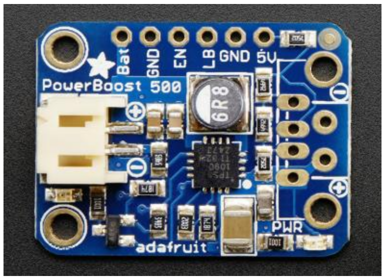

Appendix E: Detailed Supporting Analysis

E-1: Mechanical Spring Calculations

Spring Calcs

Travel Distance: $x = 1.7\,in = 0.04318\,m$

$mass_{magnet}$: $1.92\,oz = 54.43\,g$

Total Mass $= m_{magnet} + m_{washers} + m_{screw/nuts} = 68$ grams

Governing Eqns: $F = kx = ma$

$$F = k(0.04318\,m) = (0.068\,kg)(5g)(9.8\,m/s^2)$$

$$k = 77.12\,N/m$$

$$k = 77.12\,N/m \cdot \frac{1\,lbf}{4.45\,N} \cdot \frac{1\,m}{39.37\,in} = \underline{0.44\,lbf/in}$$

Resting Deflection of Spring

$$\Delta x = \frac{m \cdot g}{k} = \frac{0.068\,kg \cdot 9.8\,m/s^2}{77.12\,N/m} = 0.008641\,m = 0.34\,in$$

Desired Length: $2\,in - 0.34\,in = 1.66\,in$

To cope with 5g's need

$$\boxed{k = 0.44\,\frac{lbf}{in} \qquad L = 1.66\,in}$$

E-2: Mechanical Straps Calculations

STRAPS

Assume/given

$m_{e^-} = 250\,\text{grams} = 0.25\,\text{Kg}$

$\mu_s = 0.9$ from engineering toolbox

$a_{max} = 30g = 294\,\frac{m}{s^2}$

Find

- strap force
  - normal force between device and fork

$f = F_{straps} \cdot \mu_s$

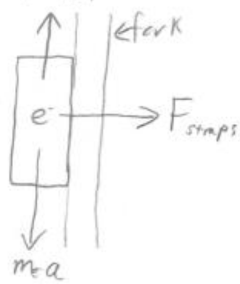

Analysis

Want

$f = m_{e^-} \cdot a$

Y direction:

$m_{e^-} \cdot a = 0.25\,\text{Kg} \cdot 294\,\frac{m}{s^2} = \underline{73.5\,N}$

$f = 73.5\,N = F_{straps} \cdot \mu_s$

$$F_{straps} = \frac{73.5}{0.9} = 81.\bar{6}\,N$$

Top View

$\theta \approx 20°$

$81.\bar{6}\,N = \underline{18.375\,\text{lbs}}$ = normal force

actual Tension in the strap

$$T = \frac{18.375\,\text{lbs}}{2 \cdot \cos\theta} = 9.777\,\text{lbs}$$

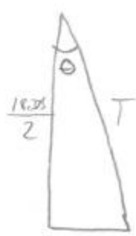

$\cos\theta = \frac{18.375}{2T}$

E-3: Casing Stress Calculations

Case Stress

m_{mag} = 64 grams

max accel: 30g = a

Travel Distance: x = 5.0cm

Rubber Pad Thickness = 0.25 in

Cross Sectional Area of Casing:

$A_c = 0.584 \, in^2$

$= 0.00037677 m^2$

Analysis

Finding Max Velocity (assuming negligible spring force)

$V_{max} = \sqrt{V_i^2 + 2(9.8m/s^2)(30g)(0.05m)} = 5.422 m/s$

Assuming Magnet Decellerates through .2 inches of pad

$0.2 in = 0.005 m$

$0 = V_{final} = \sqrt{5.422 m/s + 2 a_{pad}(0.005)} \Rightarrow a_{pad} = -542.2 m/s^2$

Force on Bottom Case:

$F_c = |m_{mag} a_{pad}| = |0.064kg \cdot (-542.2 m/s^2)| = 33.616 N$

$\sigma_{max} = P/A = F_c/A_c = \frac{33.616N}{0.00037677m^2} = \boxed{89.2 kPa}$

Rapid Prototype ABS Properties: Tensile Strength = 22MPa - 33MPa

Depending on source

Safety Factor Range: $\frac{22MPa}{89.2 kPa} \leq SF \leq \frac{33MPa}{89.2kPa} \Rightarrow \boxed{224 \leq SF \leq 369.9}$

E-4: Electrical PCB Calculations

Lynne's Devices

Bike Computer: 700mAh · 5V = ~~3.5~~ 3300 Wh

SPOT: (4AAA): 4 · 750mAh · 1.2V = 3.6Wh

GPS: (2 AA) · 2 · (1300mAh) · 1.2V = 3.12 Wh

Phone: 1900mAh · 3.8V = 7.22Wh

Total: 17.44 Wh

Test:

Phone battery increase 3%

- 10 min shaking
- 2300 mAh bat
- 3.8V bat

2300mAh · 3.8V = 8.74Wh (capacity)

(3%)(8.74) = 262.2mWh

(262.2mWh)(3600sec/hr) = 943.92J in 10 min

(943.92 J)(6) = 5663.52 J/hr

(5663.52)(.7) = 3964.46 J/hr / 3600 = 1.10W

η

$\frac{17.44\text{Wh}}{1.10\text{W}} \approx$ 15.85 hr

close

* Buck Converter Efficiency: ~ estimate 90% *

* 20% efficiency loss in charger lithium-ion. *

Appendix F: FMEA Analysis

FAILURE MODE AND EFFECTS ANALYSIS

Item:	Pedl e-	Responsibility:	Team Pedl
Model:	Current	Prepared by:	Team Pedl
Core Team:	TJ Fox, Austin Hall, Danny Stohr		
FMEA number:			
Page :	1 of 1		
FMEA Date (Orig):	2/21/15	Rev:	1

Process Function	Potential Failure Mode	Potential Effect(s) of Failure	Sev	Class	Potential Cause(s)/ Mechanism(s) of Failure	Occur	Current Process Controls	Detec	RPN	Recommended Action(s)	Responsibility and Target Completion Date	Action Results: Actions Taken	Sev	Occ	Det	RPN
Velcro Strap	*Comes Undone/Loosen/ Breaks*	*Loss/Breaking of Device*	*10*		*Excessive Force, Poor Connection, Strap Breaks*	*5*	*High F.O.S, Manufacturer Trust, Length of Strap*	*4*	*200*	*Straps with rubber on inside to increase friction*			*10*	*3*	*4*	*120*
Rubber Pad	*Falls Off Device*	*Missing Components (Devices Still Functions Normally)*	*5*		*Extreme Heat, Poor Application of Adhesive, Poor Adhesive*	*2*	*Proper Adhesive Application from Design Team, Proper Adhesive Choice*	*4*	*40*							*0*
Screw/Nut	*Break*	*Integrity of Device*	*7*		*Extreme Force, Manufacturer Defect*	*1*	*Velcro Strap Keep Casing Closed*	*1*	*7*							*0*
	Unscrews	Integrity of Device	7		Poor Installation, Vibration of Bicycle	3	None	1	21	Replace nuts with seal nuts with rubber gaskets						0
Exterior Casing	Break	Failure of Device	10		Bicycle Crash	3	Material Properties of ABS, Drop Test of Final Design	1	30							0
	Severe Crack	Dust/Particles Enter Device, Break Circuit Board, Cause Short Circuits	7		Bicycle Crash, Tree Branch or Rock	3	Placement of Device, Properties of ABS	1	21							0
Spring	Detachment	Wrong Spring Constant, Decrease in Efficiency	4		Manufacturer Defect, Poor Attachment	2	Attachment to Inner Casing	8	64							0
	Plastic Deformation	Lower Spring Constant, Decreased Efficiency	3		Fatigue, Poor Design/Manufacturing	4	Known Accelerations, Clearly State Life Span of Spring	9	108							0
Rubber Stopper	Detachment	Noise, Decreased Efficiency, Integrity to Inner Casing	6		Poor Adhesive, Attachment	2	Formed Fit and Proper Sizing, Adhesion	4	48							0
Inner Casing	Reduced Efficiency, Possible Breaking of Interior Parts	Reduced Efficiency, Possible Breaking of Interior Parts	8		Bicycle Crash, Rubber Stopper Failure or Detachment, Excessive Force from Magnet	2	Rubber Stoppers, Few Moving Parts, Spring	6	96							0
Solder Joints	Failure in Power Generation	Failure in Power Generation	10		Poor Solder Joint, Excessive Force	1	Little Moving Parts, Quality Check of Solder Joints by Visual Inspection	6	60							0

Appendix G: Design Verification Plan and Report

G-1: Outline of Test Descriptions

TEST PLAN						TEST REPORT	
Item No	Specification	Test Description	Acceptance Criteria	Test Responsibility	Test Stage	TEST Test Result	NOTES
1	Weight (grams)	Scale, device, weight	100<x<300 grams	Danny/Austin	DV/PV	298 grams	
2	USB Output Compatible	In EE lab, test for 5V output, connect to device to ensure that charging occurs	Charging occurs and USB output is present	TJ	DV/PV	Yes	Compatible with USB
3	Bike Transfer Time	Describe in words out to put on device, time user putting on (multiple cycles)	<5 minutes	Danny/Austin	PV	34 seconds	Velcor makes for fast transfer.
4	Waterproof	Water splashed against the enclosure from any direction shall have no harmful effects.	No visible water on inside of device, i.e. no harm to inerts	Austin/Danny	PV	NA	Could not test with open USB port.
5	Particle Proof	Ingress of dust is not totally prevented, but dust shall not penetrate in a sufficient quantity to interfere with satisfactory operation of the apparatus or to impair safety.	Presence of dust on inside	Danny/Austin	PV	NA	Could not test with open USB port.
6	Vibration Tolerance	Using a shake table and/or use of data logger, test the external and internal components to confirm functionality at peak forces	Withstand 30G of Acceleration	Danny/Austin	DV/PV	Yes	Used acceleration data logger.
7	Charge Rate	Using resistor or similar load (cell phone, device with battery level) calculate the amount of current being pushed from the 5V USB output	2.5 Watts	TJ	DV/PV	2.5 Watts	
8	Noise While Riding	Use a sound meter and microphone to determine the amount of decibals that the device outputs while shaking by hand	<=20 dB	Danny/Austin		8 dB	Shaking until magnet hit rubber pads.
9	Drop Test	Drop of the device from a height of 3 feet onto different types of terrain including glass, concrete, dirt/gravel and assess the structural integrity of the device in each circumstance	Casing does not show noticable damage	Danny/Austin	DV/PV	No Significant Damage	Some scratching on concrete
10	Time to Fully Charge Battery	Place device on bicycle while the battery is completely discharged and ride for about 2 hours on trail. Come back to lab to determine if battery would become fully charged in 6-15 hours	6-15 hours	All	PV	NA	

G-2: Detailed Test Descriptions

Test 1: Weight Test

Determine: An accurate weight of the final product within 1 gram of accuracy
Materials: One metric scale with less than 1 gram accuracy; One final iteration of the device
Safety: Touch only the exterior of the casing
Procedure:

1. Ensure that all necessary materials are present.
2. Place scale on a flat surface with top facing up.
3. Make sure that scale is turned on and set to the desired measuring settings.
4. Gently set the device on top of the scale.
5. Make sure that device is alone at rest and close to the center of the weighing area.
6. Record the displayed mass of the device.
7. Repeat steps 4-6 ten more times in order to ensure measurement accuracy.

8. Calculate and average and standard deviation for all of the weights measured
9. Verify that the weight of the device falls within the 200<x<300 g range

Test 2: Bike Transfer Time Test

Determine: Time required to remove device from one bike and attach it to another.
Materials: Two bikes; One final iteration of the device
Safety: Ensure that both bikes are standing properly and securely.
Procedure:

1. Ensure that all materials are present.
2. Set up bikes close to each other and stand between them.
3. Bikes should be in upright position by holding the handlebars or using a stand to keep from moving
4. Ensure that the device is attached to one of the two bikes.
5. Start timer.
6. Safely remove the device by pealing back the Velcro straps that attach it to the first bike.
7. Attach the device to the second bike by re applying the Velcro straps.
8. Try to turn the device around the bike tube that it is attached to ensure that it is snuggly secured.
9. Ride around for 1-2 minutes to ensure that the unit is securely attached.
10. Stop timer.
11. Repeat steps 4-8 two more times with other test subjects in order to ensure time accuracy.
12. Verify that the transfer time is <=5 minutes

Test 3: USB Output Compatibility Test

Determine: Output compatibility with USB output
Materials: One final iteration of the device; USB cable; cell phone with 50% battery
Safety: Ensure that the circuit has proper components installed
Procedure:

1. Charge on board battery fully using Li-Ion Fast Charger.
2. Take USB cable and install into cell phone port.
3. Plug in other end of USB cable into port on PCB.
4. Keep device plugged into PCB via USB for 15 minutes.
5. Verify that the cell phone begins to charge by observing proper charge behaviors of phone (i.e. charge symbol on battery indicator).
6. The test is a pass if the USB output can discharge to a cell phones battery.

Test 4: Waterproof Test

Determine: Accurate waterproof IP rating of the device exterior.
Materials: One final iteration of the device; one hose; one hose nozzle with shower setting; one bike
Safety: Make sure that the device is fully discharged and that the exterior screws are tightly fastened.
Procedure:

1. Ensure that all necessary materials are present.
2. Prop bike in an upright position (use kickstand if available).
3. Strap the device to the intended bike location.
4. Screw nozzle onto hose ad set on shower setting.
5. Turn hose on.
6. Spray the device from above as well as each side for 5 minutes.
7. Turn hose off.
8. Safely remove device from bicycle.
9. Inspect device exterior and interior to ensure that no water has penetrated the outer casing.
10. A waterproof rating of IP 4 will be given assuming no water damage is done to the interior or exterior.

Test 5: Particle Proof Test

Determine: Accurate IP Rating for protection against solid objects.
Materials: One final iteration of the device; one bike; sand; dirt
Safety: Make sure that the device is fully discharged and that the exterior screws are tightly fastened.
Procedure:

1. Ensure that all necessary materials are present.
2. Prop bike in an upright position (use kickstand if available).
3. Strap the device to the intended bike location.
4. Throw sand and dirt at device form different angles at varying velocities.
5. Ensure that device is hit from every direction including from below.
6. Detach device from bike.
7. Drop device in sand.
8. Inspect device for any exterior or interior damage.
9. A particle-proof rating of IP 4? Will be given assuming no particle damage was done.

Test 6: Vibration Tolerance Test

Determine: Durability of internal components when device is exposed to 30Gs.
Materials: Shake table in Cal Poly ME Lab; Rigid fixture to secure device; one final iteration of the device
Safety: Ensure that device is properly assembled and secured in fixture
Procedure:

1. Ensure that all necessary materials are present.
2. Place device into fixture and make sure that it is secured into place.
3. Place fixture on shake table
4. Turn on shake table

5. Control the frequency of the shake table until a resonant frequency is met and the magnet is steadily moving back and forth.
6. Remove device from fixture and shake table.
7. Inspect device to confirm that components are intact and not damaged
8. Device will pass test if all internal components are not noticeably damaged and the device functions properly after the test.

Test 7: Charge Rate Test

Determine: Charge rate of on board battery.
Materials: One final iteration of the device; USB cable; cell phone with 50% battery
Safety: Ensure that the circuit has proper components installed
Procedure:

1. Drain battery on board battery fully.
2. Shake device perpendicular to floor in an up and down motion for 10 minutes.
3. Plug in phone to battery via USB and confirm that charging initiates
4. After 10 minutes, record percentage of cell phone battery that was charged.
5. Perform calculations to ensure ample charge rate (2.0-2.5W).
6. The test is considered a pass if a charge rate of 2.0-2.5W is observed.

Test 8: Noise Test

Determine: Noise difference between environment where the device is and isn't being used.
Materials: One final iteration of the device; one noise reader
Safety: Make sure that the screws are tightly fastened.
Procedure:

1. Ensure that all necessary materials are present.
2. Hold device at a distance of 5 feet to the noise reader.
3. Start taking noise data.
4. Shake device and record noise difference in decibels.
5. Stop taking noise data.
6. Repeat steps 2 through 5 two more times.
7. Average the three noise readings found.
8. Ensure that the noise increases by no more than 15 dB.

Test 9: Drop Test

Determine: Integrity of device when dropped onto cement from a height of 3 feet
Materials: One final iteration of the device; phillips head screwdriver
Safety: Ensure that the exterior screws are tightly fastened.
Procedure:

1. Ensure that all necessary materials are present.
2. Go to an area where there is asphalt and level ground to measure 3 feet.
3. Measure 3 feet off the ground.
4. Hold device in hand at the 3 foot mark.

5. Drop device and ensure that you are not spinning the device or modeling it to hit the ground in a specific manner.
6. Grab device from ground.
7. Inspect the outside of the device to ensure that the exterior casing has not been penetrated or cracked.
8. Remove the screws from the device using the screwdriver
9. Inspect the inside of the device to ensure that the internal components have not been broken or damaged
10. Attempt to charge a device with a USB cable to confirm that the device still outputs a charge
11. The device will pass the test if the exterior casing has not been broken or cracked and the internal components are fully functions after the drop

Test 10: On Bicycle Battery Charging Test

Determine: Charge rate of on board battery while mounted to bicycle.
Materials: One final iteration of the device; USB cable; cell phone with 50% battery; one bike
Safety: Ensure that all components in the inner casing are secured and assembled correctly. Ensure that the circuit has proper components installed
Procedure:

1. Drain battery on board battery fully.
2. Mount device to bike following the attachment testing procedure.
3. Ride bicycle for 30 minutes.
4. Remove device from bicycle by removing the Velcro straps with the bicycle in an upright position.
5. Plug in phone to device via USB to initiate charging.
6. Record percentage of cell phone battery that was charged.
7. Perform calculations to ensure ample charge rate and extrapolate the data to ensure that the on board battery will be fully charged in 6-15 hours.

Test 11: Magnetic Clearance Test

Determine: Ensure that magnet freely moves in inner casing without noticeable resistance from inner walls
Materials: One final iteration of the inner casing assembly
Safety: Ensure that all components in the inner casing are secured and assembled correctly
Procedure:

1. Ensure that all necessary materials are present.
2. Grab device in hand with the end caps parallel to level ground
3. Shake device in an up and down motion toward and away from the ground
4. Visually inspect and confirm that the magnet is moving in a linear motion though the inner casing without noticeable resistance from walls
5. Listen to ensure that the magnet is not rubbing against the walls of the inner casing

6. The test is considered a pass if the magnet moves in a linear motion without resistance from the walls of the inner casing

Test 12: Attachment Testing

Determine: Functionality of the device's attachment mechanism.
Materials: One final iteration of the device; one bike; one helmet
Safety: Ensure that device is securely fastened and that a helmet is worn by the rider at all times.
Procedure:

1. Ensure that all necessary materials are present.
2. Securely fasten device to a bike.
3. Before riding, check to make sure that the device isn't loose and that the rider's helmet is fastened on to his/her head.
4. Ride bike on rough terrain for 1 hour checking periodically on the state of the device and attachment mechanism.
5. After the ride, examine the state of the attachment straps.

The attachment system will pass this test if the device does not come loose during the ride and if the straps do not show signs of unusable wear

Appendix H: Product User Guide

The following pages include a short user guide that describes how to use the device in a relatively simple step-by-step format.

Attaching the device to a bicycle:

- Place the long end of the device against the seat tube of the device with the rubber pads touching the bike frame.
- Move the device down the seat tube as far as possible until it makes contact with the down tube of the bicycle
- Using the included straps, wrap the straps around the bike frame and tightly secure the device to the bicycle.
- See the picture below for an example of the device safely secured to a bicycle.

Securing the Device with the Included Straps

Safely Secured Device

Detaching the device from a bicycle:

- Secure the device to the bicycle with one hand while undoing the velcro straps with the other.
- Repeat step one with both straps
- Remove the device off of the bicycle by hand

Charging mobile devices:

- Plug in your specific USB cable to the device that you would like to charge.
- Take the other end of the USB cable and plug it into the USB port on the top of the device as shown in the photo below.

Appendix I: PERT Chart

Task ID	Description	Predecessor	Start Date	Duration (days)	Responsible Party
A	3-D Print Outer Housing for Physical Verification	none	3/13/2015	5	Danny/Austin
B	3-D Print Inner Housing for Physical Verification	none	3/13/2015	5	Danny/Austin
C	Complete Purchases of New Mechanical Parts	none	3/13/2015	1	Danny/Austin
D	Verify/Obtain Tolerance and Fitting of Outer and Inner Housing Assemblies	A,B	3/30/2015	2	Danny/Austin
E	Complete Inner Casing Subassembly	C,D	4/2/2015	2	Danny/Austin
F	Complete Testing of Circuit Subassembly	none	3/13/2015	25	TJ
G	Finalize PCB Layout	F	4/7/2015	2	TJ
H	Order and Receive PCB	G	4/09/1015	7	TJ
I	Solder Battery and Coil to PCB	H	4/16/2015	1	TJ
J	Create Assembly of Outer Housing, Inner Housing, and EE Components	E,I	4/17/2015	1	All
K	Perform Mechanical Tests	J	4/19/2015	2	Danny/Austin
L	Perform Electrical Tests	J	4/19/2015	3	TJ
M	Document Findings and Implement Possible Changes to Design	K,L	4/22/2015	20	All
N	3-D Print/Machine Final Inner and Outer Housing Design	M	5/13/2015	5	Danny/Austin
O	Complete Final Assembly	N	5/18/2015	2	All
P	Final Testing	O	5/20/2015	7	All
Q	Document Results and Finalize Report	P	5/27/2015	15	All

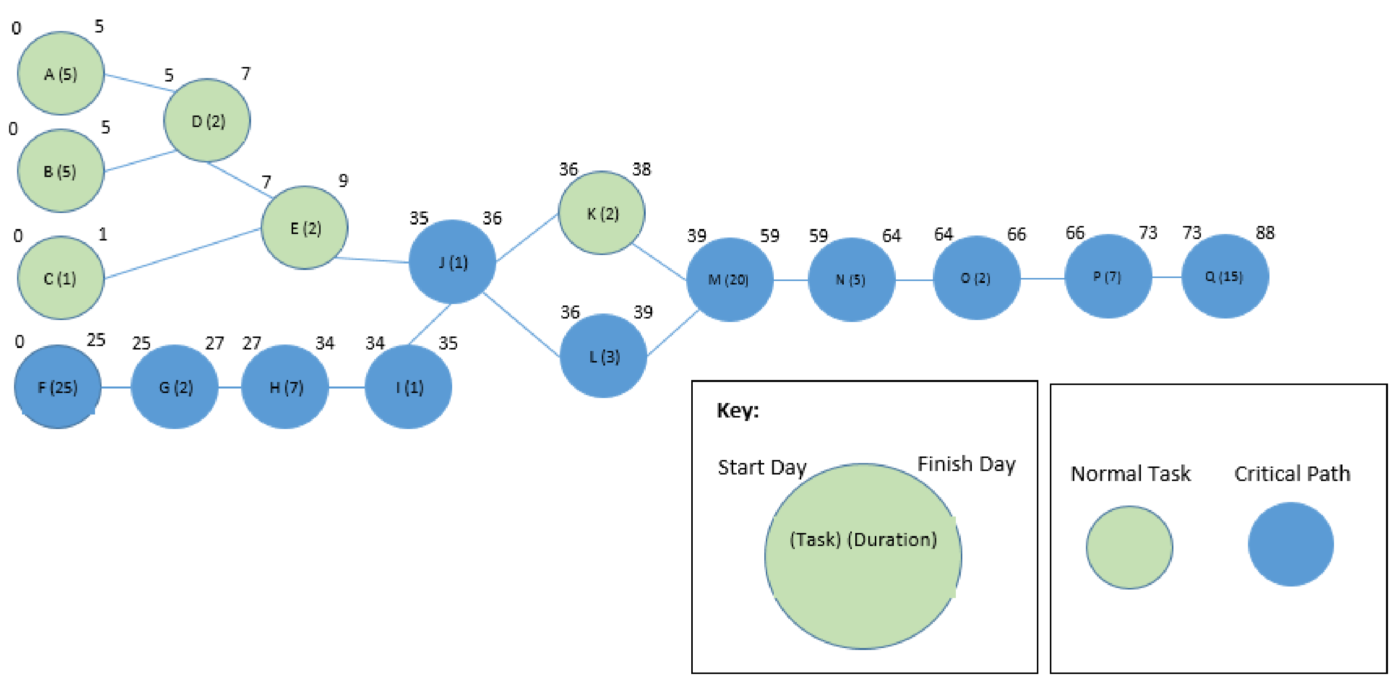

Appendix J: Vendor Supplied Component Specifications and Data Sheets

Specification Approval Sheet

Name： ***Li-18650 3.7V 5200***

Model： ______

SPEC： **3.7V 5200mAh**

Approved By	Checkup	Make

<table>
<tr><td rowspan="4">Customer Confirmation</td><td>Signature</td><td>Date</td></tr>
<tr><td></td><td></td></tr>
<tr><td colspan="2">Company Name：</td></tr>
<tr><td colspan="2">Stamp：</td></tr>
</table>

436 Kato Terrace, Fremont, CA 94539 U.S.A.

Tel: 510.687.0388 Fax: 510.687-0328

www.TenergyBattery.com

Tenergy Corporation
436 Kato Terrace
Fremont, CA 94539
Tel: 510.687-0388 Fax: 510.687.0328
www.TenergyBattery.com email: sales@tenergybattery.com

1 Scope

This specification describes the technological parameters and testing standard for the lithium ion rechargeable battery manufactured and supplied by Tenergy Corporation.

2 Products specified

2.1 Name Cylindrical Lithium Ion Rechargeable Battery
2.2 Type Li-18650 3.7V 5200

3 References

In this specification reference is made to: GB/T182847-2000, UL1642 and IEC61960-1:2000.

4 Caution:

4.1. Please read these specifications carefully before testing or using the battery as improper handling of a Li-ion battery may result in lose of efficiency, heating, ignition, electrolyte leakage or even explosion.
4.2 While testing the battery by charging and discharging, please use test-equipment especially designed for Li-ion battery. Do not use ordinary constant current and constant voltage (CC/CV) power supplies. These do not protect the battery from being overcharged and over-discharged, resulting in possible loss of functionality or danger.
4.3 When charging and discharging batteries or packing them into equipment, reversing the positive and negative terminals will result in overcharging and over-discharging of the battery(s). This could lead to serious loss of efficiency and even explosions.
4.4 Do not solder directly on the battery. Do not resolve the battery.
4.5 Do not put battery(s) in pockets or bags together with metal products such as necklaces, hairpins, coins, screws, etc. Neither stores them together without proper isolation. Do not connect the positive and negative electrode directly with each other through conductive materials. This can result in a short circuit of the battery.
4.6 Do not beat, throw or trample the batteries, do not put the battery into washing machines or high-pressure containers.
4.7 Keep the battery away from heat sources such as fires, heaters, etc. Do not use or store battery(s) at locations where the temperature can exceed 60℃, such as in direct sunlight. This may lead to the generation of excessive heat, ignition and lose of efficiency.
4.8 Do not get batteries wet or throw them into water. When not in use, place the batteries in a dry environment at low temperatures.
4.9 While during use, testing or storing batteries, batteries become hot, distribute a smell, change color, deform or show any other abnormalities, please stop using or testing immediately. Attempt to isolate the battery and keep it away from other batteries.
4.10 Should electrolyte get into the eyes, do not rub the eyes, rinse the eyes with clean water and seek medical attention if problems remain. If electrolyte gets onto the skin or clothing, wash with clean water immediately.

Tenergy Corporation
436 Kato Terrace
Fremont, CA 94539
Tel: 510.687-0388 Fax: 510.687.0328
www.TenergyBattery.com email: sales@tenergybattery.com

5 Basic characteristics

5.1 Capacity（25±5℃）	Nominal Capacity： 5200mAh (2.6A Discharge) Minimum Capacity：5090mAh (1.04A Discharge)
5.2 Nominal Voltage	3.7V
5.3 Internal Impedance	≤ 120mΩ
5.4 Discharge Cut-off Voltage	3.0V
5.5 Max Charge Voltage	4.20±0.05V
5.6 Standard Charge Current	2.6A
5.7 Rapid Charge Current	5.2A
5.8 Standard Discharge Current	2.6A
5.9 Rapid Discharge Current	5.2A
5.10 Max Pulse Discharge Current	10.4A
5.11 Weight	Appro 100g
5.12 Max. Dimension	Thickness: 18.5±0.5mm Width:37.5±0.5mm Height： 67±1mm
5.13 Operating Temperature	Charge: 0 ~ 45℃ Discharge: -20 ~ 60℃
5.14 Storage Temperature	During 1 month: -5 ~ 35℃ During 6 months: 0 ~ 35℃

6 Standard conditions for test

All the tests need to be done within one month after the delivery date under the following conditions: Ambient Temperature: 25±5℃; Relative Humidity: 65±20%

Standard Charge	Constant Current and Constant Voltage (CC/CV) Current = 2.6A Final charge voltage = 4.2V Final charge Current = 0.104A
Standard Discharge	Constant Current (CC) Current = 2.6A End Voltage = 3.0V

7 Appearance

All surfaces must be clean, without damages, leakage and corrosion. Each product will have a product label identifying the model.

8 Characteristics

In this section, the Standard Conditions of Tests are used as described in part 6.

8.1 Electrical Performances

Items	Test procedure	Requirements
8.1.1 Nominal Voltage	The average value of the working voltage during the whole discharge process.	3.7V
8.1.2 Discharge Performance	The discharge capacity of the battery, measured with 2.6A down to 3.0V within 1 hour after a completed charge.	≥114min
8.1.3 Capacity Retention	After 28 days storage at 25±5℃, after having been completely charged and discharged at 1.04A, discharge to 3.0V, the residual capacity is above 80%	Capacity≥4160mAh
8.1.4 Cycle Life	After 299 cycles at 100% DOD. Charge and discharge at 2.6A, and plus 1 day, measured under 1.04A charge and discharge, the residual discharge capacity is above 80% of initial capacity (Cycle life may be determined by conditions of charging, discharging, operating temperature and/or storage.)	300 cycles the residual capacity ≥4160mAh
8.1.5 Storage	(Within 3 months after manufactured) The battery is charged with 2.6A to 40-50% capacity and stored at ambient temperature 25±5℃, 65±20%RH for 12 months. After the 12 months storage period the battery is fully charged and discharged to 3.0V with 1.04A	Discharge time≥4h

8.2 Safety Performances

Items		Test procedure	Requirements
8.2.1	Short Circuit	The battery is to be short-circuited by connecting the positive and negative terminals of the battery directly with copper wire with a resistance of less than 0.05Ω.	No fire no explosion.
8.2.2	Impact Test	A test sample battery is to be placed on a flat surface. A 5/8 inch (15.8mm) diameter bar is to be placed across the center of the sample. A 20 pound (9.1kg) weight is to be dropped from a height of 24 ±1 inch (610±25mm) onto the sample.	No fire no explosion.
8.2.3	Overcharge (3C/10V)	The battery is connected with a thermocouple and put in a fume hood. The positive and negative terminals are connected to a DC power supply set at 15.6A and 10V until the battery reaches 10V and the current drops to approximately 0A. Monitor the temperature of battery. When the temperature of the battery is approximately 10℃ less than the peak value, the test is completed.	No fire, no explosion.
8.2.4	Thermal shock	After standard charging, heat the battery to 150±2℃ at a rate of 5±2℃ /min and keep it at this temperature during 10 minutes.	No fire, no explosion.

8.3 Environmental tests

Items	Test procedure	Requirements
8.3.1 High temperature performance	The fully charged battery is put at 55±2℃ for 2 hours and then discharged to 3.0V at 2.6A.	Capacity≥4160mAh
8.3.2 Low temperature performance	The fully charged battery is placed during 16-24 hours at -20±2℃ and then discharge to 2.75V at 1.04A.	Capacity≥3640mAh

8.3.3 Anti-vibration	The fully charged battery is fixed on a platform and vibrated in the X , Y and Z directions for 30minutes at the speed 10ct/min Frequency: 10~30Hz, Vibration amplitude 0.38mm. Frequency: 30~55Hz, Vibration amplitude 0.19mm.	No deformation should be visible. Not leak, smoke and/or explode. Voltage should be not less than 3.6V.
8.3.4 Drop Test	The fully charged battery is dropped from a height of 1m onto a 15~20mm hard board in X, Y and Z directions once for all axis. Then the battery is discharged at 2.6A to 3.0V followed by 3 or more cycles with the standard charge rate and a discharge at 2.6A.	No fire, no explosion. Discharge Time≥102min

9 Packing
Batteries are at a half-charged state when packed. The packing box surface will contain the following: name, type, nominal voltage, quantity, gross weight, date, capacity and impedance.

10 Transportation
During transport, do not subject the battery(s) or the box (es) to violent shaking, bumps, rain and direct sunlight. Keep the battery(s) at a half-charged state.

11 Long-term Storage
The battery should be used within a short period after charging because long-term storage may cause loss of capacity by self-discharging. If the battery is kept for a long time(3months or more), It is strongly recommended that the battery isstored at dry and low-temperature and Keep the battery(s) at a half-charged state. the battery should be shipped in 50% charged state. In this case, OCV is from 3.65V to 3.85V. Our shipping voltage is 3.75-3.80v . because storage at higher voltage may cause loss of characteristics.

- over a period of 1 month: -5 ~ 35℃, relative humidity: ≤75%.
- over a period of 6 months: -20~ 25℃, relative humidity: ≤75%.

12 Warranty
8.1The warranty period of this product is 12 months starting at the date of delivery from the factory.
8.2Warranty will be void if the batteries are used outside these specifications.
8.3Ryder will not be liable for any damages, personal, material, immaterial or otherwise, when the batteries are used outside these specifications.

13 Changes of specifications
The information in this specification is subject to change without prior notice.

14 For reference only
The information contained in this document is for reference only and should not be used as a basis for product guarantee or warranty. For applications other than those described here, please consult your nearest Ryder Sales Office or Distributors.

15 Pack Quality Requirement for safety and quality

15.1 The battery pack's consumption current.

- Sleep Mode : Under 250uA.
- Shut Down Mode : Under 10uA / Under 3.0V.
 Under 1uA / Under 2.5V.

15.2 Operating Charging Voltage of a battery.
- Normal operating voltage of a battery is 4.20V
- Max operating voltage of a battery is 4.25V.

15.3 Pre-charging function
- Pre-charge function should be implemented to prevent abnormal high rate charging after deep discharge.
- Pre-charging condition Operation : Under 3.0V
-Charging current : Under 150mA/Battery.(Continuous)
-Pre-charge stop (Normal Charge Start) : All batteries reach 3.0V

15.4. Battery voltage monitoring system.
- The system (Charger or Pack) should equip a device to monitor each Battery voltage and to stop
charging if a battery imbalance happened.

16 PCB Performance

16.1 Electrical characteristics

Item	Symbol	Content	Criterion
Over charge Protection	V_{DET1}	Over charge detection voltage	4.25±0.05V
	tV_{DET1}	Over charge detection delay time	0.7～1.3s
	V_{REL1}	Over charge release voltage	4.05±0.05V
Over discharge protection	V_{DET2}	Over discharge detection voltage	2.5±0.1V
	tV_{DET2}	Over discharge detection delay time	14～26ms
	V_{REL2}	Over discharge release voltage	3.0±0.05V
	VDET3	Over current detection voltage	0.2±0.015v
	IDP	Over current detection current	9.0～13.0A
	tVDET3	Detection delay time	8.0～16.0ms
		Release condition	Cut load

		Detection condition	Exterior short circuit
	TSHORT	Detection delay time	230～500us
		Release condition	Cut short circuit
	RDS	Main loop electrify resistance	VC=4.2V；RDS≤40mΩ
Current consumption	I_{DD}	Current consume in normal operation	4.0μA Type 8.0μA Max

16.2 Parts list

NO.	Location	Part name	Specification			Maker/Remark
1	U1	Battery protection IC	R5402N101KD	SOT-23-6	1	RICOH
2	U2,U3	Silicon MOSFET	FTD2017R	TSSOP-8	2	SANYO
3	R1	Resistance	SMD 330Ω±5%	0603	1	YAGEO
4	R2	Resistance	SMD 1KΩ±5%	0603	1	YAGEO
5	R3	Resistance	SMD 220Ω±5%	0603	1	YAGEO
6	C1	Capacitance	SMD 0.1μF	0603	1	TDK
7	PCB	Print circuit board	I-1661 38*4.2*0.6 mm		1	AS

Tenergy Corporation
436 Kato Terrace
Fremont, CA 94539
Tel: 510.687-0388 Fax: 510.687.0328
www.TenergyBattery.com email: sales@tenergybattery.com

16.3 Application Circuit

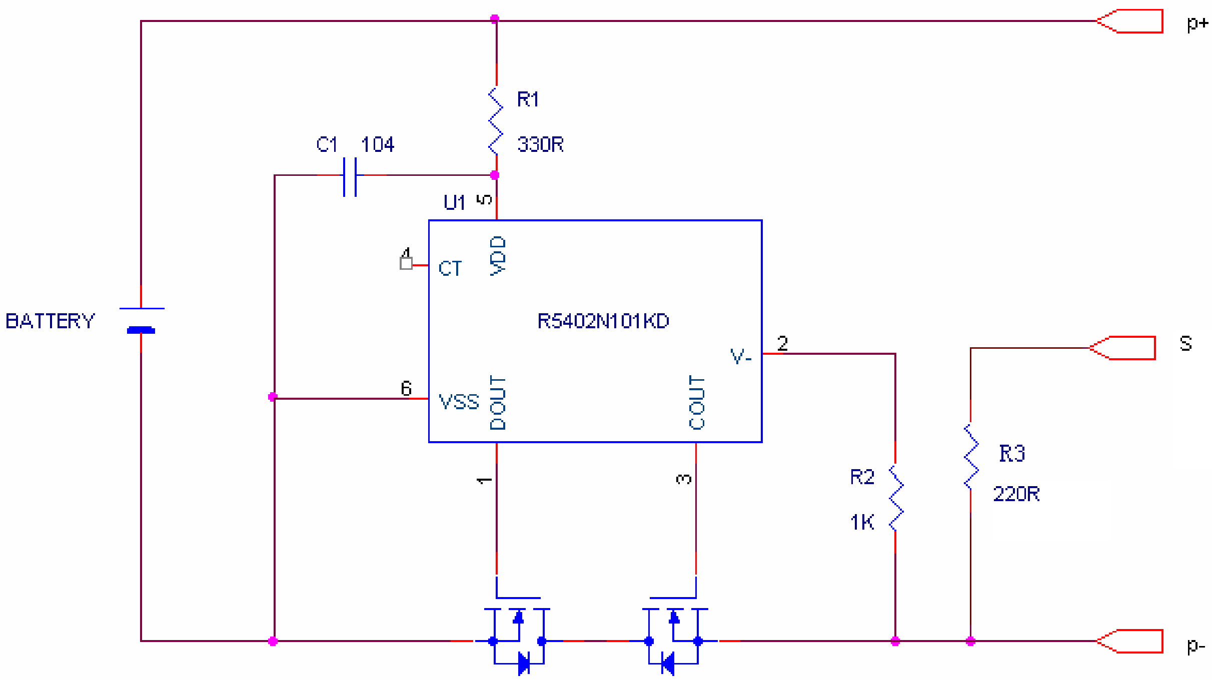

16.4 PCB layout

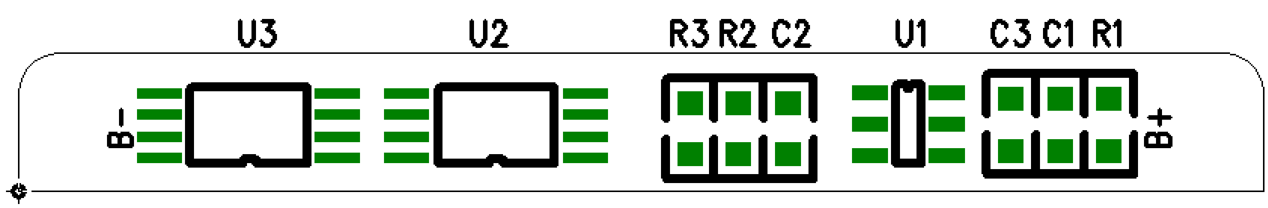

16.5 PCB Maps

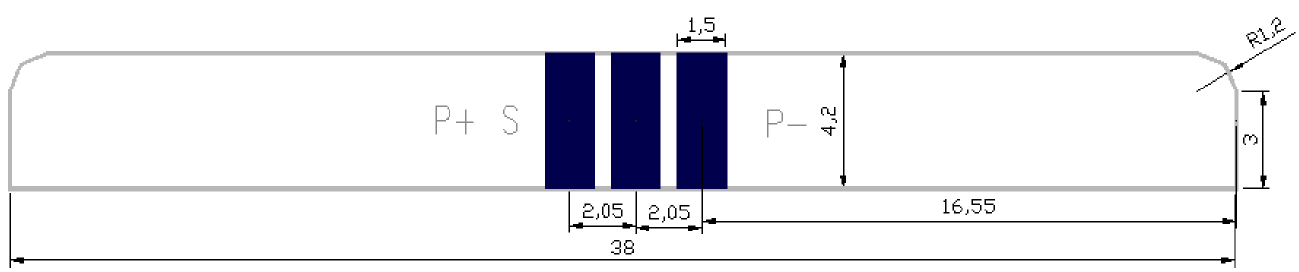

16.6 Terminal explanations

1、B+： Connected to the battery’s positive terminal

2、B-： Connected to the battery’s negative terminal

3、P+： Connected to the battery’s output or the charger’s positive terminal

4、P-： Connected to the battery’s output or the charger’s negative terminal

17 Battery Pack Drawing

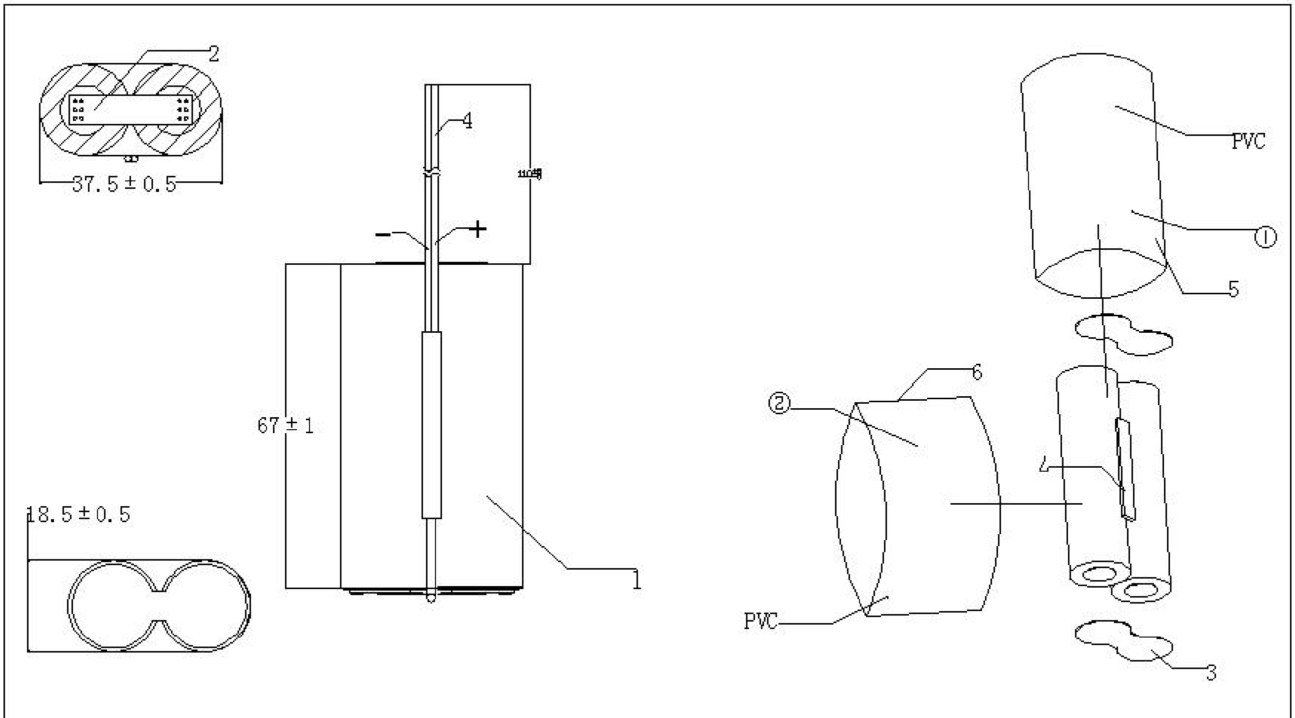

Item	materical	qty	specification	remark
7	PCB	1	F3.7V 6/9.46A	
6	PVC	1	Fold width 105	whitePVC
5	PVC	1	Fold width 50	whitePVC
4	wire	1	3135#20	
3	red strick cushion	2	3*18650	
2	connector	2	nickle belt25*6*0.15	
1	ceLL	2	Li-ion 18650 3.7V	

Item	Signature	Date	remark		ShenZhenRyder electronics co.,ltd			
drw	HouGuoSong	2009-09-24						
chk			qty	1/1	model	Li-3.7V18650-5200	unit	mm
app			edition	A/0				

bq25504 Ultra Low-Power Boost Converter With Battery Management for Energy Harvester Applications

1 Features

- Ultra Low-Power With High-Efficiency DC-DC Boost Converter/Charger
  – Continuous Energy Harvesting From Low-Input Sources: $V_{IN} \geq 80$ mV (Typical)
  – Ultra-Low Quiescent Current: $I_Q < 330$ nA (Typical)
  – Cold-Start Voltage: $V_{IN} \geq 330$ mV (Typical)
- Programmable Dynamic Maximum Power Point Tracking (MPPT)
  – Integrated Dynamic Maximum Power Point Tracking for Optimal Energy Extraction From a Variety of Energy Generation Sources
  – Input Voltage Regulation Prevents Collapsing Input Source
- Energy Storage
  – Energy Can be Stored to Rechargeable Li-ion Batteries, Thin-film Batteries, Super-Capacitors, or Conventional Capacitors
- Battery Charging and Protection
  – User Programmable Undervoltage and Overvoltage Levels
  – On-Chip Temperature Sensor With Programmable Overtemperature Shutoff
- Battery Status Output
  – Battery Good Output Pin
  – Programmable Threshold and Hysteresis
  – Warn Attached Microcontrollers of Pending Loss of Power
  – Can be Used to Enable or Disable System Loads

2 Applications

- Energy Harvesting
- Solar Chargers
- Thermal Electric Generator (TEG) Harvesting
- Wireless Sensor Networks (WSNs)
- Industrial Monitoring
- Environmental Monitoring
- Bridge and Structural Health Monitoring (SHM)
- Smart Building Controls
- Portable and Wearable Health Devices
- Entertainment System Remote Controls

3 Description

The bq25504 device is the first of a new family of intelligent integrated energy harvesting nano-power management solutions that are well suited for meeting the special needs of ultra low power applications. The device is specifically designed to efficiently acquire and manage the microwatts (µW) to miliwatts (mW) of power generated from a variety of DC sources like photovoltaic (solar) or thermal electric generators. The bq25504 is the first device of its kind to implement a highly efficient boost converter/charger targeted toward products and systems, such as wireless sensor networks (WSNs) which have stringent power and operational demands. The design of the bq25504 starts with a DC-DC boost converter/charger that requires only microwatts of power to begin operating.

Once started, the boost converter/charger can effectively extract power from low-voltage output harvesters such as thermoelectric generators (TEGs) or single- or dual-cell solar panels. The boost converter can be started with V_{IN} as low as 330 mV, and once started, can continue to harvest energy down to V_{IN} = 80 mV.

Device Information(1)

PART NUMBER	PACKAGE	BODY SIZE (NOM)
bq25504	VQFN (16)	3.00 mm x 3.00 mm

(1) For all available packages, see the orderable addendum at the end of the datasheet.

Solar Application Circuit

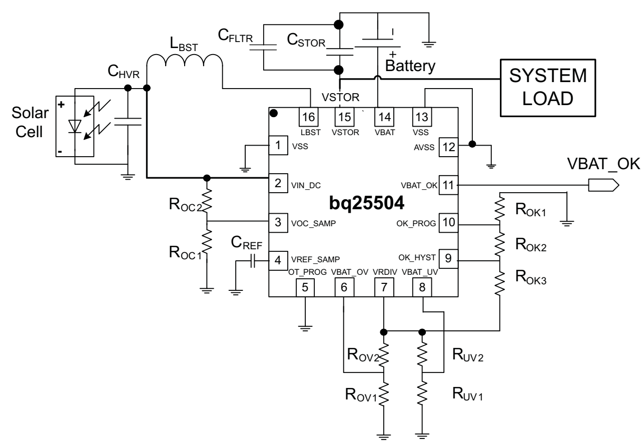

Table of Contents

4 Revision History

Changes from Revision A (September 2012) to Revision B — **Page**

- Added *Handling Rating* table, *Feature Description* section, *Device Functional Modes*, *Application and Implementation* section, *Power Supply Recommendations* section, *Layout* section, *Device and Documentation Support* section, and *Mechanical, Packaging, and Orderable Information* section ... 1

Changes from Original (October 2011) to Revision A — **Page**

- Added the INTENDED OPERATION section ... 9
- Changed the Cold -Start Operation section ... 13
- Changed the Boost Converter, Charger Operation section ... 14
- Changed the Storage Element section ... 14
- Changed the CAPACITOR SELECTION section ... 17
- Added C_{FLTR} and Notes 1 and 2 to Figure 14 ... 18
- Added C_{FLTR} and Notes 1 and 2 to Figure 21 ... 21
- Added C_{FLTR} and Notes 1 and 2 to Figure 28 ... 23

5 Description (Continued)

The bq25504 also implements a programmable maximum power point tracking sampling network to optimize the transfer of power into the device. Sampling the VIN_DC open-circuit voltage is programmed using external resistors, and held with an external capacitor (C_{REF}).

For example solar cells that operate at maximum power point (MPP) of 80% of their open-circuit voltage, the resistor divider can be set to 80% of the VIN_DC voltage and the network will control the VIN_DC to operate near that sampled reference voltage. Alternatively, an external reference voltage can be provide by a MCU to produce a more complex MPPT algorithm.

The bq25504 was designed with the flexibility to support a variety of energy storage elements. The availability of the sources from which harvesters extract their energy can often be sporadic or time-varying. Systems will typically need some type of energy storage element, such as a rechargeable battery, super capacitor, or conventional capacitor. The storage element ensures that constant power is available when needed for the systems. The storage element also allows the system to handle any peak currents that cannot directly come from the input source.

To prevent damage to a customer’s storage element, both maximum and minimum voltages are monitored against the user programmed undervoltage (UV) and overvoltage (OV) levels.

To further assist users in the strict management of their energy budgets, the bq25504 toggles the battery good flag to signal an attached microprocessor when the voltage on an energy storage battery or capacitor has dropped below a preset critical level. This warning should trigger the shedding of load currents to prevent the system from entering an undervoltage condition. The OV, UV, and battery good thresholds are programmed independently.

All the capabilities of bq25504 are packed into a small-footprint, 16-lead, 3-mm x 3-mm VQFN package.

6 Pin Configuration and Functions

RGT Package
16 Pins
Top View

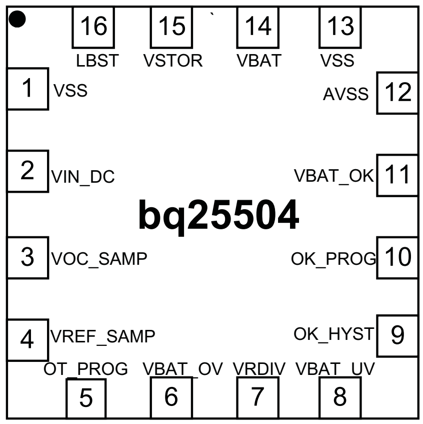

Pin Functions

PIN		I/O	DESCRIPTION
NAME	NO.		
AVSS	12	Supply	Signal ground connection for the device
LBST	16	Input	Inductor connection for the boost charger switching node. Connect a 22 µH inductor between this pin and pin 2 (VIN_DC).
OK_HYST	9	Input	Connect to the mid-point of external resistor divider between VRDIV and GND for setting the VBAT_OK hysteresis threshold. If not used, connect this pin to GND.
OK_PROG	10	Input	Connect to the mid-point of external resistor divider between VRDIV and GND for setting the VBAT_OK threshold. If not used, connect this pin to GND.
OT_PROG	5	Input	Digital Programming input for IC overtemperature threshold. Connect to GND for 60 C threshold or VSTOR for 120 C threshold.
VBAT	14	I/O	Connect a rechargeable storage element with at least 100 uF of equivalent capacitance to this pin.
VBAT_OK	11	Output	Digital output for battery good indicator. Internally referenced to the VSTOR voltage. Leave floating if not used.
VBAT_OV	6	Input	Connect to the mid-point of external resistor divider between VRDIV and GND for setting the VSTOR = VBAT overvoltage threshold.
VBAT_UV	8	Input	Connect to the mid-point of external resistor divider between VRDIV and GND for setting the VBAT undervoltage threshold. The PFET between VBAT and VSTOR opens if the voltage on VSTOR is below this threshold.
VIN_DC	2	Input	DC voltage input from energy harvesters. Connect at least a 4.7 µF capacitor as close as possible between this pin and pin 1.
VOC_SAMP	3	Input	Sampling pin for MPPT network. Connect to the mid-point of external resistor divider between VIN_DC and GND for setting the MPP threshold voltage which will be stored on the VREF_SAMP pin. To disable the MPPT sampling circuit, connect to VSTOR.
VRDIV	7	Output	Resistor divider biasing voltage.
VREF_SAMP	4	Input	Connect a 0.01 µF low leakage capacitor from this pin to GND to store the voltage to which VIN_DC will be regulated. This voltage is provided by the MPPT sample circuit. When MPPT is disabled, either use an external voltage source to provide this voltage or tie this pin to GND to disable input voltage regulation (i.e. operate from a low impedance power supply).
VSS	1	Input	General ground connection for the device
VSS	13	Supply	General ground connection for the device
VSTOR	15	Output	Connection for the output of the boost charger, which is typically connected to the system load. Connect at least a 4.7 µF capacitor in parallel with a 0.1 µF capacitor as close as possible to between this pin and pin 1 (VSS).

7 Specifications

7.1 Absolute Maximum Ratings (1)

over operating free-air temperature range (unless otherwise noted)

		MIN	MAX	UNIT
Input voltage	VIN_DC, VOC_SAMP, VREF_SAMP, VBAT_OV, VBAT_UV, VRDIV, OK_HYST, OK_PROG, VBAT_OK, VBAT, VSTOR, LBST (2)	–0.3	5.5	V
Peak Input Power, P_{IN_PK}			400	mW
Operating junction temperature range, T_J		–40	125	°C

(1) Stresses beyond those listed under *Absolute Maximum Ratings* may cause permanent damage to the device. These are stress ratings only and functional operation of the device at these or any other conditions beyond those indicated under *Recommended Operating Conditions* is not implied. Exposure to absolute–maximum–rated conditions for extended periods may affect device reliability.
(2) All voltage values are with respect to V_{SS}/ground terminal.

7.2 Handling Ratings

			MIN	MAX	UNIT
T_{stg}	Storage temperature range		–65	150	°C
$V_{(ESD)}$	Electrostatic discharge	Human body model (HBM), per ANSI/ESDA/JEDEC JS-001, all pins (1)		2	kV
		Charged device model (CDM), per JEDEC specification JESD22-C101, all pins (2)		500	V

(1) JEDEC document JEP155 states that 500-V HBM allows safe manufacturing with a standard ESD control process.
(2) JEDEC document JEP157 states that 250-V CDM allows safe manufacturing with a standard ESD control process.

7.3 Recommended Operating Conditions

		MIN	NOM	MAX	UNIT
$V_{IN\ (DC)}$	DC input voltage into VIN_DC (1)	0.13		3	V
VBAT	Battery voltage range (2)	2.5		5.25	V
C_{HVR}	Input capacitance	4.23	4.7	5.17	µF
C_{STOR}	Storage capacitance	4.23	4.7	5.17	µF
C_{BAT}	Battery pin capacitance or equivalent battery capacity	100			µF
C_{REF}	Sampled reference storage capacitance	9	10	11	nF
$R_{OC1} + R_{OC2}$	Total resistance for setting for MPPT reference.	18	20	22	MΩ
$R_{OK}1 + R_{OK}2 + R_{OK3}$	Total resistance for setting reference voltage.	9	10	11	MΩ
$R_{UV1} + R_{UV2}$	Total resistance for setting reference voltage.	9	10	11	MΩ
$R_{OV1} + R_{OV2}$	Total resistance for setting reference voltage.	9	10	11	MΩ
L_{BST}	Input inductance	19.8	22	24.2	µH
T_A	Operating free air ambient temperature	–40		85	°C
T_J	Operating junction temperature	–40		105	°C

(1) Maximum input power ≤ 300 mW. Cold start has been completed
(2) VBAT_OV setting must be higher than VIN_DC

7.4 Thermal Information

THERMAL METRIC (1)		bq25504 QFN 16 PINS	UNIT
$R_{\theta JA}$	Junction-to-ambient thermal resistance	48.5	°C/W
$R_{\theta JC(top)}$	Junction-to-case (top) thermal resistance	63.9	
$R_{\theta JB}$	Junction-to-board thermal resistance	22	
ψ_{JT}	Junction-to-top characterization parameter	1.8	
ψ_{JB}	Junction-to-board characterization parameter	22	
$R_{\theta JC(bot)}$	Junction-to-case (bottom) thermal resistance	6.5	

(1) For more information about traditional and new thermal metrics, see the *IC Package Thermal Metrics* application report, SPRA953.

7.5 Electrical Characteristics

Over recommended temperature range, typical values are at T_A = 25°C. Unless otherwise noted, specifications apply for conditions of VIN_DC = 1.2V, VBAT = VSTOR = 3V. External components L_{BST} = 22 µH, C_{HVR} = 4.7 µF C_{STOR}= 4.7 µF.

PARAMETER		TEST CONDITIONS	MIN	TYP	MAX	UNIT
BOOST CONVERTER \ CHARGER STAGE						
$V_{IN(DC)}$	DC input voltage into VIN_DC	Cold-start completed	130		3000	mV
$I_{IN(DC)}$	Peak Current flowing from V_{IN} into VIN_DC input	0.5V < V_{IN} < 3 V; VSTOR = 4.2 V		200	300	mA
P_{IN}	Input power range for normal charging	VBAT > VIN_DC; VIN_DC = 0.5 V	0.01		300	mW
$V_{IN(CS)}$	Cold-start Voltage. Input voltage that will start charging of VSTOR	VBAT < VBAT_UV; VSTOR = 0 V; 0°C < T_A < 85°C		330	450	mV
$P_{IN(CS)}$	Minimum cold-start input power to start normal charging	VBAT < VBAT_UV; VSTOR = 0 V; Input source impedance 0 Ω		10	50	µW
V_{STOR_CHGEN}	Voltage on VSTOR when cold start operation ends and normal charger operation begins		1.6	1.77	1.95	V
$R_{BAT(on)}$	Resistance of switch between VBAT and VSTOR when turned on.	VBAT = 4.2 V; VSTOR load = 50 mA			2	Ω
$R_{DS(on)}$	Charger Low Side switch ON resistance	VBAT = 2.1 V			2	Ω
		VBAT = 4.2 V			2	
	Charger rectifier High Side switch ON resistance	VBAT = 2.1 V			5	Ω
		VBAT = 4.2 V			5	
f_{SW_BST}	Boost converter mode switching frequency				1	MHz
BATTERY MANAGEMENT						
I_{VBAT}	Leakage on VBAT pin	VBAT = 2.1 V; VBAT_UV = 2.3 V, T_J = 25°C VSTOR = 0 V		1	5	nA
		VBAT = 2.1 V; VBAT_UV = 2.3 V, –40°C < T_J < 65°C, VSTOR = 0 V			80	nA
I_{VSTOR}	VSTOR Quiescent current Charger Shutdown in UV Condition	VIN_DC = 0V; VBAT < VBAT_UV = 2.4V; VSTOR = 2.2V, No load on VBAT		330	750	nA
	VSTOR Quiescent current Charger Shutdown in OV Condition	VIN_DC = 0V, VBAT > VBAT_OV, VSTOR = 4.25, No load on VBAT		570	1400	nA
V_{BAT_OV}	Programmable voltage range for overvoltage threshold (Battery voltage is rising)	VSTOR increasing	2.5		5.25	V
$V_{BAT\_OV\_HYST}$	Battery voltage overvoltage hysteresis threshold (Battery voltage is falling), internal threshold	VSTOR decreasing	18	35	89	mV
V_{BAT_UV}	Programmable voltage range for under voltage threshold (Battery voltage is falling)	VSTOR decreasing; VBAT_UV > V_{Bias}	2.2		VBAT_OV	V
$V_{BAT\_UV\_HYST}$	Battery under voltage threshold hysteresis, internal thershold	VSTOR increasing	40	80	125	mV
V_{BAT_OK}	Programmable voltage range for threshold voltage for high to low transition of digital signal indicating battery is OK,	VSTOR decreasing	VBAT_UV		VBAT_OV	V
$V_{BAT\_OK\_HYST}$	Programmable voltage range for threshold voltage for low to high transition of digital signal indicating battery is OK,	VSTOR increasing	50		VBAT_OV-VBAT_UV	mV
$V_{BAT\_ACCURACY}$	Overall Accuracy for threshold values, UV, OV, VBAT_OK	Selected resistors are 0.1% tolerance	–5%		5%	
V_{BAT_OKH}	VBAT OK (High) threshold voltage	Load = 10 µA			VSTOR-200mV	V
V_{BAT_OKL}	VBAT OK (Low) threshold voltage	Load = 10 µA			100	mV
TSD_PROTL	The temperature at which the boost converter is disabled and the switch between VBAT and VSTOR is disconnected to protect the battery	OT_Prog = LO		65		°C
TSD_PROTH		OT_Prog = HI		120		
OT_Prog	Voltage for OT_PROG High setting		2			V
	Voltage for OT_PROG Low setting				0.3	V
BIAS and MPPT CONTROL STAGE						
VOC_sample	Sampling period of VIN_DC open circuit voltage			16		s
VOC_Settling	Sampling period of VIN_DC open circuit voltage			256		ms
VIN_Reg	Regulation of VIN_DC during charging	0.5 V <V_{IN} < 3 V; I_{IN} (DC) = 10 mA	–10%		10%	
VIN_shutoff	DC input voltage into VIN_DC when charger is turned off		40	80	130	mV
MPPT_Disable	Threshold on VOC_SAMP to disable MPPT functionality		VSTOR-15 mV			V
VBIAS	Voltage node which is used as reference for the programmable voltage thresholds	VIN_DC ≥ 0.5V; VSTOR ≥ 1.8 V	1.21	1.25	1.27	V

7.6 Typical Characteristics

VSTOR = Keithley Sourcemeter configured to measure current & voltage source set to hold the VSTOR voltage = 1.8V, 3.0V or 5.5V; VBAT_OV = 5.5V and measurement taken between MPPT measurements

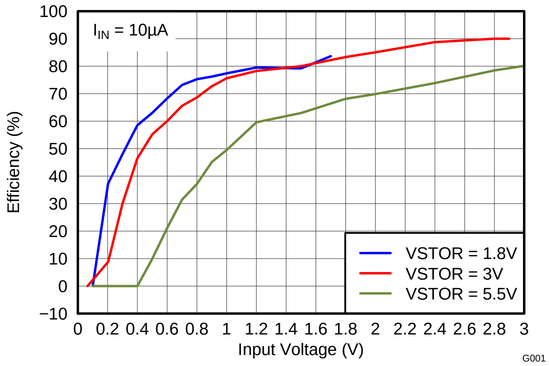

VIN_DC = Keithley Source Meter configured with I_{COMP} = 10 µA and outputting 0 to 3.0 V

Figure 1. Efficiency vs Input Voltage

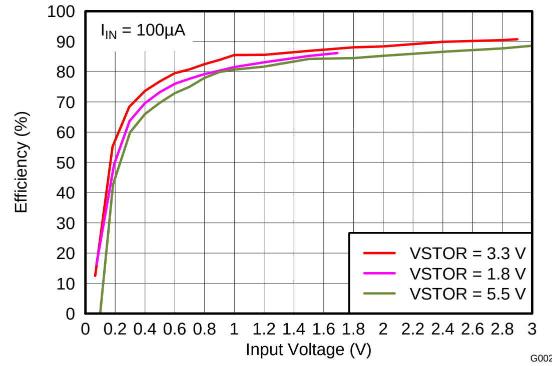

VIN_DC = Keithley Source Meter configured with I_{COMP} = 100 µA and voltage source varied from 0.1 V to 3.0 V

Figure 2. Efficiency vs Input Voltage

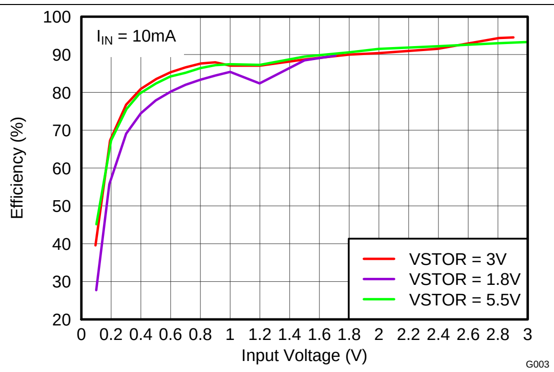

VIN_DC = Keithley Source Meter configured with I_{COMP} = 10 mA and voltage source varied from 0.1 V to 3.0 V

Figure 3. Efficiency vs Input Voltage

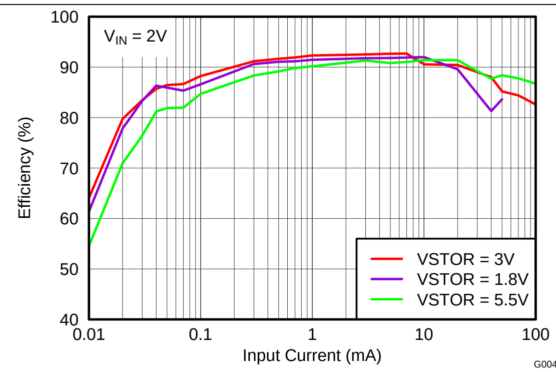

VIN_DC = Keithley Source Meter configured with voltage source = 2.0 V and I_{COMP} varied from 0.01 mA to 100 mA

Figure 4. Efficiency vs Input Current

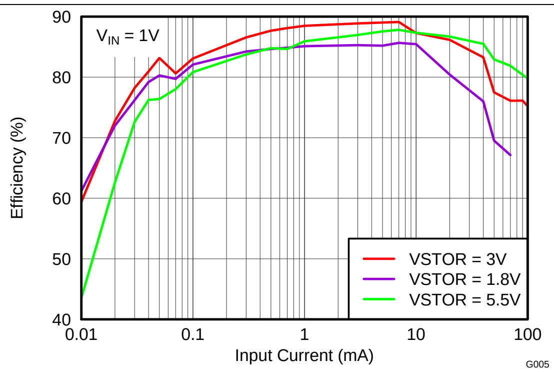

VIN_DC = Keithley Source Meter configured with voltage source = 1.0 V and I_{COMP} varied from 0.01 mA to 100 mA

Figure 5. Efficiency vs Input Current

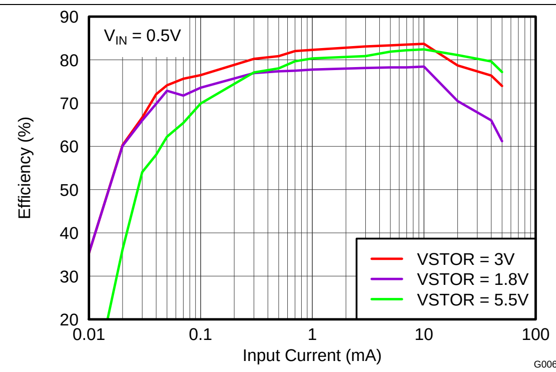

VIN_DC = Keithley Source Meter configured with voltage source = 0.5 V and I_{COMP} varied from 0.01 mA to 100 mA

Figure 6. Efficiency vs Input Current

Typical Characteristics (continued)

VSTOR = Keithley Sourcemeter configured to measure current & voltage source set to hold the VSTOR voltage = 1.8V, 3.0V or 5.5V; VBAT_OV = 5.5V and measurement taken between MPPT measurements

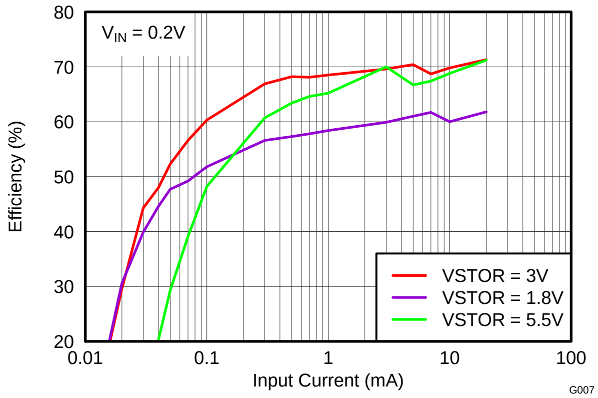

VIN_DC = Keithley Source Meter configured with voltage source = 0.2 V and I_{COMP} varied from 0.01 mA to 100 mA

VSTOR = Keithley Source Meter configured to measure current and voltage source set to hold the VSTOR voltage = 2.0 V, 3.0 V or 5.5 V

Figure 7. Efficiency vs Input Current

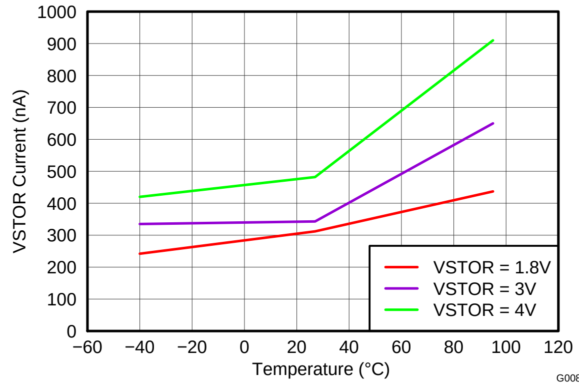

VIN_DC = floating

VBAT = Keithley Sourcemeter configured to measure current and voltage source varied from 1.8 V, 3 V or 4 V

Figure 8. VSTOR Quiescent Current vs Temperature

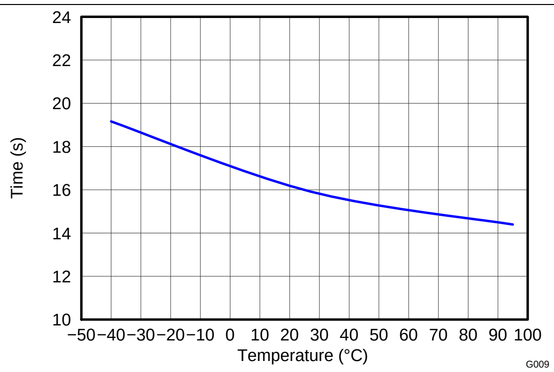

Figure 9. Sample Period vs Temperature

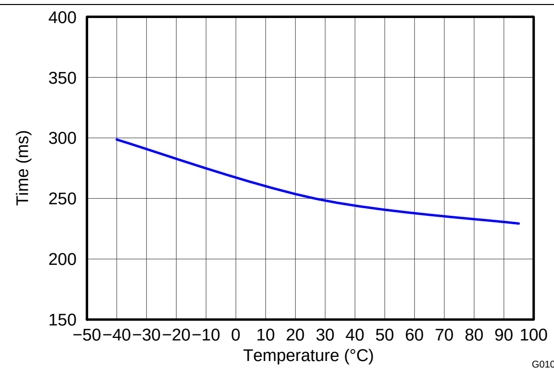

Figure 10. Settling Period vs Temperature

8 Detailed Description

8.1 Overview

The bq25504 is the first of a new family of intelligent integrated energy harvesting Nano-Power management solutions that are well suited for meeting the special needs of ultra low power applications. The product is specifically designed to efficiently acquire and manage the microwatts (µW) to miliwatts (mW) of power generated from a variety of DC sources like photovoltaic (solar) or thermal electric generators (TEGs). The bq25504 is a highly efficient boost charger targeted toward products and systems, such as wireless sensor networks (WSN) which have stringent power and operational demands. The design of the bq25504 starts with a DCDC boost charger that requires only microwatts of power to begin operating.

Once the VSTOR voltage is above VSTOR_CHGEN (1.8V typical), for example, after a partially discharged battery is attached to VBAT, the boost charger can effectively extract power from low voltage output harvesters such as TEGs or single or dual cell solar panels outputing voltages down to VIN(DC) (130mV minimum). When starting from VSTOR=VBAT < 100mV, the cold start circuit needs at least VIN(CS), 330 mV typical, to charge VSTOR up to 1.8V.

The bq25504 implements a programmable maximum power point tracking (MPPT) sampling network to optimize the transfer of power into the device. Sampling of the VIN_DC open circuit voltage is programmed using external resistors, and that sample voltage is held with an external capacitor connected to the VREF_SAMP pin.

For example solar cells that operate at maximum power point (MPP) of 80% of their open circuit voltage, the resistor divider can be set to 80% of the VIN_DC voltage and the network will control the VIN_DC to operate near that sampled reference voltage. Alternatively, an external reference voltage can be applied directly to the VREF_SAMP pin by a MCU to implement a more complex MPPT algorithm.

The bq25504 was designed with the flexibility to support a variety of energy storage elements. The availability of the sources from which harvesters extract their energy can often be sporadic or time-varying. Systems will typically need some type of energy storage element, such as a re-chargeable battery, super capacitor, or conventional capacitor. The storage element will make certain constant power is available when needed for the systems. The storage element also allows the system to handle any peak currents that can not directly come from the input source. To prevent damage to the storage element, both maximum and minimum voltages are monitored against the user programmable undervoltage (VBAT_UV) and overvoltage (VBAT_OV) levels.

To further assist users in the strict management of their energy budgets, the bq25504 toggles the battery good flag to signal an attached microprocessor when the voltage on an energy storage battery or capacitor has dropped below a pre-set critical level. This should trigger the shedding of load currents to prevent the system from entering an undervoltage condition. The OV and battery good (VBAT_OK) thresholds are programmed independently.

8.2 Functional Block Diagram

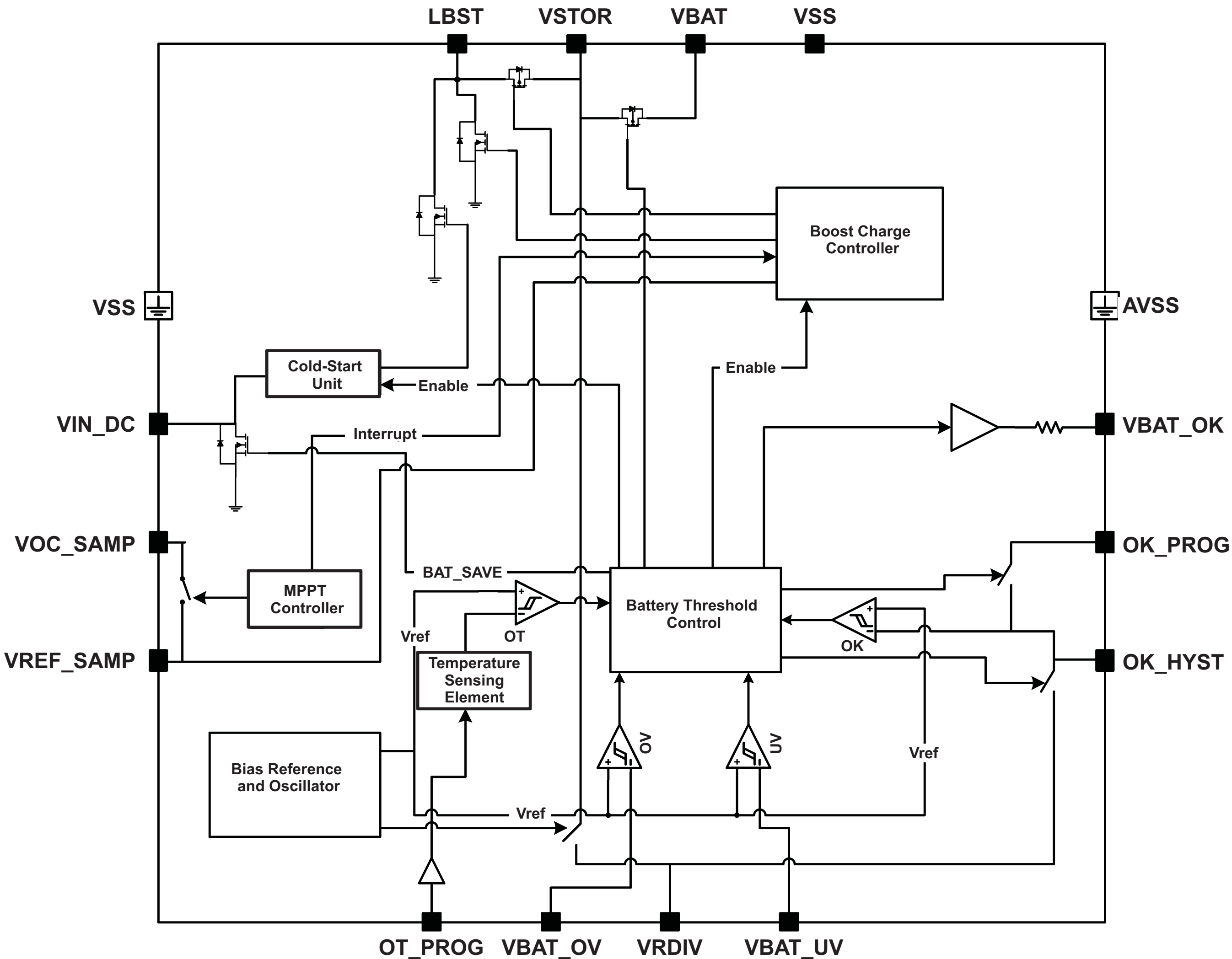

8.3 Feature Description

8.3.1 Maximum Power Point Tracking

Maximum power point tracking (MPPT) is implemented in order to maximize the power extracted from an energy harvester source. The boost converter indirectly modulates the input impedance of the main boost charger by regulating the charger's input voltage, as sensed by the VIN_DC pin, to the sampled reference voltage stored on the VREF_SAMP pin. The MPPT circuit obtains a new reference voltage every 16 s (typical) by periodically disabling the charger for 256 ms (typical) and sampling a fraction of the harvester's open-circuit voltage (VOC). For solar harvesters, the maximum power point is typically 70%-80% of VOC and for thermoelectric harvesters, the MPPT is typically 50%. The exact ratio for MPPT can be optimized to meet the needs of the input source being used by connecting external resistors R_{OC1} and R_{OC2} between VIN_DC and GND with mid-point at VOC_SAMP.

$$VREF\_SAMP = VIN\_DC(OpenCircuit)\left(\frac{R_{OC1}}{R_{OC1} + R_{OC2}}\right) \tag{1}$$

Spreadsheet SLUC484 provides help on sizing and selecting the resistors.

Feature Description (continued)

The internal MPPT circuitry and the periodic sampling of VIN_DC can be disabled by tying the VOC_SAMP pin to VSTOR. An external reference voltage can be fed to the VREF_SAMP pin. The boost converter will then regulate VIN_DC to the externally provided reference. If input regulation is not desired (i.e. the input source is a low-impedance output battery or power supply instead of a high impedance output energy harvester), VREF_SAMP can be tied to GND.

8.3.2 Battery Undervoltage Protection

To prevent rechargeable batteries from being deeply discharged and damaged, and to prevent completely depleting charge from a capacitive storage element, the undervoltage (VBAT_UV) threshold must be set using external resistors. The VBAT_UV threshold voltage when the battery voltage is decreasing is given by Equation 2:

$$VBAT\_UV = VBIAS\left(1 + \frac{R_{UV2}}{R_{UV1}}\right) \tag{2}$$

The sum of the resistors is recommended to be no higher than 10 MΩ that is, $R_{UV1} + R_{UV2}$ = 10 MΩ. Spreadsheet SLURAQ1 provides help on sizing and selecting the resistors.

The undervoltage threshold when the battery voltage is increasing is VBAT_UV plus an internal hysteresis voltage denoted by VBAT_UV_HYST. For the VBAT_UV feature to function properly, the load must be connected to the VSTOR pin while the storage element should be connected to the VBAT pin. Once the VSTOR pin voltage goes above VBAT_UV plus VBAT_UV_HYST threshold, the VSTOR pin and the VBAT pins are effectively shorted through an internal PMOS FET. The switch remains closed until the VSTOR pin voltage falls below the VBAT_UV threshold. The VBAT_UV threshold should be considered a fail safe to the system. The system load should be removed or reduced based on the VBAT_OK threshold which should be set above the VBAT_UV threshold.

8.3.3 Battery Overvoltage Protection

To prevent rechargeable batteries from being exposed to excessive charging voltages and to prevent over charging a capacitive storage element, the over-voltage (VBAT_OV) threshold level must be set using external resistors. This is also the voltage value to which the charger will regulate the VSTOR/VBAT pin when the input has sufficient power. The VBAT_OV threshold when the battery voltage is rising is given by Equation 3:

$$VBAT\_OV = \frac{3}{2}VBIAS\left(1 + \frac{R_{OV2}}{R_{OV1}}\right) \tag{3}$$

The sum of the resistors is recommended to be no higher 10 MΩ that is, $R_{OV1} + R_{OV2}$ = 10 MΩ. Spreadsheet SLURAQ1 provides help with sizing and selecting the resistors.

The overvoltage threshold when the battery voltage is decreasing is given by VBAT_OV - VBAT_OV_HYST. Once the voltage at the battery reaches the VBAT_OV threshold, the boost converter is disabled. The charger will start again once the battery voltage drop by VBAT_OV_HYST. When there is excessive input energy, the VBAT pin voltage will ripple between the VBAT_OV and the VBAT_OV - VBAT_OV_HYST levels.

CAUTION

If VIN_DC is higher than VSTOR and VSTOR is higher than VBAT_OV, the input VIN_DC is pulled to ground through a small resistance to stop further charging of the attached battery or capacitor. It is critical that if this case is expected, the impedance of the source attached to VIN_DC be higher than 20 Ω and not a low impedance source.

8.3.4 Battery Voltage in Operating Range (VBAT_OK Output)

The IC allows the user to set a programmable voltage independent of the overvoltage and undervoltage settings to indicate whether the VSTOR voltage (and therefore the VBAT voltage when the PFET between the two pins is turned on) is at an acceptable level. When the battery voltage is decreasing the threshold is set by Equation 4:

Feature Description (continued)

$$VBAT\_OK\_PROG = VBIAS\left(1 + \frac{R_{OK2}}{R_{OK1}}\right) \quad (4)$$

When the battery voltage is increasing, the threshold is set by Equation 5:

$$VBAT\_OK\_HYST = VBIAS\left(1 + \frac{R_{OK2} + R_{OK3}}{R_{OK1}}\right) \quad (5)$$

The sum of the resistors are recommended to be approximately 10 MΩ i.e., R_{OK1} + R_{OK2} + R_{OK3}= 10 MΩ. Spreadsheet SLURAQ1 provides help on sizing and selecting the resistors.

The logic high level of this signal is equal to the VSTOR voltage and the logic low level is ground. The logic high level has ~20 KΩ internally in series to limit the available current to prevent MCU damage until it is fully powered. The VBAT_OK_PROG threshold must be greater than or equal to the UV threshold. Figure 11 shows the relative position of the various threshold voltages.

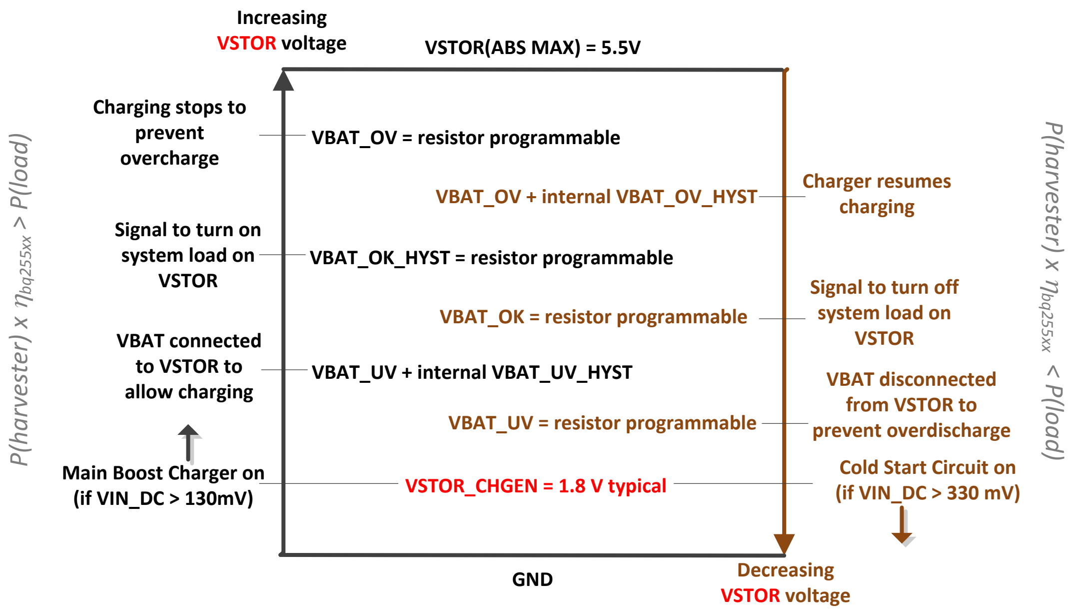

Figure 11. Summary of VSTOR Threshold Voltages

8.3.5 Nano-Power Management and Efficiency

The high efficiency of the bq25504 charger is achieved via the proprietary Nano-Power management circuitry and algorithm. This feature essentially samples and holds the VSTOR voltage in order to reduce the average quiescent current. That is, the internal circuitry is only active for a short period of time and then off for the remaining period of time at the lowest feasible duty cycle. A portion of this feature can be observed in Figure 19 where the VRDIV node is monitored. Here the VRDIV node provides a connection to the VSTOR voltage (first pulse) and then generates the reference levels for the VBAT_OV and VBAT_OK resistor dividers for a short period of time. The divided down values at each pin arecompared against VBIAS as part of the hysteretic control. Since this biases a resistor string, the current through these resistors is only active when the Nano-Power management circuitry makes the connection—hence reducing the overall quiescent current due to the resistors. This process repeats every 64 ms.

The bq25504's boost charger efficiency is shown for various input power levels in Figure 1 through Figure 7. All data points were captured by averaging the overall input current. This must be done due to the periodic biasing scheme implemented via the Nano-Power management circuitry. In order to properly measure the resulting input current when calculating the output to input efficiency, the input current efficiency data was gathered using a source meter set to average over at least 50 samples. Quiescent current curves into VSTOR over temperature and voltage is shown at Figure 8.

8.4 Device Functional Modes

The bq25504 has three functional modes: cold-start operation, main boost charger enabled and thermal shutdown. The cold start circuitry is powered from VIN_DC. The main boost charger circuitry is powered from VSTOR while the boost power stage is powered from VIN_DC. Details of entering and exiting each mode are explained below.

8.4.1 Cold-Start Operation (VSTOR < VSTOR_CHGEN, VIN_DC > VIN(CS) and PIN > PIN(CS))

Whenever VSTOR < VSTOR_CHGEN, VIN_DC ≥ VIN(CS) and PIN > PIN(CS), the cold-start circuit is on. This could happen when there is not input power at VIN_DC to prevent the load from discharging the battery or during a large load transient on VSTOR. During cold start, the voltage at VIN_DC is clamped to VIN(CS) so the energy harvester's output current is critical to providing sufficient cold start input power, PIN(CS) = VIN(CS) X IIN(CS). The cold-start circuit is essentially an unregulated, hysteretic boost converter with lower efficiency compared to the main boost charger. None of the other features function during cold start operation. The cold start circuit's goal is to charge VSTOR higher than VSTOR_CHGEN so that the main boost charger can operate. When a depleted storage element is initially attached to VBAT, as shown in Figure 12 and the harvester can provide a voltage > VIN(CS) and total power at least > PIN(CS), assuming minimal system load or leakage at VSTOR and VBAT, the cold start circuit can charge VSTOR above VSTOR_CHGEN. Once the VSTOR voltage reaches the VSTOR_CHGEN threshold, the IC

1. first performs an initialization pulse on VRDIV to reset the feedback voltages,
2. then disables the charger for 32 ms (typical) to allow the VIN_DC voltage to rise to the harvester's open-circuit voltage which will be used as the input voltage regulation reference voltage until the next MPPT sampling cycle and
3. lastly performs its first feedback sampling using VRDIV, approximately 64 ms after the initialization pulse.

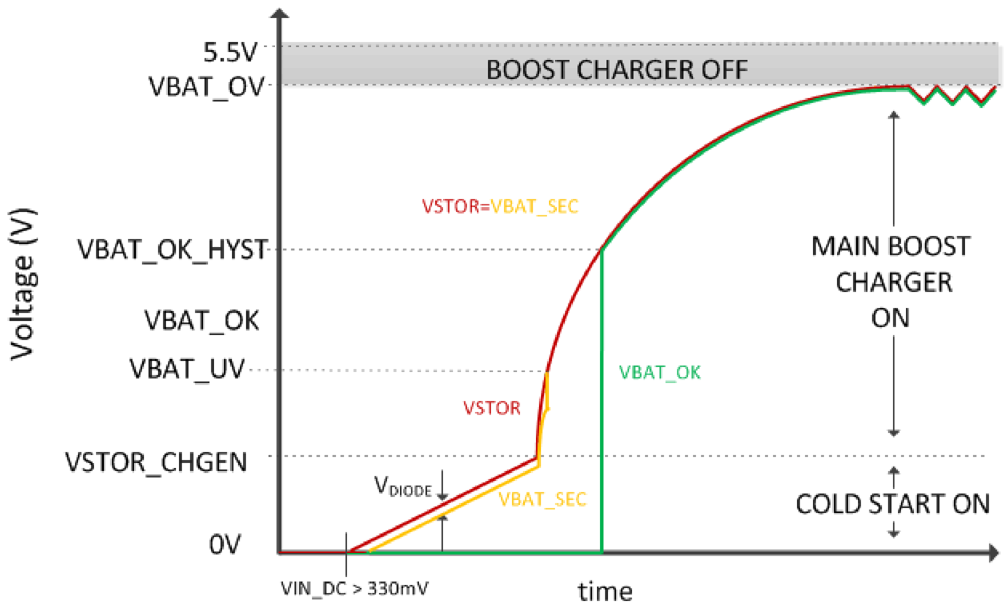

Figure 12. Charger Operation After a Depleted Storage Element is Attached and Harvester is Available

The energy harvester must supply sufficient power for the IC to exit cold start. Due to the body diode of the PFET connecting VSTOR and VBAT, the cold start circuit must charge both the capacitor on CSTOR up to the VSTOR_CHGEN and the storage element connected to VBAT up to VSTOR_CHGEN less a diode drop. When a rechargeable battery with an open protector is attached, the intial charge time is typically short due to the minimum charge needed to close the battery's protector FETs. When large, discharged super capacitors with high DC leakage currents are attached, the intial charge time can be signficant.

Device Functional Modes (continued)

When the VSTOR voltage reaches VSTOR_CHGEN, the main boost charger starts up. When the VSTOR voltage rises to the VBAT_UV threshold, the PMOS switch between VSTOR and VBAT turns on, which provides additional loading on VSTOR and could result in the VSTOR voltage dropping below both the VBAT_UV threshold and the VSTOR_CHGEN voltage, especially if system loads on VSTOR or VBAT are active during this time. Therefore, it is not uncommon for the VSTOR voltage waveform to have incremental pulses (i.e. stair steps) as the IC cycles between cold-start and main boost charger operation before eventually maintaing VSTOR above VSTOR_CHGEN.

The cold start circuit initially clamps VIN_DC to VIN(CS) = 330 mV typical. If sufficient input power (i.e.,output current from the harvester clamped to VIN(CS)) is not available, it is possible that the cold start circuit cannot raise the VSTOR voltage above VSTOR_CHGEN in order for the main boost conveter to start up. It is highly recommended to add an external PFET between the system load and VSTOR. An inverted VBAT_OK signal can be used to drive the gate of this system-isolating, external PFET. See the *Power Supply Recommendations* section for guidance on minimum input power requirements.

8.4.2 Main Boost Charger Enabled (VSTOR > VSTOR_CHGEN, VIN_DC > VIN(DC) and $\overline{\text{EN}}$ = LOW)

One way to avoid cold start is to attach a partially charged storage element as shown in Figure 13.

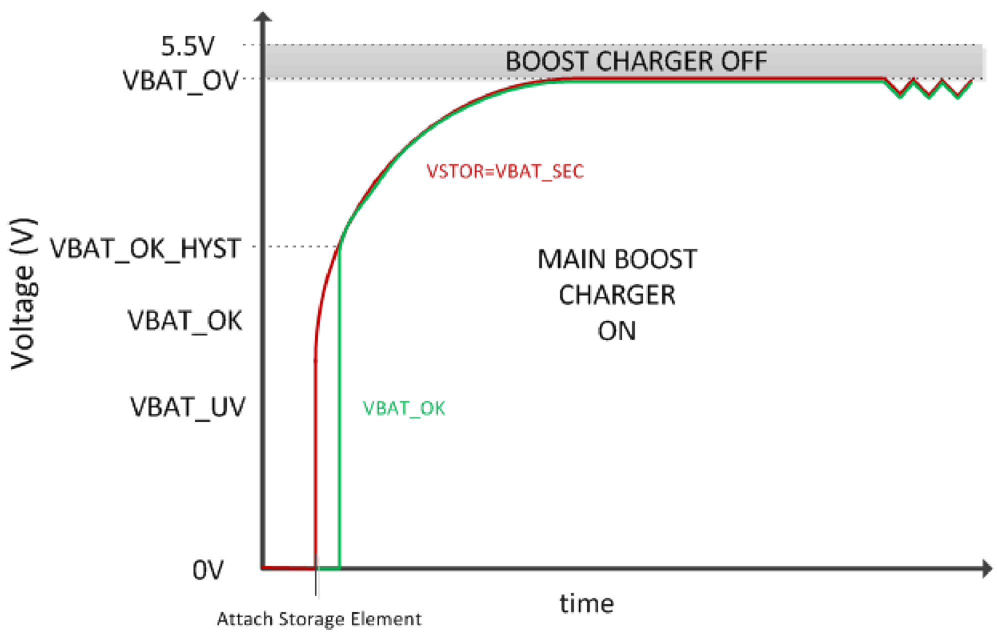

Figure 13. Charger Operation after a Partially Charged Storage Element is Attached and Harvester Power is Available

When no input source is attached, the VSTOR node should be discharged to ground before attaching a storage element. Hot-plugging a storage element that is charged (e.g., the battery protector PFET is closed) and with the VSTOR node more than 100 mV above ground results in the PFET between VSTOR and VBAT remaining off until an input source is attached.

Assuming the voltages on VSTOR and VBAT are both below 100mV, when a charged storage element is attached (i.e. hot-plugged) to VBAT, the IC.

1. first turns on the internal PFET between the VSTOR and VBAT pins for $t_{BAT\_HOT\_PLUG}$ (45ms) in order to charge VSTOR to VSTOR_CHGEN then turns off the PFET to prevent the battery from overdischarge,
2. then performs an initialization pulse on VRDIV to reset the feedback voltages,
3. then disables the charger for 32 ms (typical) to allow the VIN_DC voltage to rise to the harvester's open-circuit voltage which will be used as the input voltage regulation reference voltage until the next MPPT sampling cycle and
4. lastly performs its first feedback sampling using VRDIV, approximately 64 ms after the initialization pulse.

Device Functional Modes (continued)

If the VSTOR pin voltage remains above the internal under voltage threshold (VBAT_UV) for the additional 64 ms after the VRDIV initialization pulse (following the 45-ms PFET on time), the internal PFET turns back on and the main boost charger begins to charge the storage element assuming there is sufficient power available from the harvester at the VIN_DC pin. If VSTOR does not reach the VBAT_UV threshold, then the PFET remains off until the main boost charger can raise the VSTOR voltage to VBAT_UV. If a system load tied to VSTOR discharges VSTOR below VSTOR_GEN or below VBAT_UV during the 32 ms initial MPPT reference voltage measurement or within 110 ms after hot plug, it is recommended to add an external PFET between the system load and VSTOR. An inverted VBAT_OK signal can be used to drive the gate of this system-isolating, external PFET. Otherwise, the VSTOR voltage waveform will have incremental pulses as the IC turns on and off the internal PFET controlled by VBAT_UV or cycles between cold-start and main boost charger operation.

Once VSTOR is above VSTOR_CHGEN, the main boost charger employs pulse frequency modulation (PFM) mode of control to regulate the voltage at VIN_DC close to the desired reference voltage. The reference voltage is set by the MPPT control scheme as described in the features section. Input voltage regulation is obtained by transferring charge from the input to VSTOR only when the input voltage is higher than the voltage on pin VREF_SAMP. The current through the inductor is controlled through internal current sense circuitry. The peak current in the inductor is dithered internally to up to three pre-determined levels in order to maintain high efficiency of the charger across a wide input current range. The charger transfers up to a maximum of 100 mA average input current (230mA typical peak inductor current). The boost charger is disabled when the voltage on VSTOR reaches the user set VBAT_OV threshold to protect the battery connected at VBAT from overcharging. In order for the battery to charge to VBAT_OV, the input power must exceed the power needed for the load on VSTOR. See the *Power Supply Recommendations* section for guidance on minimum input power requirements.

Steady state operation for the boost charger is shown in Figure 16. These plots highlight the inductor current, the VSTOR voltage ripple, input voltage regulation and the LBOOST switching node. The cycle-by-cycle minor switching frequency is a function of the boost converter's inductor value, peak current limit and voltage levels on each side of each inductor. Once the VSTOR capacitor, CSTOR, droops below a minimum value, the hysteretic switching repeats.

CAUTION

If VIN_DC is higher than VSTOR and VSTOR is higher than VBAT_OV, the input VIN_DC is pulled to ground through a small resistance to stop further charging of the attached battery or capacitor. It is critical that if this case is expected, the impedance of the source attached to VIN_DC be higher than 20 Ω and not a low impedance source.

8.4.3 Thermal Shutdown

Rechargeable Li-ion batteries need protection from damage due to operation at elevated temperatures. The application should provide this battery protection and ensure that the ambient temperature is never elevated greater than the expected operational range of 85°C.

The bq25504 uses an integrated temperature sensor to monitor the junction temperature of the device. If the OT_PROG pin is tied low, then the temperature threshold for thermal protection is set to TSD_ProtL which is 65°C typically. If the OT_PROG is tied high, then the temperature is set to TSD_ProtH which is 120°C typically. Once the temperature threshold is exceeded, the boost converter/charger is disabled and charging ceases. Once the temperature of the device drops below this threshold, the boost converter and or charger can resume operation. To avoid unstable operation near the overtemp threshold, a built-in hysteresis of approximately 5°C has been implemented. Care should be taken to not over discharge the battery in this condition since the boost converter/charger is disabled. However, if the supply voltage drops to the VBAT_UV setting, then the switch between VBAT and VSTOR will open and protect the battery even if the device is in thermal shutdown.

9 Application and Implementation

NOTE

Information in the following applications sections is not part of the TI component specification, and TI does not warrant its accuracy or completeness. TI's customers are responsible for determining suitability of components for their purposes. Customers should validate and test their design implementation to confirm system functionality.

9.1 Application Information

9.1.1 Storage Element Selection

In order for the charge management circuitry to protect the storage element from over-charging or discharging, the storage element must be connected to VBAT pin and the system load tied to the VSTOR pin. Many types of elements can be used, such as capacitors, super capacitors or various battery chemistries. A storage element with 100 uF equivalent capacitance is required to filter the pulse currents of the PFM switching charger. The equivalent capacitance of a battery can be computed as computed as:

$$C_{EQ} = 2 \text{ x } mAHr_{BAT(CHRGD)} \text{ x } 3600 \text{ s/Hr} / V_{BAT(CHRGD)} \quad (6)$$

In order for the storage element to be able to charge VSTOR capacitor (CSTOR) within the $t_{VB\_HOT\_PLUG}$ (50 ms typical) window at hot-plug; therefore preventing the IC from entering cold start, the time constant created by the storage element's series resistance (plus the resistance of the internal PFET switch) and equivalent capacitance must be less than $t_{VB\_HOT\_PLUG}$. For example, a battery's resistance can be computed as:

$$R_{BAT} = V_{BAT} / I_{BAT(CONTINUOUS)} \text{ from the battery specifications.} \quad (7)$$

The storage element must be sized large enough to provide all of the system load during periods when the harvester is no longer providing power. The harvester is expected to provide at least enough power to fully charge the storage element while the system is in low power or sleep mode. Assuming no load on VSTOR (i.e., the system is in low power or sleep mode), the following equation estimates charge time from voltage VBAT1 to VBAT2 for given input power is:

Refer to SLUC462 for a design example that sizes the storage element.

$$PIN \times \eta_{EST} \times t_{CHRG} = 1/2 \times CEQ \text{ X } (VBAT2^2 - VBAT1^2) \quad (8)$$

Note that if there are large load transients or the storage element has significant impedance then it may be necessary to increase the CSTOR capacitor from the 4.7uF minimum or add additional capacitance to VBAT in order to prevent a droop in the VSTOR voltage. See below for guidance on sizing capacitors.

9.1.2 Inductor Selection

The boost charger needs an appropriately sized inductor for proper operation. The inductor's saturation current should be at least 25% higher than the expected peak inductor currents recommended below if system load transients on VSTOR are expected. Since this device uses hysteretic control, the boost charger is considered naturally stable systems (single order transfer function).

For the boost charger to operate properly, an inductor of appropriate value must be connected between LBOOST, pin 20, and VIN_DC, pin 2. The boost charger internal control circuitry is designed to control the switching behavior with a nominal inductance of 22 µH ± 20%. The inductor must have a peak current capability of > 300 mA with a low series resistance (DCR) to maintain high efficiency.

A list of inductors recommended for this device is shown in Table 1.

Table 1. Recommended Inductors

Inductance (µH)	Dimensions (mm)	Part Number	Manufacturer (1)
22	4.0x4.0x1.7	LPS4018-223M	Coilcraft
22	3.8x3.8x1.65	744031220	Wurth
22	2.8x2.8x2.8	744025220	Wurth

(1) See **WHAT?** concerning recommended third-party products.

9.1.3 Capacitor Selection

In general, all the capacitors need to be low leakage. Any leakage the capacitors have will reduce efficiency, increase the quiescent current and diminish the effectiveness of the IC for energy harvesting.

9.1.3.1 VREF_SAMP Capacitance

The MPPT operation depends on the sampled value of the open circuit voltage and the input regulation follows the voltage stored on the CREF capacitor. This capacitor is sensitive to leakage since the holding period is around 16 seconds. As the capacitor voltage drops due to any leakage, the input regulation voltage also drops preventing proper operation from extraction the maximum power from the input source. Therefore, it is recommended that the capacitor be an X7R or COG low leakage capacitor.

9.1.3.2 VIN_DC Capacitance

Energy from the energy harvester input source is initially stored on a capacitor, CIN, connected to VIN_DC, pin 2, and VSS, pin 1. For energy harvesters which have a source impedance which is dominated by a capacitive behavior, the value of the harvester capacitor should scaled according to the value of the output capacitance of the energy source, but a minimum value of 4.7 µF is recommended.

9.1.3.3 VSTOR Capacitance

Operation of the bq25504 requires two capacitors to be connected between VSTOR, pin 15, and VSS, pin 1. A high frequency bypass capacitor of at 0.1 µF should be placed as close as possible between VSTOR and VSS. In addition, a low ESR capacitor of at least 4.7 µF should be connected in parallel.

9.1.3.4 Additional Capacitance on VSTOR or VBAT

If there are large, fast system load transients and/or the storage element has high resistance, then the CSTOR capacitors may momentarily discharge below the VBAT_UV threshold in response to the transient. This causes the bq25504 to turn off the PFET switch between VSTOR and VBAT and turn on the boost charger. The CSTOR capacitors may further discharge below the VSTOR_CHGEN threshold and cause the bq25504 to enter Cold Start. For instance, some Li-ion batteries or thin-film batteries may not have the current capacity to meet the surge current requirements of an attached low power radio. To prevent VSTOR from drooping, either increasing the CSTOR capacitance or adding additional capacitance in parallel with the storage element is recommended. For example, if boost charger is configured to charge the storage element to 4.2 V and a 500 mA load transient of 50 µs duration infrequently occurs, then, solving I = C x dv/dt for CSTOR gives:

$$\text{CSTOR} \geq \frac{500\ \text{mA} \times 50\ \mu\text{s}}{(4.2\ \text{V} - 1.8\ \text{V})} = 10.5\ \mu\text{F} \tag{9}$$

Note that increasing CSTOR is the recommended solution but will cause the boost charger to operate in the less efficient cold start mode for a longer period at startup compared to using CSTOR = 4.7 µF. If longer cold start run times are not acceptable, then place the additional capacitance in parallel with the storage element.

For a recommended list of standard components, see the EVM User's Guide (SLUUAA8).

9.2 Typical Applications

9.2.1 Solar Application Circuit

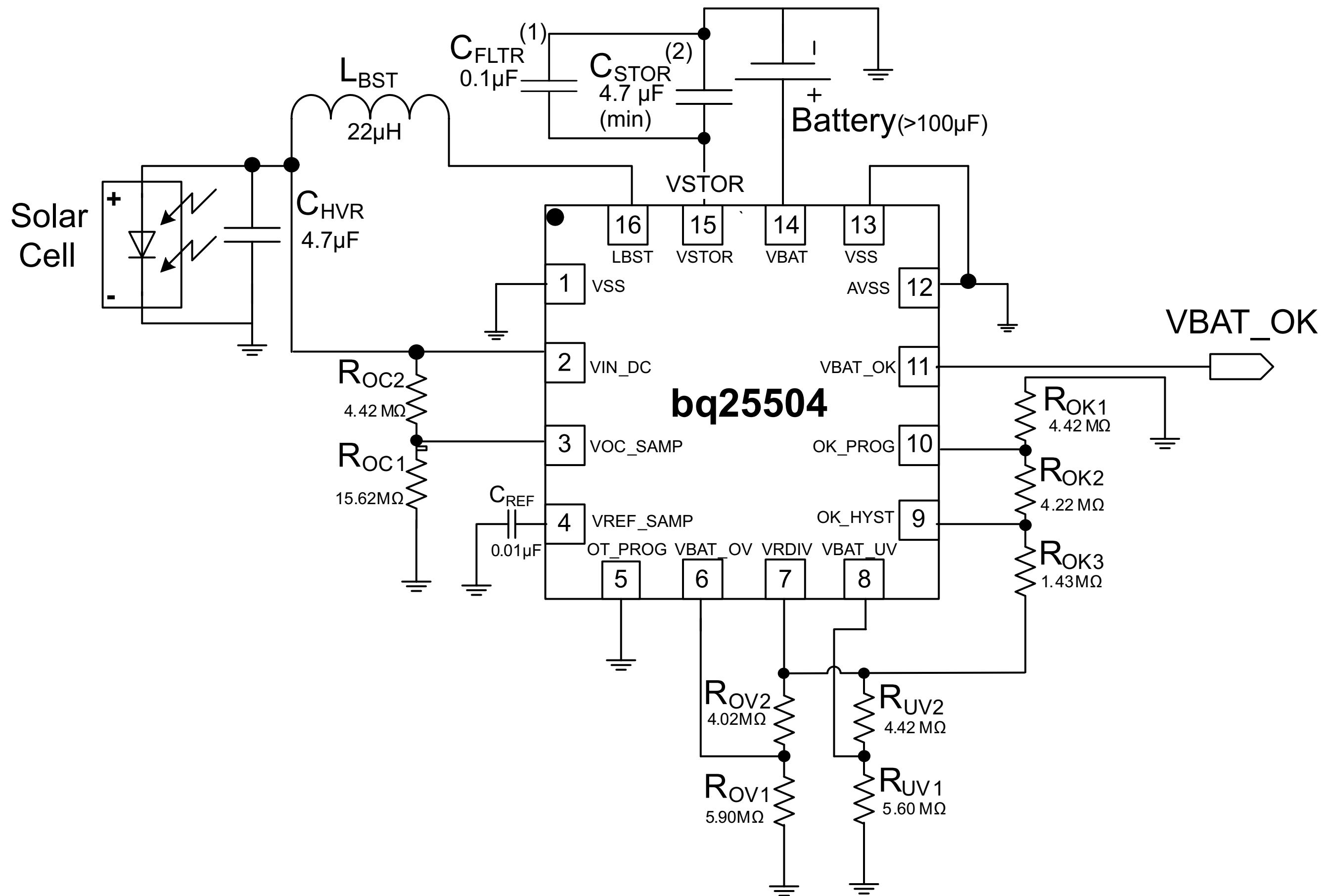

(1) Place close as possible to IC pin 15 (VSTOR) and pin 13 (VSS)

(2) See the Capacitor Selection section for guidance on sizing C_{STOR}

Figure 14. Typical Solar Application Circuit

9.2.1.1 Design Requirements

The desired voltage levels are VBAT_OV = 3.15 V, VBAT_UV = 2.20 V, VBAT_OK = 2.44 V, VBAT_OK_HYST = 2.80 V and MPP (V_{OC}) = 78% which is typical for solar panels. There are no large load transients expected. The IC must stop charging if its junction temperature is above 65°C. The simulated solar panel open circuit voltage is 1.0 V.

9.2.1.2 Detailed Design Procedure

The recommended L1 = 22 µH, CBYP=0.1 µF and low leakage CREF = 10 nF are selected. In order to ensure the fastest recovery of the harvester output voltage to the MPPT level following power extraction, the minimum recommended CIN = 4.7 µF is selected. Because no large system load transients are expected and to ensure fast charge time during cold start, the minimum recommended CSTOR = 4.7 µF. To stop charging when the IC junction temperature is above 65°C, the OT_PROG pin is tied to ground.

- With VBAT_UV < VBAT_OV ≤ 5.5 V, to size the VBAT_OV resistors, first choose $RSUM_{OV} = R_{OV1} + R_{OV2}$ = 10 MΩ then solve Equation 3 for

$$R_{OV1} = \frac{3}{2} \times \frac{RSUM_{OV} \times VBIAS}{VBAT\_OV} \times \frac{3}{2}\frac{10\ M\Omega \times 1.25\ V}{3.15\ V} = 5.95\ M\Omega \rightarrow 5.90\ M\Omega \text{ closest 1\% value then} \quad (10)$$

- $R_{OV2} = RSUM_{OV} - R_{OV1}$ = 10 MΩ - 5.95 MΩ = 4.05 MΩ → 4.02 MΩ resulting in VBAT_OV = 3.15 V

Typical Applications (continued)

- To size the VBAT_UV resistors, first choose $RSUM_{UV} = R_{UV1} + R_{UV2} = 10\ M\Omega$ then solve Equation 2 for

$$R_{UV1} = \frac{RSUM_{UV} \times VBIAS}{VBAT_{UV}} = \frac{10\ M\Omega \times 1.25\ V}{2.2\ V} = 5.68\ M\Omega \rightarrow 5.60\ M\Omega \text{ closest 1\% value then} \tag{11}$$

- $R_{UV2} = RSUM_{UV} - R_{UV1} = 10\ M\Omega - 5.60\ M\Omega = 4.4\ M\Omega \rightarrow 4.42\ M\Omega$ closest 1% resistor resulting in VBAT_UV = 2.2 V.
- With VBAT_OV ≥ VBAT_OK_HYST > VBAT_OK ≥ VBAT_UV, to size the VBAT_OK and VBAT_OK_HYST resistors,
  first choose $RSUM_{OK} = R_{OK1} + R_{OK2} + R_{OK3} = 10\ M\Omega$ then solve Equation 4 and Equation 5 for

$$R_{OK1} = \frac{VBIAS \times RSUM_{OK}}{VBAT\_OK\_HYST} = \left(\frac{1.25\ V}{2.8\ V}\right) \times 10\ M\Omega = 4.46\ M\Omega \rightarrow 4.42\ M\Omega \text{ closest 1\% resistor then} \tag{12}$$

$$R_{OK2} = \left(\frac{VBAT\_OK\_PROG}{VBIAS} - 1\right) \times R_{OK1} = \left(\frac{2.45\ V}{1.25\ V} - 1\right) \times 4.24\ M\Omega = 4.07\ M\Omega, \text{ then} \tag{13}$$

- $R_{OK3} = RSUM_{OK} - R_{OK1} - R_{OK2} = 10\ M\Omega - 4.42\ M\Omega - 4.22\ M\Omega = 1.36\ M\Omega \rightarrow 1.43\ M\Omega$ to give VBAT_OK = 2.44 V and VBAT_OK_HYST = 2.85 V.
- Keeping in mind that VREF_SAMP stores the MPP voltage for the harvester, first choose $RSUM_{OC} = R_{OC1} + R_{OC2} = 20\ M\Omega$ then solve Equation 1 for

$$R_{OC1} = \left(\frac{VREF\_SAMP}{VIN\_DC(OC)}\right) \times RSUM_{OC} = 0.78 \times 20\ M\Omega = 15.6\ M\Omega, \text{ then} \tag{14}$$

$$R_{OC2} = RSUM_{OC} \times \left(1 - \frac{VREF\_SAMP}{VIN\_DC(OC)}\right) = 20\ M\Omega(1 - 0.78) = 4.4\ M\Omega \text{ closest 1\% resistors} \tag{15}$$

- SLURAQ1 provides help on sizing and selecting the resistors.

9.2.1.3 Application Curves

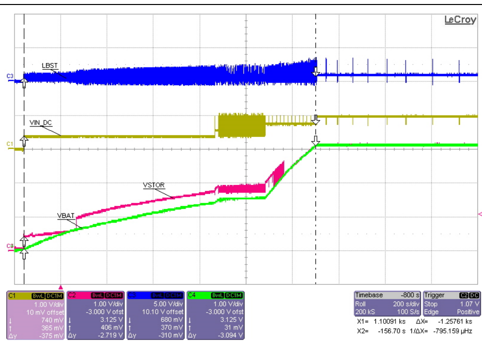

VINDC = sourcemeter with V_{SOURCE} = 1.0 V and compliance of 2.75 mA
VBAT connected to 0.1 F depleted supercap
No resistance load on VSTOR

Figure 15. Startup into Depleted Storage Element

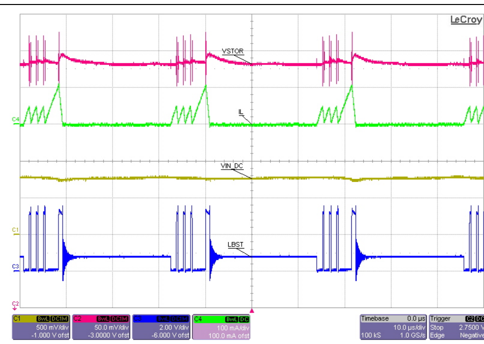

VIN_DC = sourcemeter with V_{SOURCE} = 1 V and compliance of 10.5 mA
VBAT = 0.1 F supercap
VSTOR = 2 kΩ resistive load

Figure 16. Boost Charger Operational Waveforms

Typical Applications (continued)

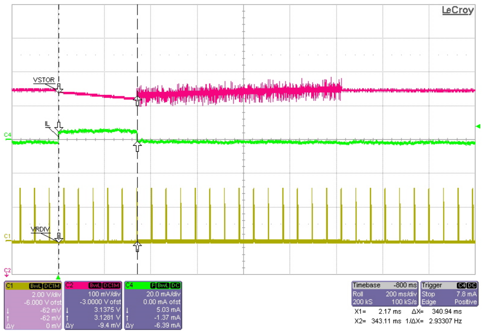

VIN_DC = sourcemeter with V_{SOURCE} = 1 V and compliance of 10.5 mA

VBAT = 0.1 F supercap

VSTOR = open to 500 Ω to open resistive load (IL = load current on VSTOR)

Figure 17. 5 mA Load Transient on VSTOR

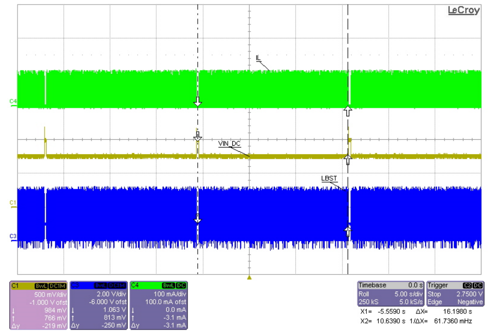

VIN_DC = sourcemeter with V_{SOURCE} = 1 V and compliance of 10.5 mA

VBAT = sourcemeter with V_{SOURCE} = 2.8V and compliance of 1A

IL = inductor current

Figure 18. MPPT Operation

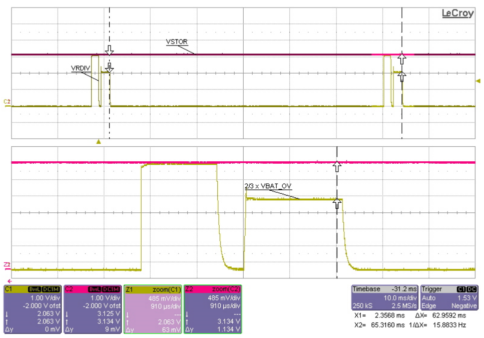

VIN_DC = sourcemeter with V_{SOURCE} = 1 V and compliance of 10.5 mA

VBAT = sourcemeter with V_{SOURCE} = 2.8 V and compliance of 1A

Figure 19. VRDIV Operation

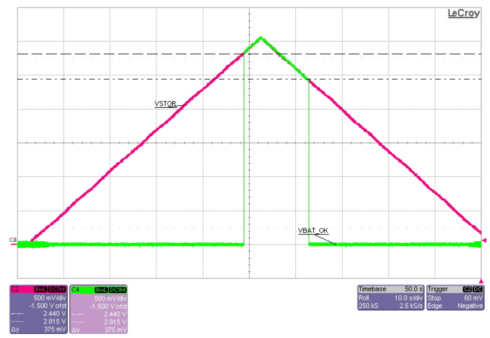

VIN_DC = sourcemeter with V_{SOURCE} = 1 V and compliance of 2.75 mA

No storage element on VBAT

VSTOR artificially ramped from 0V to 3.15 V to 0 V using a power amp driven by a function generator

Figure 20. VBAT_OK Operation

Typical Applications (continued)

9.2.2 TEG Application Circuit

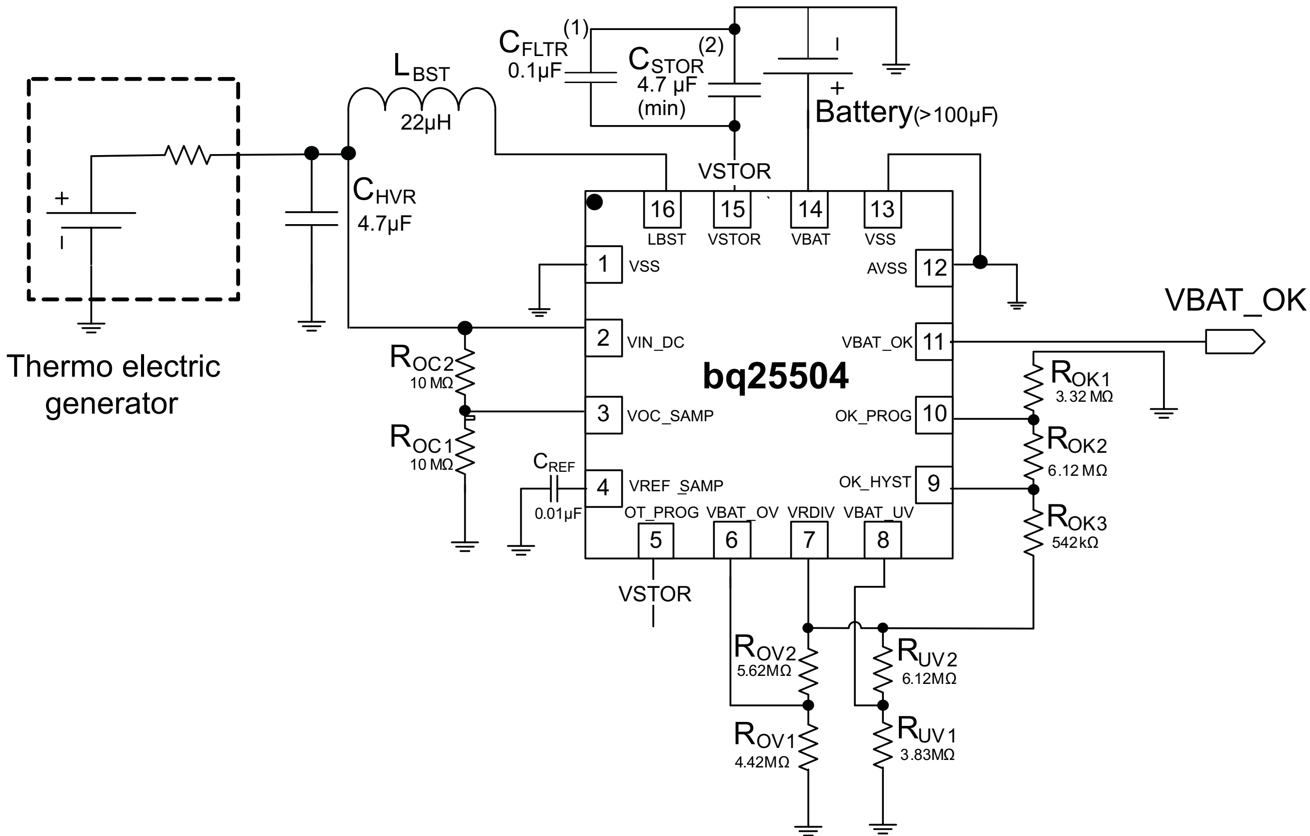

(1) Place close as possible to IC pin 15 (VSTOR) and pin 13 (VSS)

(2) See the Capacitor Selection section for guidance on sizing C_{STOR}

Figure 21. Typical TEG Application Circuit

9.2.2.1 Design Requirements

The desired voltage levels are VBAT_OV = 4.25 V, VBAT_UV = 3.20 V, VBAT_OK = 3.55 V, VBAT_OK_HYST = 3.76 V and MPP (V_{OC}) = 50% which is typical for TEG harvesters. The IC must stop charging if its junction temperature is above 120°C. The simulated TEG open circuit voltage is 1.0 V.

9.2.2.2 Detailed Design Procedure

The recommended L1 = 22 µH, CBYP=0.1 µF and low leakage CREF = 10 nF are selected. In order to ensure the fastest recovery of the harvester output voltage to the MPPT level following power extraction, the minimum recommended CIN = 4.7 µF is selected. Because no large system load transients are expected and to ensure fast charge time during cold start, the minimum recommended CSTOR = 4.7 µF. To stop charging when the IC junction temperature is above 120°C, the OT_PROG pin is tied to VSTOR.

Referring back to the procedure in *Detailed Design Procedure* or using the spreadsheet calculator at SLURAQ1 gives the following values:

- R_{OV1} = 4.42 MΩ, R_{OV2} = 5.49 MΩ resulting in VBAT_OV = 4.26 V due to rounding to the nearest 1% resistor.
- R_{UV1} = 3.83 MΩ, R_{UV2} = 6.04 MΩ resulting in VBAT_UV = 3.22 V due to rounding to the nearest 1% resistor
- R_{OK1} = 3.32 MΩ, R_{OK2} = 6.04 MΩ, R_{OK3} = 0.536 MΩ resulting in VBAT_OK = 3.52 V and VBAT_OK_HYST = 3.73 V after rounding.
- R_{OC1} = 10 MΩ and R_{OC2} = 10 MΩ gives 50% MPP voltage.

Typical Applications (continued)

9.2.2.3 Application Curves

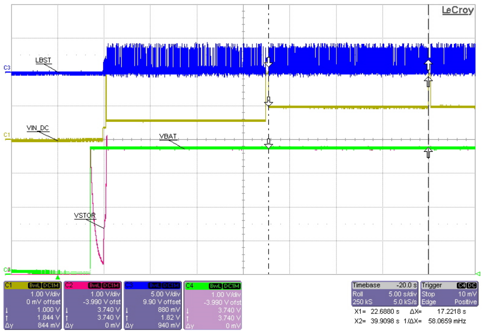

VINDC = sourcemeter with V_{SOURCE} = 2.0 V and compliance of 1 mA

VBAT connected to LiIon battery

VSTOR = 50 kΩ resistor

Figure 22. Startup by Attaching Charged Storage Element

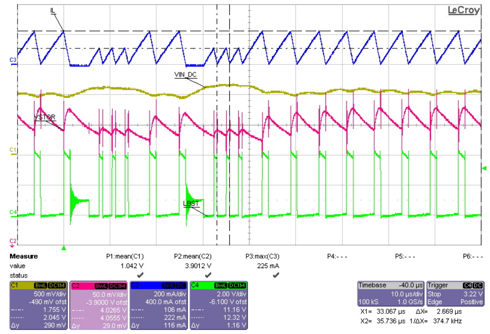

VIN_DC = sourcemeter with V_{SOURCE} = 2.0 V and compliance of 100 mA

VBAT connected to LiIon battery

VSTOR = 100 kΩ resistive load (IL = inductor current)

Figure 23. Boost Charger Operational Waveforms

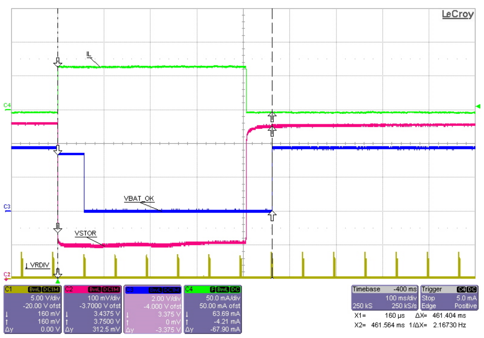

VIN_DC = sourcemeter with V_{SOURCE} = 2.0 V and compliance of 1 mA

VBAT connected to LiIon battery

VSTOR = open to 50Ω to open resistive load (IL = load current on VSTOR)

Figure 24. 50 mA Load Transient on VSTOR

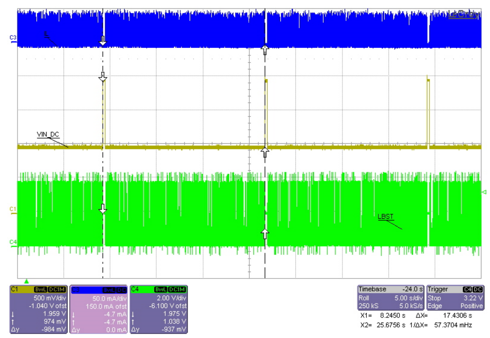

VIN_DC = sourcemeter with V_{SOURCE} = 2.0 V and compliance of 1 mA

VBAT connected to LiIon battery

IL = inductor current

Figure 25. MPPT Operation

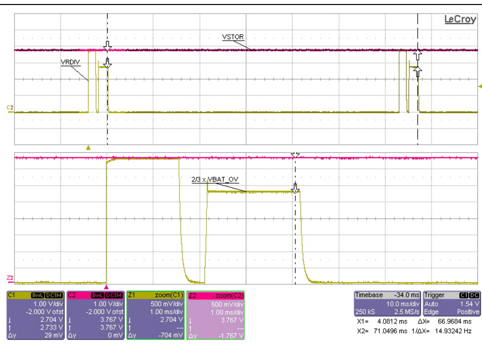

VIN_DC = sourcemeter with V_{SOURCE} = 2.0 V and compliance of 1 mA

VBAT connected to LiIon battery

Figure 26. VRDIV Operation

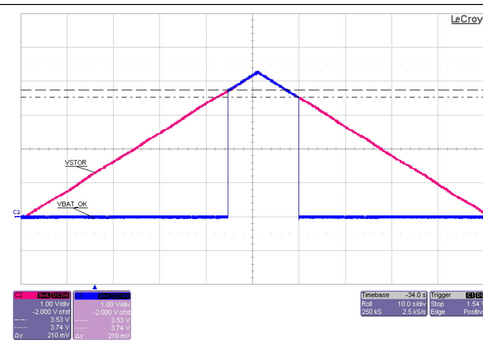

VIN_DC = sourcemeter with V_{SOURCE} = 2.0 V and compliance of 1 mA

No storage element on VBAT

VSTOR artificially ramped from 0V to 4.25V to 0V using a power amp driven by a function generator

Figure 27. VBAT_OK Operation

Typical Applications (continued)

9.2.3 MPPT Disabled, Low Impedance Source Application Circuit

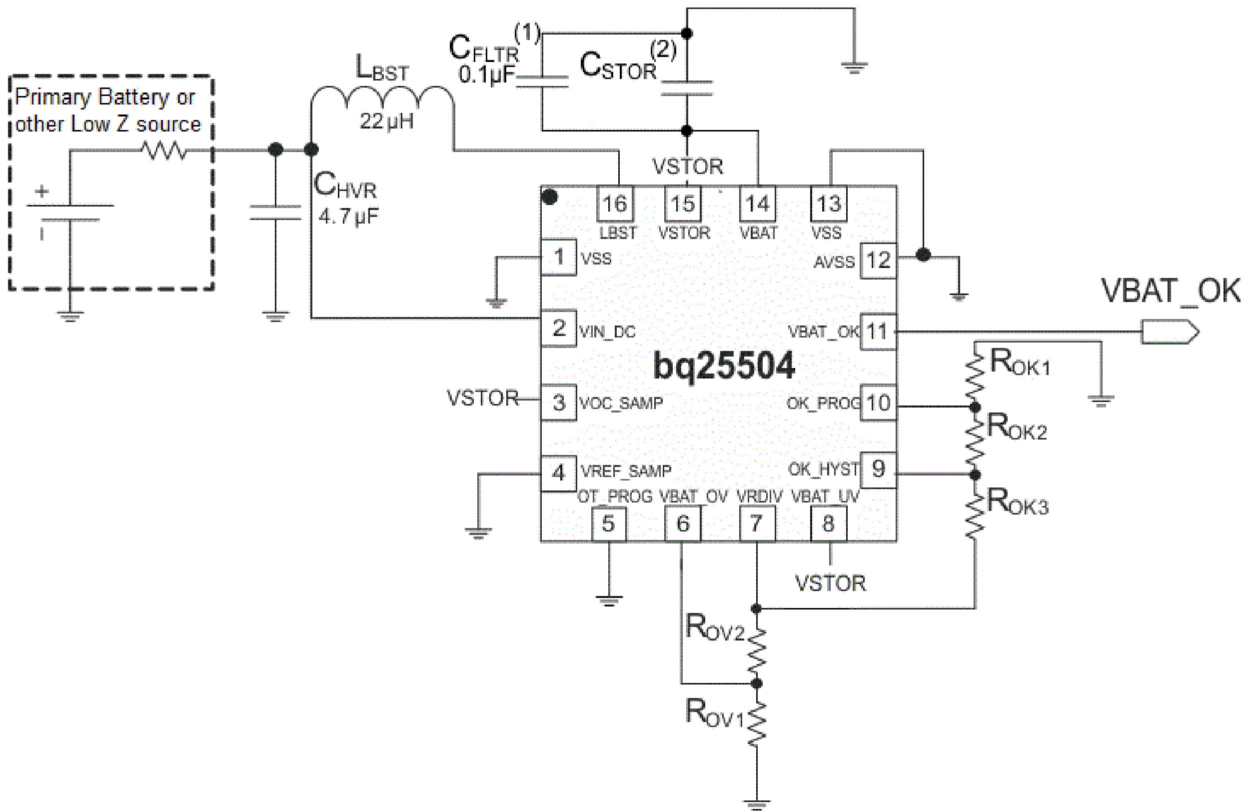

(1) Place close as possible to IC pin 15 (VSTOR) and pin 13 (VSS)

(2) See the Capacitor Selection section for guidance on sizing C_{STOR}

Figure 28. Typical MPPT Disabled Application Circuit (Low Iq Boost Converter from Low Impedance Source)

9.2.3.1 Design Requirements

The input source is a low impedance 1.2 V battery therefore MPPT is not needed. The output will be a low ESR capacitor therefore VSTOR can be tied to VBAT and VBAT_UV is not needed. The desired voltage levels are VBAT_OV = 3.30 V, VBAT_OK = 2.80 V, VBAT_OK_HYST = 3.10 V, and MPPT disabled. The IC must stop charging if its junction temperature is above 65°C. Load transients are expected.

9.2.3.2 Detailed Design Procedure

The recommended L1 = 22 µH, CBYP=0.1 µF and low leakage CREF = 10 nF are selected. The minimum recommended CIN = 4.7 µF is selected. To prevent VSTOR from drooping during system load transients, CSTOR is set to 100 µF. To disable the sampling for MPPT, the VOC_SAMP pin is tied to VSTOR. To disable the input voltage regulation circuit, the VREF_SAMP pin is tied to GND. Since the VBAT_UV function is not needed, the VBAT_UV can be tied to VSTOR. To stop charging when the IC junction temperature is above 65°C, the OT_PROG pin is tied to GND.

Referring back to the procedure in *Detailed Design Procedure* or using the spreadsheet calculator at SLURAQ1 gives the following values:

- R_{OV1} = 5.62 MΩ, R_{OV2} = 4.22 MΩ resulting in VBAT_OV = 3.28 V due to rounding to the nearest 1% resistor.
- R_{OK1} = 4.12 MΩ, R_{OK2} = 5.11 MΩ, R_{OK3} = 0.976 MΩ resulting in VBAT_OK = 2.80 V and VBAT_OK_HYST = 3.10 V after rounding.

Typical Applications (continued)

9.2.3.3 Application Curves

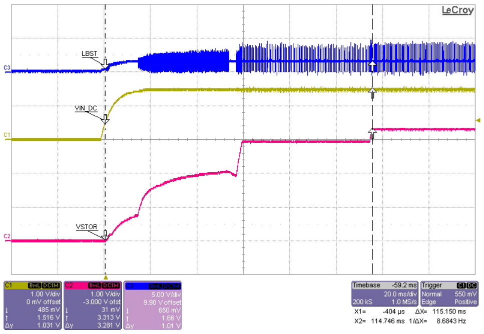

VIN_DC = low impedance voltage source = 1.5 V
VBAT = VSTOR = 100 µF
VSTOR = 500 Ω resistor

Figure 29. Startup

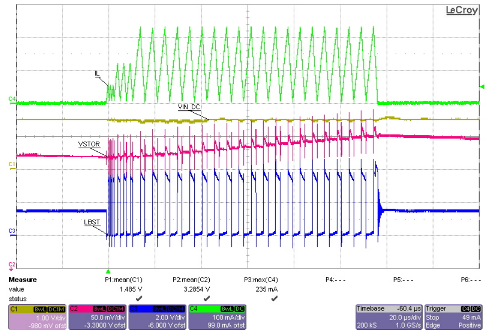

VIN_DC = low impedance voltage source = 1.5 V
VBAT = VSTOR = 100 µF
VSTOR = 330 Ω resistive load (IL = inductor current)

Figure 30. Boost Charger Operational Waveforms

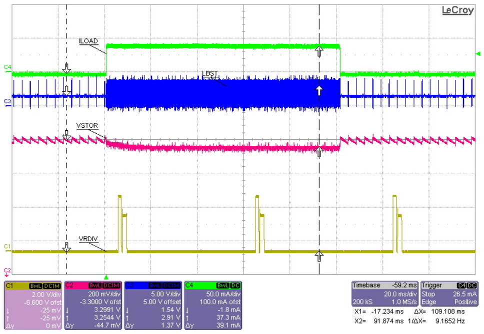

VIN_DC = low impedance voltage source = 1.5 V)
VBAT = VSTOR = 100 µF
VSTOR = open to 75 Ω to open resistive load (IL = load current on VSTOR

Figure 31. 40 mA Load Transient on VSTOR

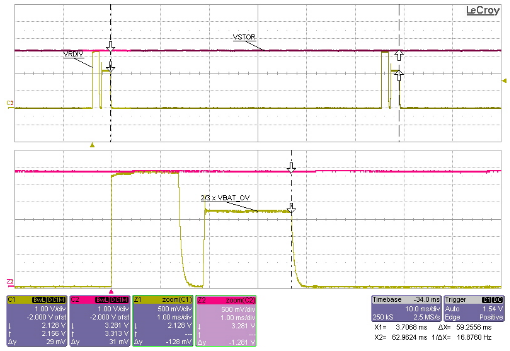

VIN_DC = low impedance voltage source = 1.5 V
VBAT = VSTOR = 100 µF

Figure 32. VRDIV Operation

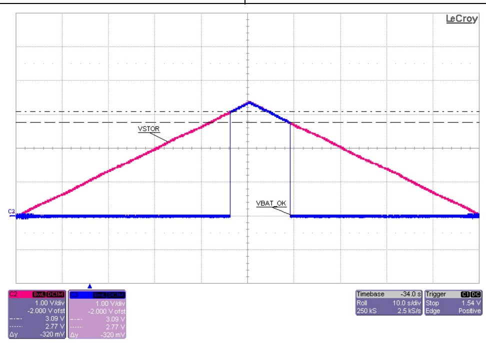

VIN_DC = low impedance voltage source = 1.5 V
VBAT = VSTOR = 100 µF
VSTOR artificially ramped from 0 V to 3.3 V to 0 V using a power amp driven by a function generator

Figure 33. VBAT_OK Operation

10 Power Supply Recommendations

The energy harvesting source (e.g., solar panel, TEG, vibration element) must provide a minimum level of power for the IC to operate as designed. The IC's minimum input power required to exit cold start can be estimated as:

$$PIN > PIN(CS) = VIN(CS) \times IIN(CS) > \frac{\left(I-STR\_ELM\_LEAK_{@1.8V} \times 1.8V\right) + \frac{(1.8V)^2}{RSTOR(CS)}}{0.05} \quad (16)$$

where I-STR_ELM_LEAK$_{@1.8V}$ is the storage element leakage current at 1.8V and

RSTOR(CS) is the equivalent resistive load on VSTOR during cold start and 0.05 is an estimate of the worst case efficiency of the cold start circuit.

Once the IC is out of cold start and the system load has been activated (e.g., using the VBAT_OK signal), the energy harvesting element must provide the main boost charger with at least enough power to meet the average system load. Assuming RSTOR(AVG) represents the average resistive load on VSTOR, the simplified **equation below** gives an estimate of the IC's minimum input power needed during system operation:

$$PIN \times \eta_{EST} > PLOAD = \frac{(VBAT\_OV)^2}{RSTOR(AVG)} + VBAT\_OV \times I-STR\_ELM\_LEAK_{@VBAT\_OV} \quad (17)$$

where η_{EST} can be derived from the datasheet efficiency curves for the given input voltage and current and VBAT_OV. The simplified equation above assumes that, while the harvester is still providing power, the system goes into low power or sleep mode long enough to charge the storage element so that it can power the system when the harvester eventually is down. Refer to spreadsheet SLUC462 for a design example that sizes the energy harvester.

11 Layout

11.1 Layout Guidelines

As for all switching power supplies, the PCB layout is an important step in the design, especially at high peak currents and high switching frequencies. If the layout is not carefully done, the boost charger could show stability problems as well as EMI problems. Therefore, use wide and short traces for the main current path and for the power ground paths. The input and output capacitors as well as the inductors should be placed as close as possible to the IC. For the boost charger, first priority are the output capacitors, including the 0.1 uF bypass capacitor (CBYP), followed by CSTOR, which should be placed as close as possible between VSTOR, pin 15, and VSS, pin 1 or 13. Next, the input capacitor, CIN, should be placed as close as possible between VIN_DC, pin 2, and VSS, pin 1. Last in priority is the boost charger inductor, L1, which should be placed close to LBOOST, pin 16, and VIN_DC, pin 2 if possible. It is best to use vias and bottom traces for connecting the inductor to its respective pins instead of the capacitors.

To minimize noise pickup by the high impedance voltage setting nodes (VBAT_OV, VBAT_UV, OK_PROG, OK_HYST), the external resistors should be placed so that the traces connecting the midpoints of each divider to their respective pins are as short as possible. When laying out the non-power ground return paths (e.g. from resistors and CREF), it is recommended to use short traces as well, separated from the power ground traces and connected to AVSS pin 12. This avoids ground shift problems, which can occur due to superimposition of power ground current and control ground current. The PowerPad should not be used as a power ground return path.

The remaining pins are digital signals with minimal layout restrictions. See Figure 34 for an example layout.

In order to maximize efficiency at light load, the use of voltage level setting resistors > 1 MΩ is recommended. In addition, the sample and hold circuit output capacitor on VREF_SAMP must hold the voltage for 16 s. During board assembly, contaminants such as solder flux and even some board cleaning agents can leave residue that may form parasitic resistors across the physical resistors/capacitors and/or from one end of a resistor/capacitor to ground, especially in humid, fast airflow environments. This can result in the voltage regulation and threshold levels changing significantly from those expected per the installed components. Therefore, it is highly

Layout Guidelines (continued)

recommended that no ground planes be poured near the voltage setting resistors or the sample and hold capacitor. In addition, the boards must be carefully cleaned, possibly rotated at least once during cleaning, and then rinsed with de-ionized water until the ionic contamination of that water is well above 50 Mohm. If this is not feasible, then it is recommended that the sum of the voltage setting resistors be reduced to at least 5X below the measured ionic contamination.

11.2 Layout Example

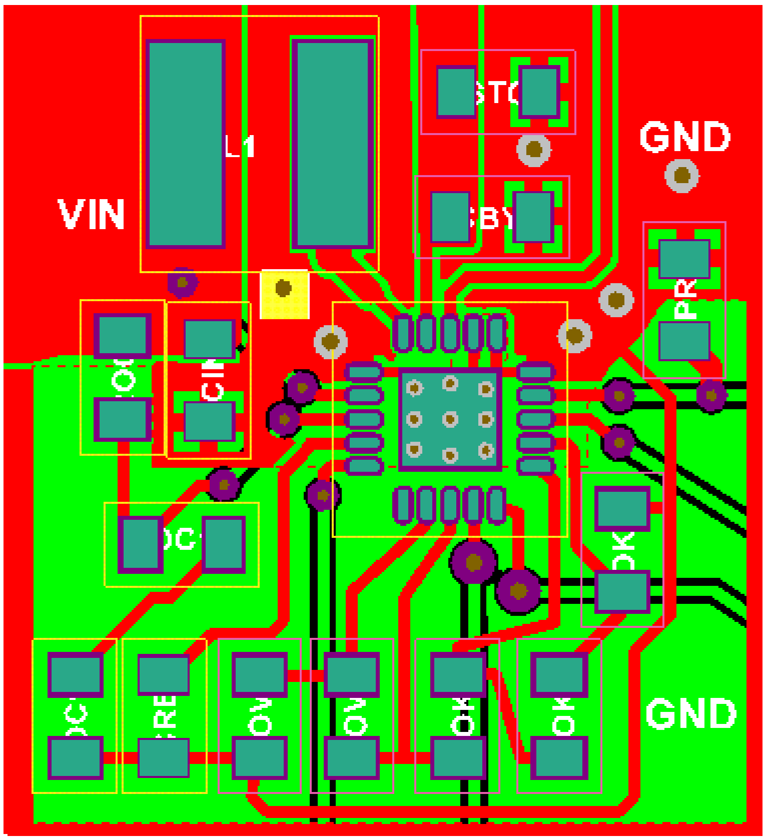

Figure 34. Recommended Layout

11.3 Thermal Considerations

Implementation of integrated circuits in low-profile and fine-pitch surface-mount packages typically requires special attention to power dissipation. Many system-dependent issues such as thermal coupling, airflow, added heat sinks and convection surfaces, and the presence of other heat-generating components affect the power-dissipation limits of a given component.

Three basic approaches for enhancing thermal performance are listed below.

- Improving the power-dissipation capability of the PCB design
- Improving the thermal coupling of the component to the PCB
- Introducing airflow in the system

For more details on how to use the thermal parameters in the Thermal Table, check the Thermal Characteristics Application Note (SZZA017) and the IC Package Thermal Metrics Application Note (SPRA953).

12 Device and Documentation Support

12.1 Device Support

12.1.1 Third-Party Products Disclaimer

TI'S PUBLICATION OF INFORMATION REGARDING THIRD-PARTY PRODUCTS OR SERVICES DOES NOT CONSTITUTE AN ENDORSEMENT REGARDING THE SUITABILITY OF SUCH PRODUCTS OR SERVICES OR A WARRANTY, REPRESENTATION OR ENDORSEMENT OF SUCH PRODUCTS OR SERVICES, EITHER ALONE OR IN COMBINATION WITH ANY TI PRODUCT OR SERVICE.

12.1.2 Zip Files

- http://www.ti.com/lit/zip/SLUC484
- http://www.ti.com/lit/zip/SLURAQ1
- http://www.ti.com/lit/zip/SLUC462

12.2 Documentation Support

12.2.1 Related Documentation

For related documentation see the following:

- EVM User's Guide, SLUUAA8
- Thermal Characteristics Application Note, SZZA017
- IC Package Thermal Metrics Application Note, SPRA953

12.3 Trademarks

All trademarks are the property of their respective owners.

12.4 Electrostatic Discharge Caution

These devices have limited built-in ESD protection. The leads should be shorted together or the device placed in conductive foam during storage or handling to prevent electrostatic damage to the MOS gates.

12.5 Glossary

SLYZ022 — *TI Glossary*.

This glossary lists and explains terms, acronyms, and definitions.

13 Mechanical, Packaging, and Orderable Information

The following pages include mechanical, packaging, and orderable information. This information is the most current data available for the designated devices. This data is subject to change without notice and revision of this document. For browser-based versions of this data sheet, refer to the left-hand navigation.

PACKAGING INFORMATION

Orderable Device	Status (1)	Package Type	Package Drawing	Pins	Package Qty	Eco Plan (2)	Lead/Ball Finish (6)	MSL Peak Temp (3)	Op Temp (°C)	Device Marking (4/5)	Samples
BQ25504RGTR	ACTIVE	QFN	RGT	16	3000	Green (RoHS & no Sb/Br)	CU NIPDAU	Level-2-260C-1 YEAR	-40 to 85	B5504	Samples
BQ25504RGTT	ACTIVE	QFN	RGT	16	250	Green (RoHS & no Sb/Br)	CU NIPDAU	Level-2-260C-1 YEAR	-40 to 85	B5504	Samples

(1) The marketing status values are defined as follows:
ACTIVE: Product device recommended for new designs.
LIFEBUY: TI has announced that the device will be discontinued, and a lifetime-buy period is in effect.
NRND: Not recommended for new designs. Device is in production to support existing customers, but TI does not recommend using this part in a new design.
PREVIEW: Device has been announced but is not in production. Samples may or may not be available.
OBSOLETE: TI has discontinued the production of the device.

(2) Eco Plan - The planned eco-friendly classification: Pb-Free (RoHS), Pb-Free (RoHS Exempt), or Green (RoHS & no Sb/Br) - please check http://www.ti.com/productcontent for the latest availability information and additional product content details.
TBD: The Pb-Free/Green conversion plan has not been defined.
Pb-Free (RoHS): TI's terms "Lead-Free" or "Pb-Free" mean semiconductor products that are compatible with the current RoHS requirements for all 6 substances, including the requirement that lead not exceed 0.1% by weight in homogeneous materials. Where designed to be soldered at high temperatures, TI Pb-Free products are suitable for use in specified lead-free processes.
Pb-Free (RoHS Exempt): This component has a RoHS exemption for either 1) lead-based flip-chip solder bumps used between the die and package, or 2) lead-based die adhesive used between the die and leadframe. The component is otherwise considered Pb-Free (RoHS compatible) as defined above.
Green (RoHS & no Sb/Br): TI defines "Green" to mean Pb-Free (RoHS compatible), and free of Bromine (Br) and Antimony (Sb) based flame retardants (Br or Sb do not exceed 0.1% by weight in homogeneous material)

(3) MSL, Peak Temp. - The Moisture Sensitivity Level rating according to the JEDEC industry standard classifications, and peak solder temperature.

(4) There may be additional marking, which relates to the logo, the lot trace code information, or the environmental category on the device.

(5) Multiple Device Markings will be inside parentheses. Only one Device Marking contained in parentheses and separated by a "~" will appear on a device. If a line is indented then it is a continuation of the previous line and the two combined represent the entire Device Marking for that device.

(6) Lead/Ball Finish - Orderable Devices may have multiple material finish options. Finish options are separated by a vertical ruled line. Lead/Ball Finish values may wrap to two lines if the finish value exceeds the maximum column width.

Important Information and Disclaimer: The information provided on this page represents TI's knowledge and belief as of the date that it is provided. TI bases its knowledge and belief on information provided by third parties, and makes no representation or warranty as to the accuracy of such information. Efforts are underway to better integrate information from third parties. TI has taken and continues to take reasonable steps to provide representative and accurate information but may not have conducted destructive testing or chemical analysis on incoming materials and chemicals. TI and TI suppliers consider certain information to be proprietary, and thus CAS numbers and other limited information may not be available for release.

In no event shall TI's liability arising out of such information exceed the total purchase price of the TI part(s) at issue in this document sold by TI to Customer on an annual basis.

TAPE AND REEL INFORMATION

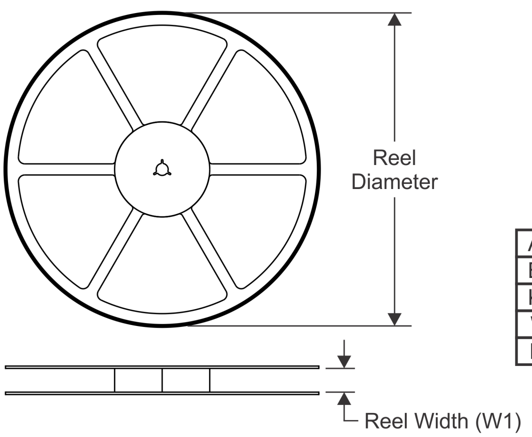

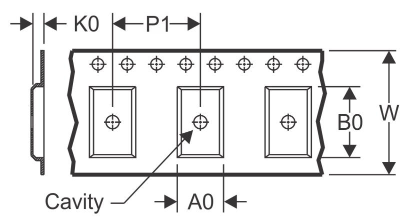

A0	Dimension designed to accommodate the component width
B0	Dimension designed to accommodate the component length
K0	Dimension designed to accommodate the component thickness
W	Overall width of the carrier tape
P1	Pitch between successive cavity centers

QUADRANT ASSIGNMENTS FOR PIN 1 ORIENTATION IN TAPE

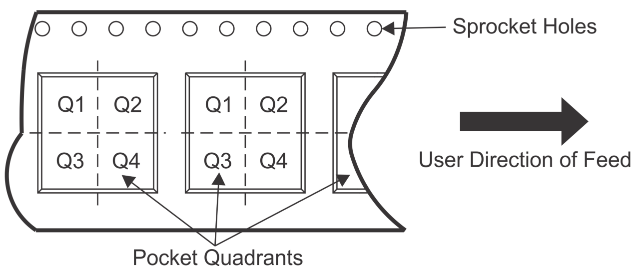

*All dimensions are nominal

Device	Package Type	Package Drawing	Pins	SPQ	Reel Diameter (mm)	Reel Width W1 (mm)	A0 (mm)	B0 (mm)	K0 (mm)	P1 (mm)	W (mm)	Pin1 Quadrant
BQ25504RGTR	QFN	RGT	16	3000	330.0	12.4	3.3	3.3	1.1	8.0	12.0	Q2
BQ25504RGTT	QFN	RGT	16	250	180.0	12.4	3.3	3.3	1.1	8.0	12.0	Q2

TAPE AND REEL BOX DIMENSIONS

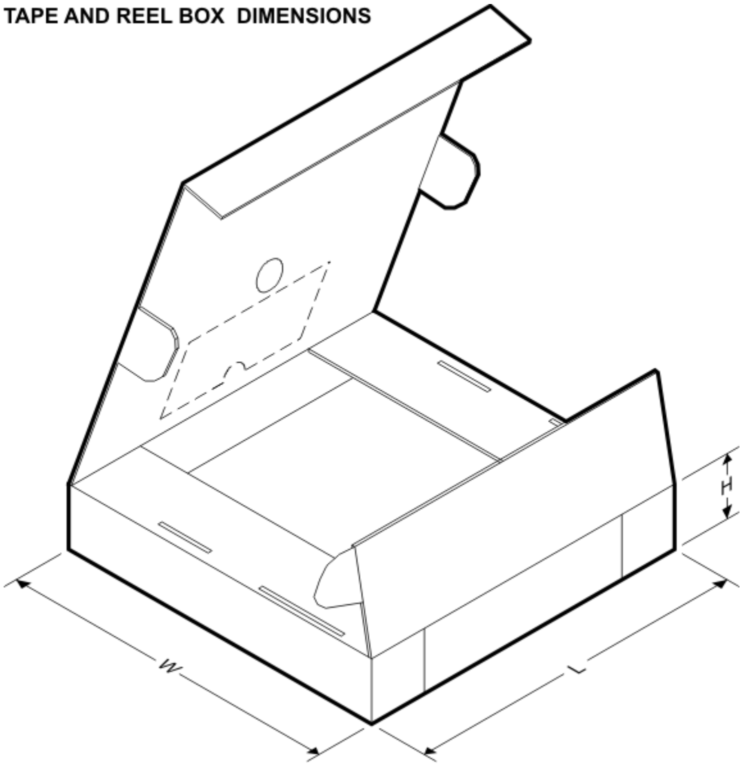

*All dimensions are nominal

Device	Package Type	Package Drawing	Pins	SPQ	Length (mm)	Width (mm)	Height (mm)
BQ25504RGTR	QFN	RGT	16	3000	367.0	367.0	35.0
BQ25504RGTT	QFN	RGT	16	250	210.0	185.0	35.0

RGT (S-PVQFN-N16) PLASTIC QUAD FLATPACK NO-LEAD

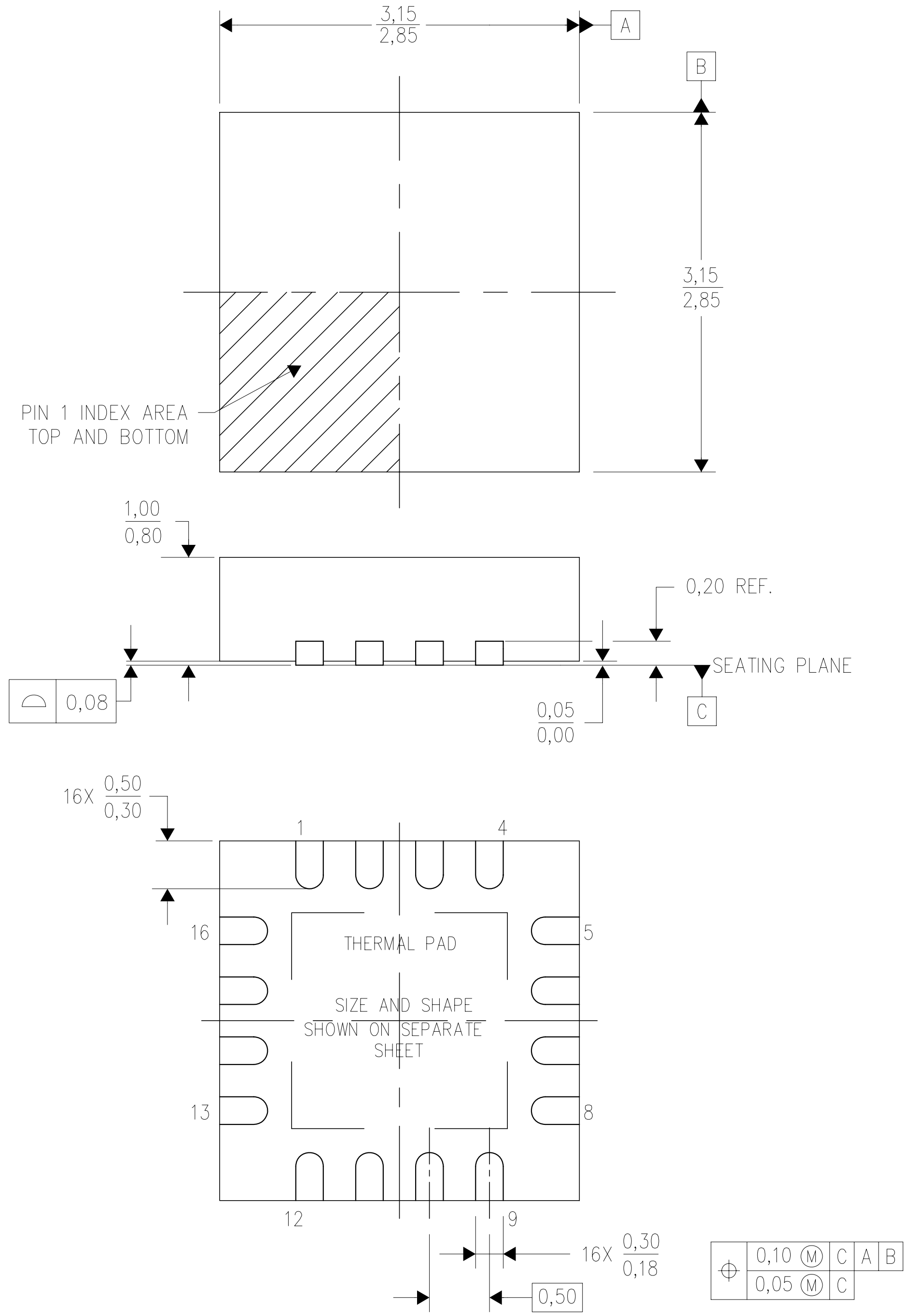

4203495/H 10/11

NOTES:
A. All linear dimensions are in millimeters. Dimensioning and tolerancing per ASME Y14.5M-1994.
B. This drawing is subject to change without notice.
C. Quad Flatpack, No-leads (QFN) package configuration.
D. The package thermal pad must be soldered to the board for thermal and mechanical performance.
E. See the additional figure in the Product Data Sheet for details regarding the exposed thermal pad features and dimensions.
F. Falls within JEDEC MO-220.

RGT (S–PVQFN–N16) PLASTIC QUAD FLATPACK NO–LEAD

THERMAL INFORMATION

This package incorporates an exposed thermal pad that is designed to be attached directly to an external heatsink. The thermal pad must be soldered directly to the printed circuit board (PCB). After soldering, the PCB can be used as a heatsink. In addition, through the use of thermal vias, the thermal pad can be attached directly to the appropriate copper plane shown in the electrical schematic for the device, or alternatively, can be attached to a special heatsink structure designed into the PCB. This design optimizes the heat transfer from the integrated circuit (IC).

For information on the Quad Flatpack No–Lead (QFN) package and its advantages, refer to Application Report, QFN/SON PCB Attachment, Texas Instruments Literature No. SLUA271. This document is available at www.ti.com.

The exposed thermal pad dimensions for this package are shown in the following illustration.

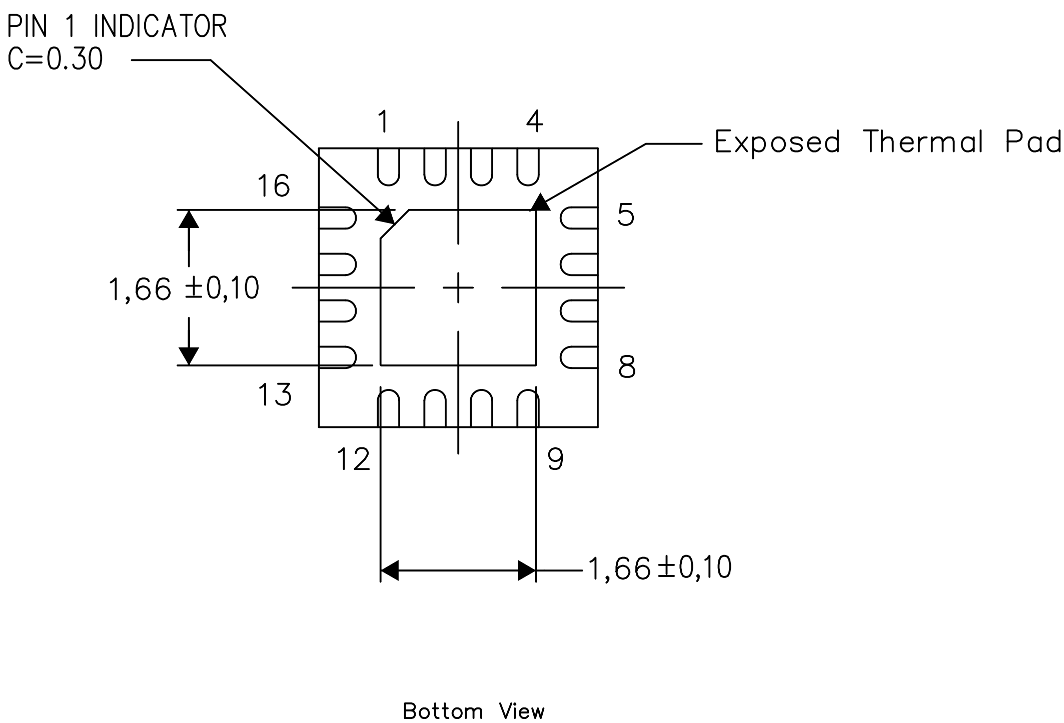

Exposed Thermal Pad Dimensions

4206349–10/W 10/14

NOTE: All linear dimensions are in millimeters

Products		**Applications**	
Audio	www.ti.com/audio	Automotive and Transportation	www.ti.com/automotive
Amplifiers	amplifier.ti.com	Communications and Telecom	www.ti.com/communications
Data Converters	dataconverter.ti.com	Computers and Peripherals	www.ti.com/computers
DLP® Products	www.dlp.com	Consumer Electronics	www.ti.com/consumer-apps
DSP	dsp.ti.com	Energy and Lighting	www.ti.com/energy
Clocks and Timers	www.ti.com/clocks	Industrial	www.ti.com/industrial
Interface	interface.ti.com	Medical	www.ti.com/medical
Logic	logic.ti.com	Security	www.ti.com/security
Power Mgmt	power.ti.com	Space, Avionics and Defense	www.ti.com/space-avionics-defense
Microcontrollers	microcontroller.ti.com	Video and Imaging	www.ti.com/video
RFID	www.ti-rfid.com		
OMAP Applications Processors	www.ti.com/omap	**TI E2E Community**	e2e.ti.com
Wireless Connectivity	www.ti.com/wirelessconnectivity		

Mailing Address: Texas Instruments, Post Office Box 655303, Dallas, Texas 75265

adafruit learning system

Adafruit PowerBoost 500 Basic

Created by lady ada

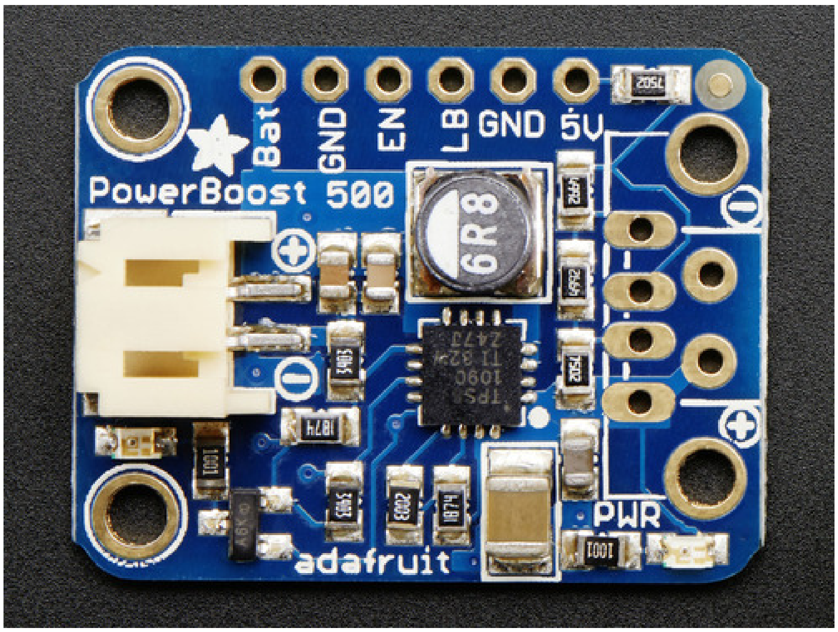

Last updated on 2015-01-15 11:00:12 PM EST

Guide Contents

Overview

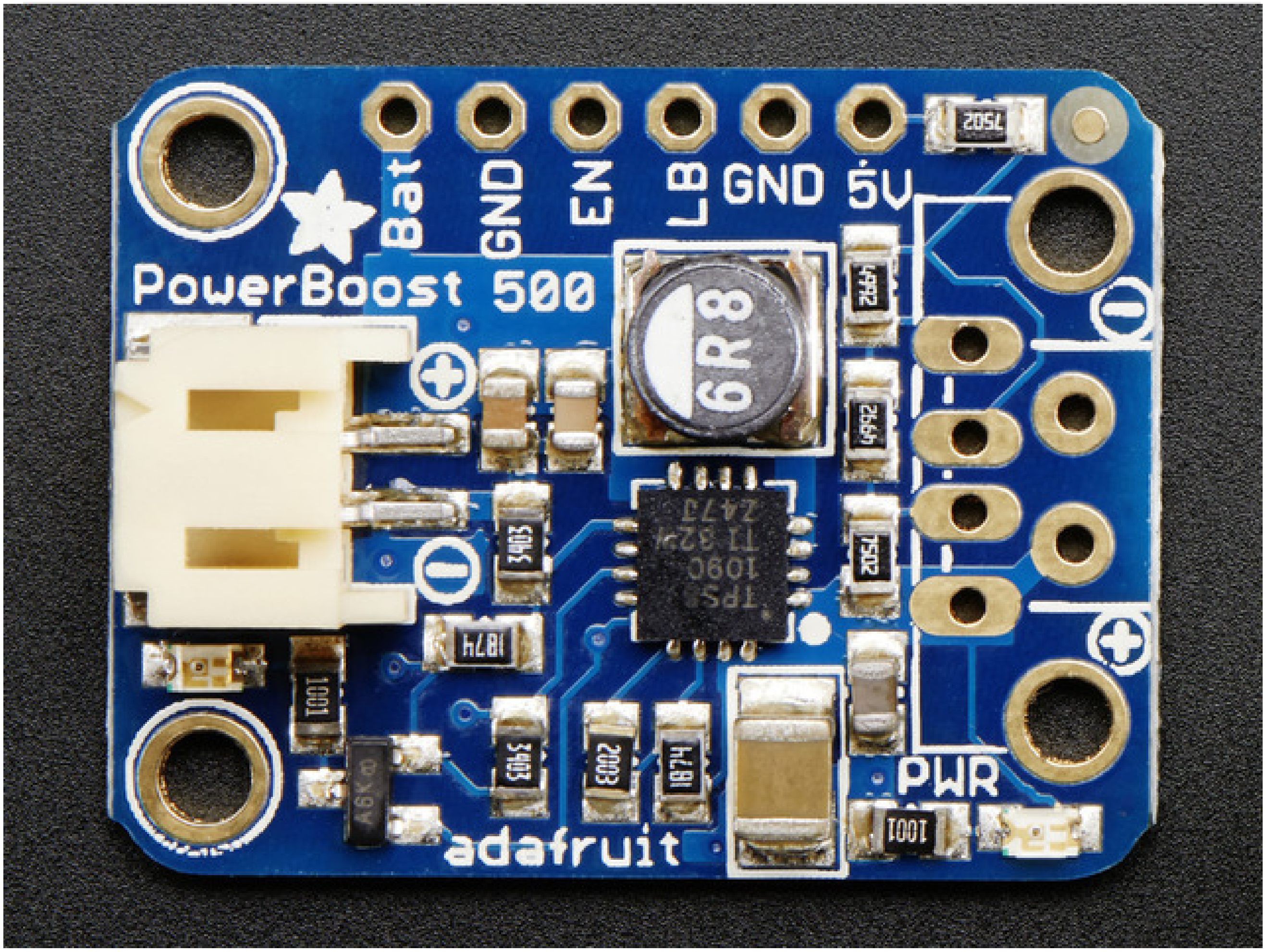

PowerBoost is the perfect power supply for your portable project! (http://adafru.it/dFq)This little DC/DC boost converter module can run from 1.8V batteries or higher, and convert that voltage to 5.2V DC for running your 5V projects. Like our popular 5V 1A USB wall adapter (http://adafru.it/duP), we tweaked the output to be 5.2V instead of a straight-up 5.0V so that there's a little bit of 'headroom' for long cables, high draw, the addition of a diode on the output if you wish, etc. The 5.2V is safe for all 5V-powered electronics like Arduino, Raspberry Pi, or Beagle Bone while preventing icky brown-outs during high current draw because of USB cable resistance.

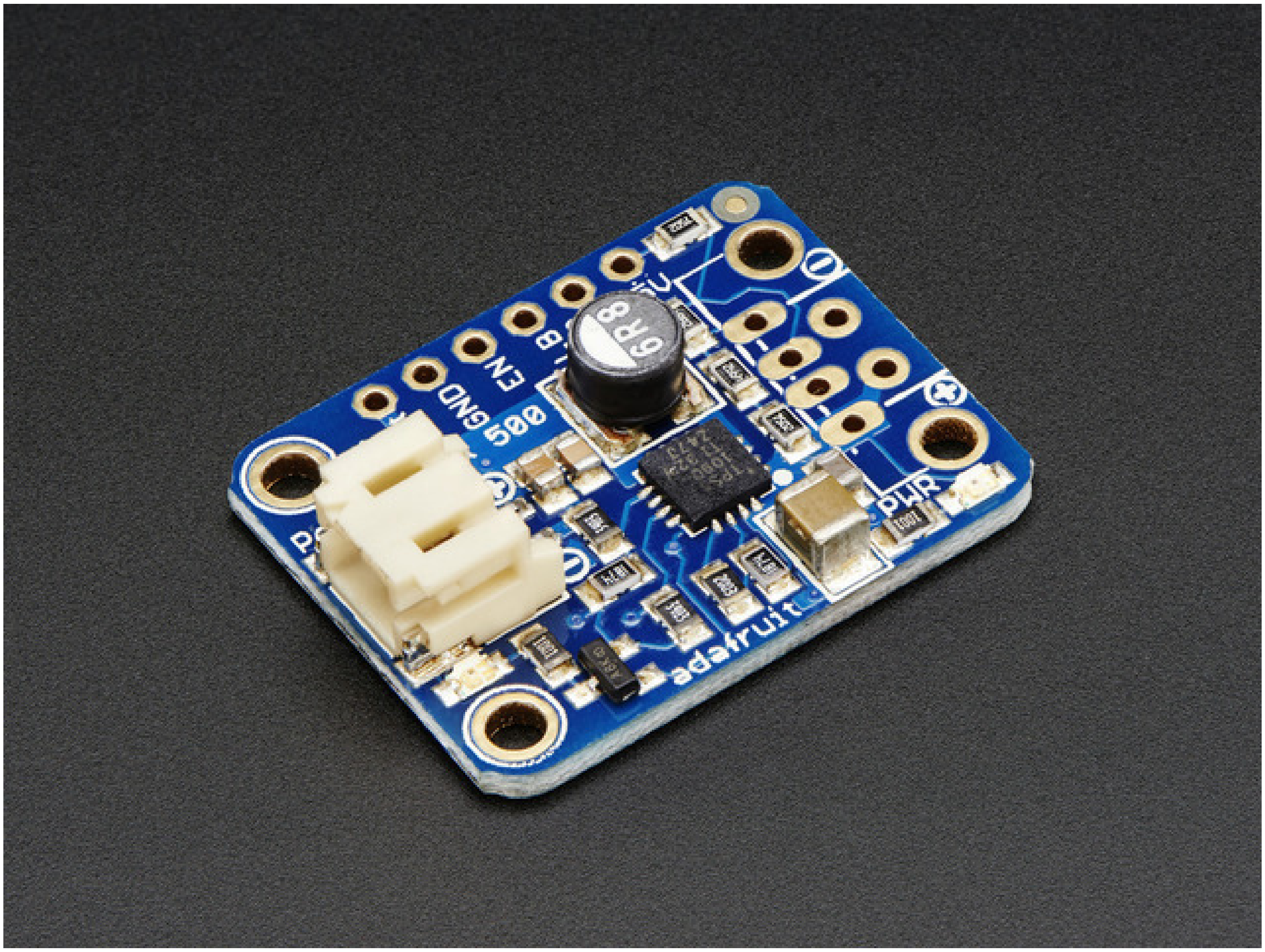

The PowerBoost 500 (http://adafru.it/dFq) has at the heart a TPS61090 boost converter from TI (http://adafru.it/duQ). This boost converter chip has some really nice extras such as low battery detection, 2A internal switch, synchronous conversion, excellent efficiency, and 700KHz high-frequency operation. Check out these specs!

- Synchronous operation means you can disconnect the output completely by connecting the **EN**able pin to ground. This will completely turn off the output
- 2A internal switch (~2.5A peak limiting) means you can get **500mA+ from as low as 1.8V**, **750mA+ from 2 NiMH** or Alkaline batteries, and at least **1000mA from a 3.7V LiPoly/LiIon** battery or 3 NiMH/Alkalines.
- Low battery indicator LED lights up red when the voltage dips below 3.2V, optimized for the most common usage of LiPo/LiIon battery usage
- Onboard 500mA charge-rate 'iOS' data resistors. Solder in the USB connector and you can plug in any iPhone or iPod for 500mA charge rate. Not suggested for iPad (which really needs 1A charge rate).
- Full breakout for battery in, control pins and power out
- 90%+ operating efficiency in most cases (see datasheet for efficiency graphs), and low quiescent current: 5mA when enabled and power LED is on, 20uA when disabled (power and low batt LED are off)

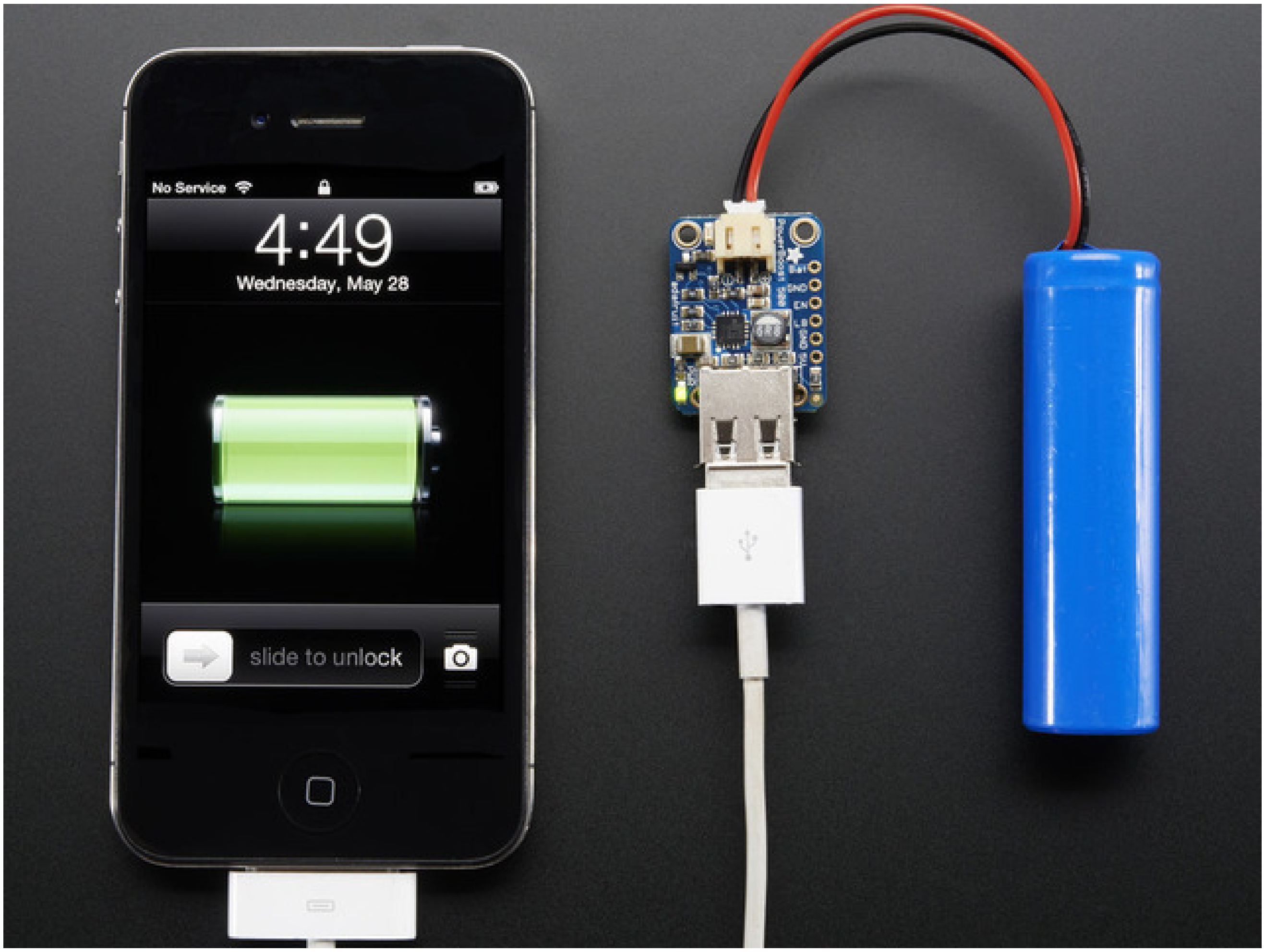

Great for powering your robot, Arduino project, single-board-computer such as Raspberry Pi or BeagleBone! Each order comes with one fully assembled and tested PCB and a loose USB A jack. If you are powering your project from USB, solder the USB A jack in (a 3-minute soldering task). If you would like to use a terminal block, pick up a 3.5mm 2pin block here (http://adafru.it/duR) and solder to the output spot where the USB jack would go. Or dont solder anything in for a more compact power pack.

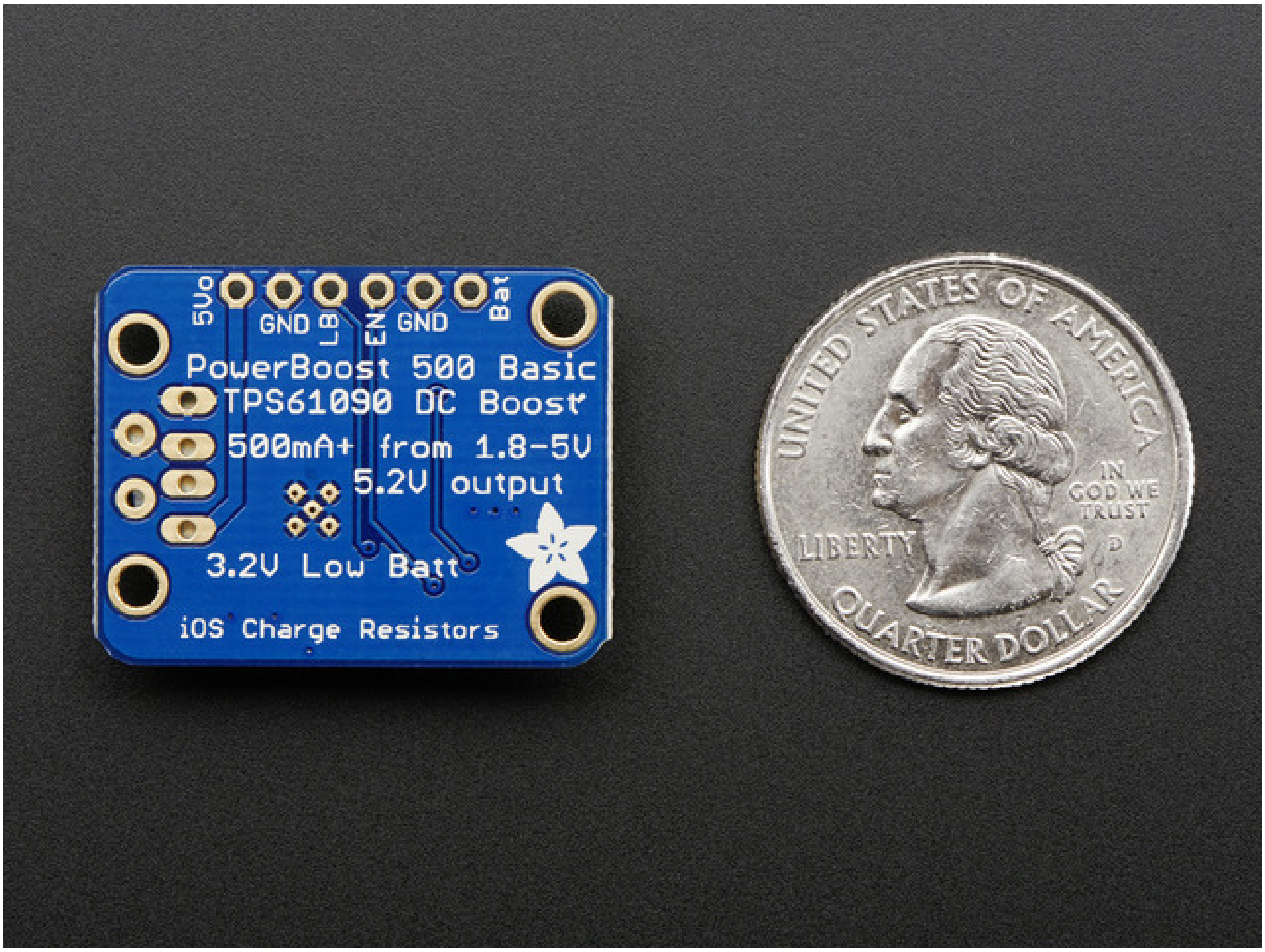

If you're trying to figure out how much current your project is using, check out the CHARGER DOCTOR! (http://adafru.it/1852)

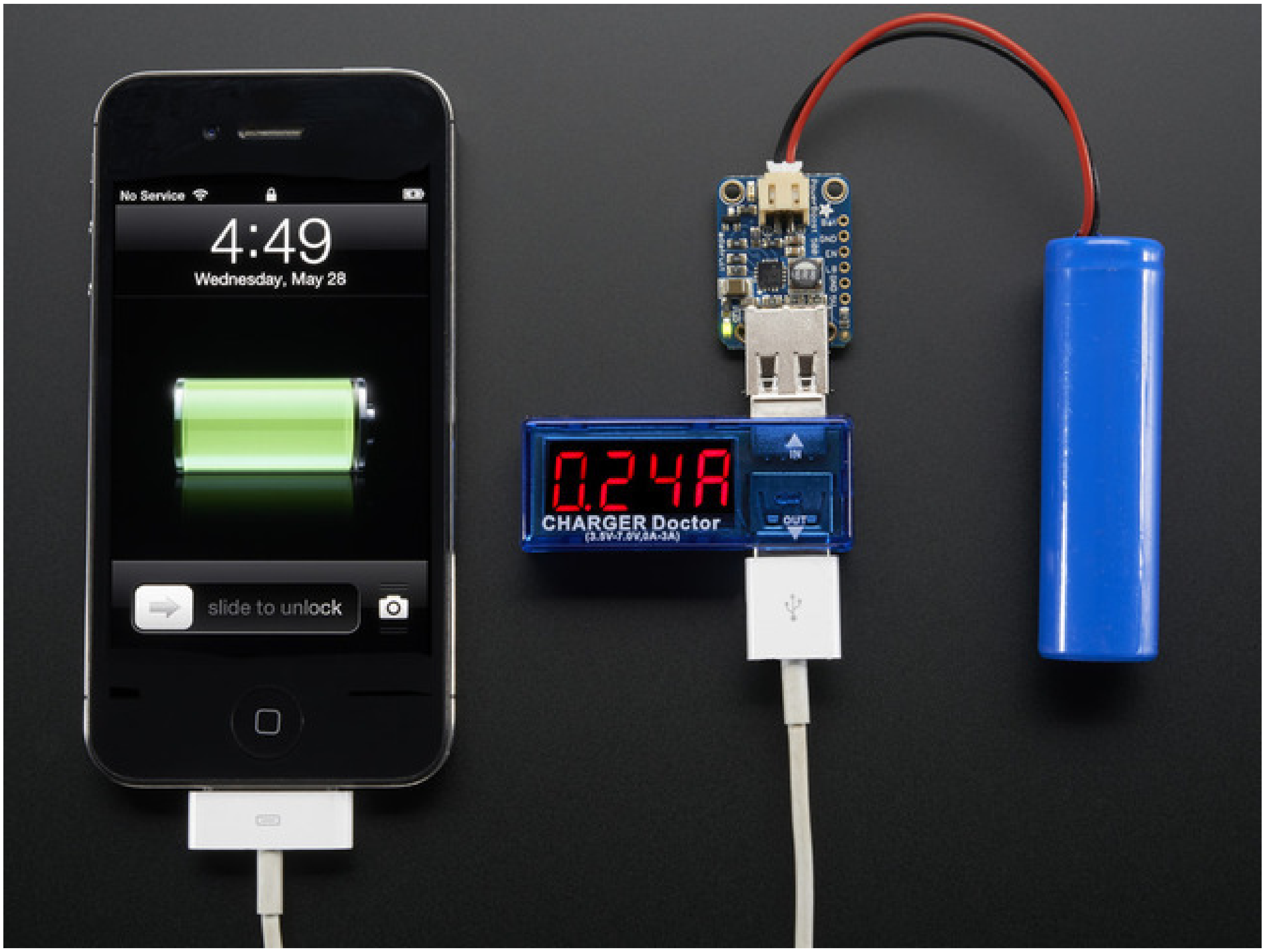
No Service
4:49
Wednesday, May 28
slide to unlock
0.24A
CHARGER Doctor
IN
OUT

Pinouts

For many people, the PowerBoost can be used with just the power input and power outputs. However, we have a couple handy breakouts so lets get started!

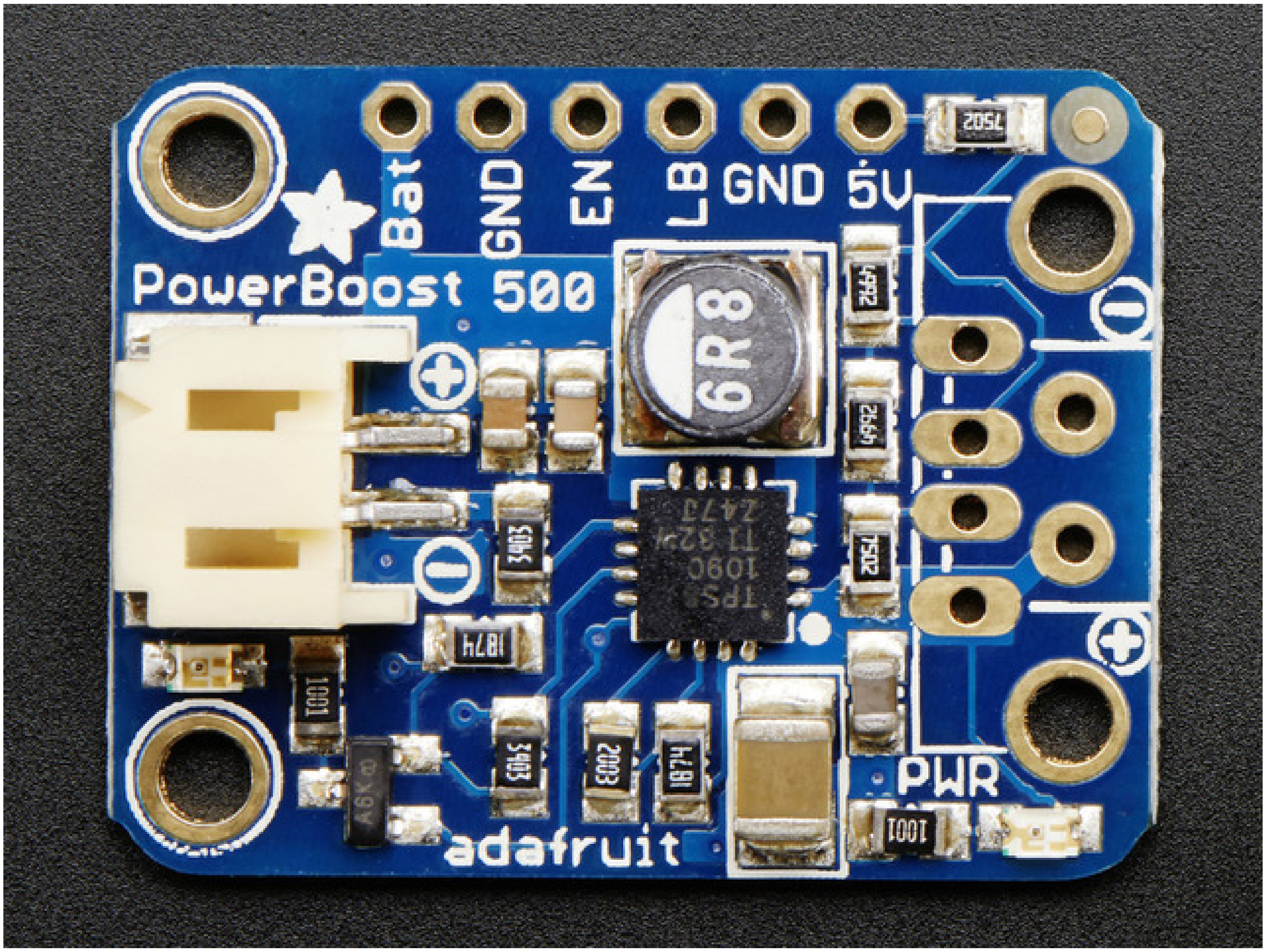

Power Pins

There's two power 'ports' - an input (called **BAT**) and an output (called **5V**)

- **BAT** - this is the battery input, it can range from 1.8V to 5V. Higher voltages will let you draw more current and in general, are more efficient. Try to keep the wires going to this pin nice and short - 3" or less is best!
- **GND** - this is the power ground. This boost converter is not 'isolated' - the ground input is the same as the ground output
- **5V** - this is the boosted output. When the board is running, the voltage will be 5.2V approximately. It may dip down to 5V as the current draw starts to go up (over 500mA). When the board is disabled, this output is 'floating' but you should still try not to apply a voltage to it while the board is disabled. There's a green LED connected to this pin which will let you know when there's power output

Control Pins

There's two 'control' pins.

- **EN** - this is the 'enable' pin. By default it is pulled 'high' to **VBAT**. To turn off the booster, connect this pin to ground. The switch can be as small as you like, it is just a signal. Contrast this to an inline power switch which would have to be able to handle up to 2A of current! When the chip is disabled the output is completely disconnected from the input.
- **LBO** - not a leveraged buy out! this is the **Low Battery Output**. By default it is pulled high to **BAT** but when the charger detects a low voltage (under 3.2V) the pin will drop down to 0V. You can use this to signal when its time to shut down or alert the user that the battery is low. There is also a red LED connected to this pin.

LEDs

There are two onboard LEDs. The Green LED sits next to the USB connector socket, and indicates the 5V output power state. The Red LED is next to the battery JST port and indicates when the battery voltage is below 3.2VDC

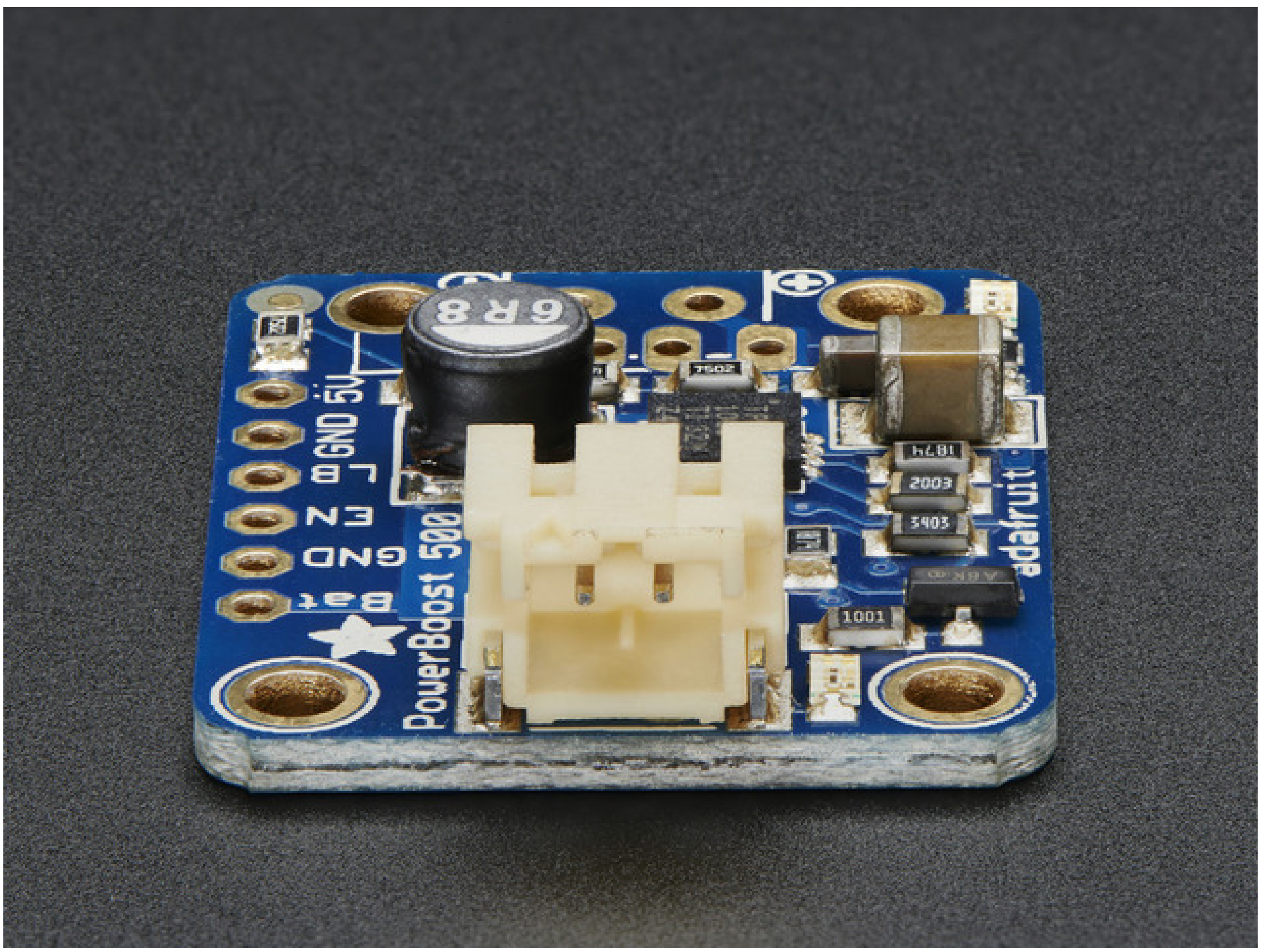

Battery and USB connection

You can connect a battery to the breakout strip or to the JST connector. All of Adafruit batteries come with JST cables that will plug in nicely. **Watch the polarity of the cable!** the + and - markings next to the JST will let you know which way is which.

The USB connector can be soldered on to create a portable 'USB power pack'. The two data lines on USB have resistor dividers that match Apple charger values so that you can plug any iOS device in to charge. 99% of other phones, devices and tables are totally cool with these resistors as well. You can always short the D+ and D- lines if you happen to have a phone that wants shorted data lines.

If you don't want a USB connector attached, there are two holes that are designed for a 3.5mm spaced terminal block (not included)

Downloads

- TPS61090 datasheet (http://adafru.it/duS)(the DC/DC boost control chip used)

Schematic

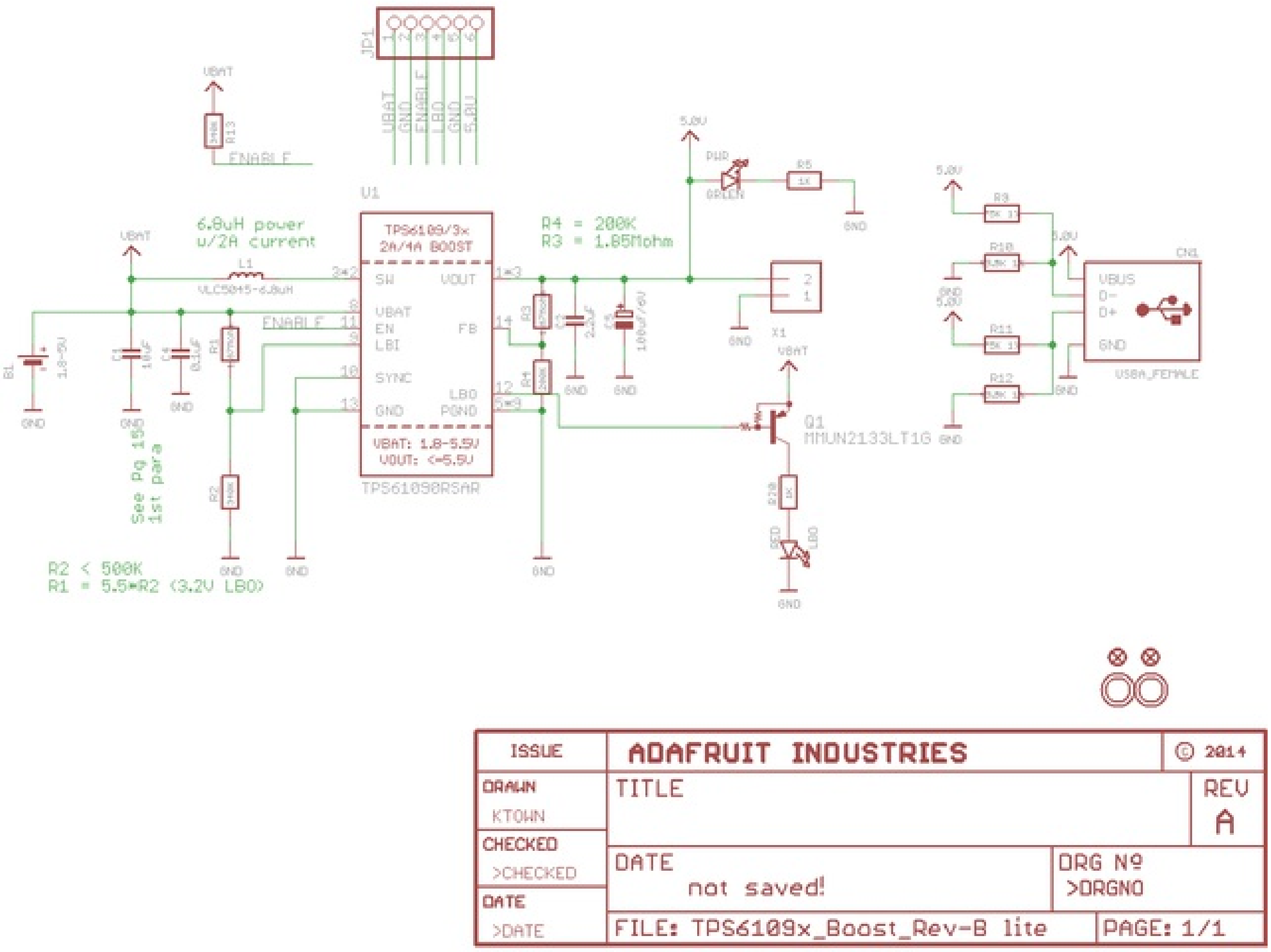

Fabrication Print

Dimensions in Inches

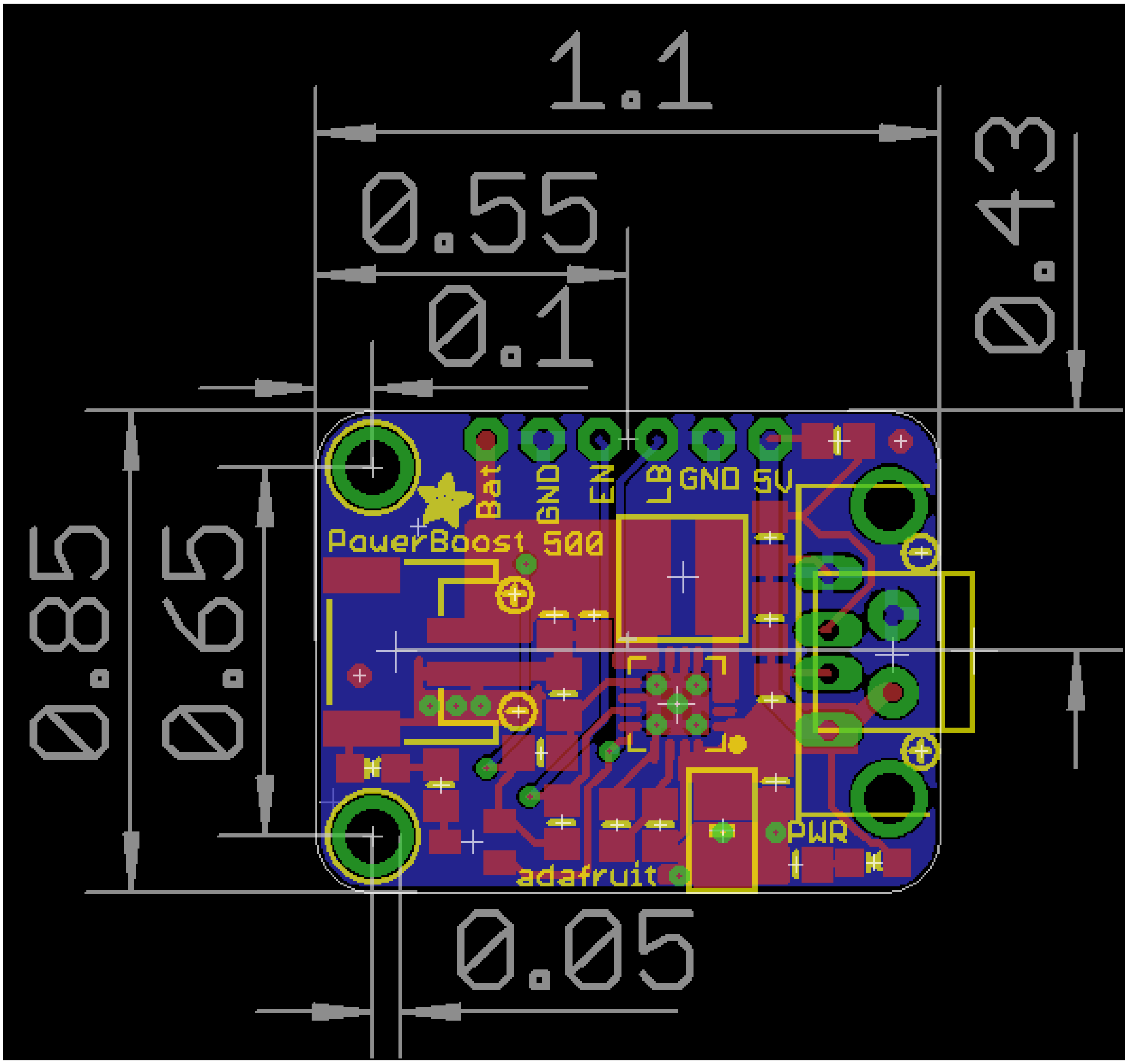
1.1
0.55
0.1
0.43
0.85
0.65
0.05
Bat
GND
EN
LB
GND
5V
PowerBoost 500
PWR
adafruit